# THE INFLUENCE OF OXYGEN UPON THE LIFESTYLE CHOICES OF *STAPHYLOCOCCUS AUREUS*

by

**Ameya Ashutosh Mashruwala**

A dissertation submitted to the

Graduate School-New Brunswick

Rutgers, The State University of New Jersey

In partial fulfillment of the requirements

for the degree of

Doctor of Philosophy

Graduate Program in Microbial Biology

Written under the direction of

Dr. Jeffrey M Boyd

And approved by

_____

_____

_____

_____

New Brunswick, New Jersey

May 2017

**ABSTRACT OF THE DISSERTATION**

The Influence of Oxygen Upon the Lifestyle Choices of *Staphylococcus aureus*

by Ameya Ashutosh Mashruwala

Dissertation Director:

Dr. Jeffrey M Boyd

Biofilms are communities of microorganisms attached to a surface or each other. Biofilm associated cells are the etiologic agents of recurrent *Staphylococcus aureus* infections. Oxygen is utilized by *S. aureus* as a terminal electron acceptor (TEA). Infected human tissues are hypoxic or anoxic. *S. aureus* increases biofilm formation in response to hypoxia, but how this occurs is unknown. This thesis reports that oxygen influences biofilm formation in its capacity as a TEA for cellular respiration. Genetic, physiological, or chemical inhibition of respiratory processes elicited increased biofilm formation. Impaired respiration led to increased cell lysis via divergent regulation of two processes: increased expression of the AtlA murein hydrolase and decreased expression of the AtlA-inhibitory glycopolymers, WTA. The AltA-dependent release of cytosolic DNA contributed to increased biofilm formation. The fibronectin binding protein A, which is known to interact with AtlA, was also found to be involved in fermentative biofilm formation. Further, cell lysis and biofilm formation were governed by the SrrAB and the SaeRS two-component regulatory systems (TCRS). Genetic evidence suggests that SrrAB-dependent biofilm formation

occurs in response to the accumulation of reduced menaquinone. SaeRS-dependent biofilm formation also occurred in response to changes in the respiratory status of the cell, via an as yet undefined signal molecule(s). Further, a high cellular titer of phosphorylated SaeR is required for biofilm formation. Epistasis analyses found that SaeRS and SrrAB influence biofilm formation independent of one another, *in vitro*. SrrAB and SaeRS governed host colonization *in vivo*, in the context of a mouse model of orthopedic implant-associated biofilm formation. Of these two TCRS, SrrAB is the dominant system driving biofilm formation *in vivo*. Biofilms impart protection from innate immunity as well as therapeutic agents. Data presented suggest that pre-formed biofilms, established by fermenting *S. aureus*, can be prompted to detach and disperse upon exposure to a TEA (oxygen or nitrate). Exposure to oxygen (reaeration) results in increased growth but decreased transcription of *atlA* and decreased release of DNA. Reaeration is also accompanied by increased transcription of *sspA* which encodes for a protease capable of cleaving AtlA. Biofilm dispersal was blocked in a strain that is incapable of respiration, suggesting changes in cellular respiratory status are being sensed to trigger dispersal. The transcription of *atlA* and *sspA* upon reaeration was modulated in a divergent manner by SrrAB. Data presented suggest that SrrAB achieves divergent regulation of *atlA*, in two separate growth conditions, via the small RNA, *rsaE*, as an intermediary. In summation, the results presented define the bases for how oxygen dictates the lifestyle choices of *S. aureus*. The studies also establish the mechanistic and

regulatory bases underlying the formation of anaerobic and fermentative biofilms by *S. aureus*.

## ACKNOWLEDGEMENTS

When I arrived in New Jersey I did not know anybody. I thank my graduate mentor Jeff Boyd and his wife Laura Boyd for welcoming me to NJ, and for their friendship over the years. Having been in graduate school for over a decade, I am well aware of the pressures and requirements upon an assistant professor. Thus I am sincerely grateful to Jeff, for he always believed in me and never really 'trimmed my wings', but in fact allowed me to freely pursue any and all scientific endeavors and helped me grow as an independent thinker and scientist.

I extend my gratitude to Dr. William Belden and the members of his group (especially Hamidah and Allison) for their help and guidance in learning the many and varied techniques in molecular biology; and on the many discussions on science we had that were of immeasurable help during my PhD work. I am grateful to Dr. Ann Stock and the members of her group (especially Paul & Ian) for their help in the approach and study of regulatory networks. I thank Dr. Debashish Bhattacharya and the members of his group (especially Nicole) for their guidance with genomics. Dr. Ann Stock, Dr. William Belden and Dr. Debashish Bhattacharya advised me as members of my dissertation committee, and I thank them for their encouragement and guidance throughout my PhD program. I also sincerely appreciate their help and advise during my search for a postdoctoral position.

It is said that current science builds upon the endeavors of previous scientists. The truism of the communal aspect of science was never clearer to me, than during my time at Rutgers. My work upon biofilms and programmed cell death was conducted in a lab with no previous expertise in these lines of inquiry. This work would have been near impossible without being able to refer to the work of previous scientists. It helped me to build my hypotheses and learn the methods and techniques involved in studying my topic. Although in the interests of space I am unable to acknowledge everyone individually, I extend my gratitude to the many scientists from the James Imlay, Kenneth Bayles, Suzanne Walker, James P. O'Gara, Alex Horswill, Richard Losick and Andreas Peschel research groups, who without their knowing essentially served as my teachers.

I gratefully acknowledge the kind endowment of Dennis Fenton and Douglas Eveleigh; and SEBS Rutgers, for funding my research.

Life in graduate school is stodgy without friends around you. I will miss my friends Hassan, Christina, Shiming, Shiven, Adriana, Carly, Chengsheng and Hamidah when I leave Rutgers. I will miss the lab baking competitions and the Kabobs! I wish you guys the best for all your future endeavors. And I will miss working with the two great undergraduate researchers, Adriana and Carly, who helped with my experiments. Adriana and Carly, a ton of thanks!

As a foreign national, the vagaries of the US immigration service and academic life have prevented me from visiting my home country for almost nine years. I thank my uncle, aunt and cousin for our annual family gatherings in

Texas, which helped alleviate my homesickness. It would have been tough going indeed without you guys!

My love for science and microbiology originated with my Mother, herself a microbiologist. Her stories about science, her love for microbiology and investigating scientific mysteries, have much to do with my being in science. I am grateful to her for that, and her for all the love and blessings throughout these years. A big thanks to my father, my brother and my maternal grandmother for their love, encouragement and constant support, during both good times and bad. Without them, I would have long ago given up on graduate school.

Ralph Emerson once said, "Art is a jealous mistress". I think it is a saying readily applied to science. Thus above all else, I thank my wife Vidisha for bearing with my scientific pursuits. Her unwavering love, encouragement and her patient support is the bedrock on which our life in the last eight years has been built.

I dedicate this thesis to my family, especially my paternal grandmother (Malini Mashruwala), who has lost her memory to Alzheimer's since I last met her.

## TABLE OF CONTENTS

## LIST OF TABLES

## ABBREVIATIONS

| | |
|---|---|
| *Bacillus subtilis* | *B. subtilis* |
| Catalase | Kat |
| Cell-wall associated proteins were detached | CW-extracts |
| Endo-β-N-acetylglucosaminidase | GL |
| *Escherichia coli* | *E. coli* |
| High-molecular weight extracellular DNA | eDNA |
| Histidine kinase | HK |
| Hyperbaric oxygen therapy | HBOT |
| N-acetylmuramyl-L-alanine amidase | AM |
| Nitric oxide | NO |
| Not-significant | NS |
| Phosphate buffered saline | PBS |
| Polysaccharide intercellular adhesin | PIA |
| Programmed cell death | PCD |
| Programmed cell lysis | PCL |
| Response regulator | RR |
| Small colony variants | SCV |
| *Staphylococcus aureus* | *S. aureus* |
| Terminal electron acceptor | TEA |
| Tricarboxylic acid cycle | TCA |
| Two-component regulatory system | TCRS |
| Wall-teichoic acids | WTA |

| | |
|---|---|
| Wild-type | WT |

## LIST OF FIGURES

## PREFACE

Chapter 2 has been published in ELife as "Impaired respiration elicits SrrAB-dependent programmed cell lysis and biofilm formation in *Staphylococcus aureus*", 2017, Mashruwala A.A., Guchte A.V.D., Boyd J.M.

Mashruwala A.A. conducted all the work reported in Chapter 2, with the following exception: he contributed design, analysis, curation and visualization for the data presented in Figures 2.2B and 2.5F, but did not participate in data accquisition.

Chapter 3 is under revision at Infection and Immunity as "SaeRS is responsive to the cellular respiratory status and regulates fermentative biofilm formation in *Staphylococcus aureus*.", Mashruwala A.A., Gries C.M., Scherr T.D., Kielian T., Boyd J.M.

Mashruwala A.A. conducted all the work reported in Chapter 3, with with the following exception: he contributed only data visualization in Figure 3.6 and Figure 3.S5 (animal model of infection).

Chapter 4 is in preparation for submission as " Resumption of respiration results in the detachment and dispersal of pre-formed fermentative *Staphylococcus aureus* biofilms", Mashruwala A.A., Guchte A.V.D., Boyd J.M.

Mashruwala A.A. conducted all the work reported in Chapter 4 with the following exception: he contributed to the design, analysis, curation and visualization for

the data presented in Figures 4.1B and 4.2B, but did not participate in data accquisition.

# CHAPTER 1

# INTRODUCTION

## *Staphylococcus aureus*: A human commensal

*Staphylococcus aureus* is an immobile, gram-positive bacterium that froms characteristic golden-yellow colonies when cultured upon solid medium (128). *S. aureus* was first isolated by Sir Alexander Ogston, in 1882, from the pus of surgical abcesses of a patient in Aberdeen, Scotland (90). However, Rosenbach first described a proper nomenclature for *S. aureus*, in 1884 (128). Rosenbach described the two pigmented colony types of staphylococci, *S. aureus* (derived from the Latin word aurum for gold) and *Staphylococcus albus* (derived from the Latin word albus for white) (128). *S. aureus* is a commensal bacterium that colonizes both animals and humans. *S. aureus* has been determined to colonize between 20-50% of the healthy human population (38, 51, 108, 114, 164). Colonization typically occurs in the nares, throat, or on the skin (53, 114, 164).

## *Staphylococcus aureus*: A facultative pathogen

Typically *S. aureus* does not cause the human carrier harm, however, under select conditions, it is capable of causing both invasive as well as non-invasive infections (78, 150, 159). The factors in either the host or the bacterium, that lead to the establishment of the carrier state are still unclear. It is also unclear what prompts the bacterium to invade and infect human tissues.

However, once *S. aureus* switches to a pathogenic state it is capable of causing rapidly progressing, and often fatal, infections in a number of tissues and organs in the human body (78, 150). While *S. aureus* causes a variety of suppurative infections and toxinoses, the dominant fraction of invasive infections caused by this bacterium occur in the context of bacteremia (34, 78).

Historically, *S. aureus* infections were acquired within a hospital environment (termed as noscomial or healthcare-associated infections) (128). Indeed, *S. aureus* was reported as being the leading cause of nosocomial infections in the US (reported by the National Nosocomial Infections Surveillance System) (128). However, the onset or occurrence of *S. aureus* infections is increasingly transpiring in community settings (78, 148).

### ***Staphylococcus aureus*: Modes of energy generation**

Bacteria require a source of carbon and energy for growth and replication. These are usually derived from the enzymatic breakdown of more-complex organic molecules such as carbohydrates, lipids, and proteins. *S. aureus*, at least transiently, derives it's carbon and energy from the host organism (34, 127, 142). This is accomplished in part by the synthesis of a wide assortment of virulence determinants that are capable of killing host cells and catabolizing macromolecules (142).

*S. aureus* is a facultative anaerobe, and therefore, it can derive energy for growth using either fermentative or respiratory pathways (97). It has complete

metabolic pathways for the glycolytic, oxidative pentose phosphate pathway and the tricarboxylic acid cycle (TCA) (127, 142). Under laboratory conditions, *S. aureus* displays diauxic growth upon glucose. Initial growth is achieved via fermentation upon glucose during which growth is exponential (142). Post-exponential growth requires the uptake and catabolism of the fermentative by-products, such as acetate, formed during the exponential phase of growth (142). Thus during post-exponential growth the TCA cycle is active to provide both reducing power and biosynthetic intermediates and energy is derived via respiration. This switch to respiration dramatically alters the metabolic status of the cell and also coincides with increased expression of virulence factors (to extract more nutrients from the surroundings) (142). *S. aureus* can utilize either oxygen or nitrate as a terminal electron acceptor (TEA) to support respiration. Respiration is the preferred mode of energy generation (142). Oxygen is the dominant TEA utilized for growth and when allowed to select between the usuage of oxygen or nitrate, *S. aureus* prefers oxygen as the TEA. In the laboratory, anaerobic growth of *S. aureus* upon sodium nitrate results in the respiratory reduction to nitrite. NO is an acidificed derivative of nitrite. Thus, NO can arise during respiration upon nitrate in cells cultured in tryptic soy broth. NO is toxic to *S. aureus*. Data presented in this study use nitrate as a TEA to gain insights into staphylococcal physiology. However, due the inherent complications arising from growth in the presence of nitrate, the principal data accquisition and analyses were predicated upon the usuage of oxygen as a TEA.

**Biofilm formation in *Staphylococcus aureus***

*S. aureus* is a leading cause of infections associated with bio-medical devices, such as catheters, pacemakers, and artificial heart valves (2). *S. aureus* has the ability to adhere to these indwelling devices and form architecturally complex structures termed as biofilms (2). *S. aureus* can also adhere directly upon human tissues (2). Biofilms structures are mini-ecosystems that can be either mono- or poly-organismal in composition. *S. aureus* typically froms mono-microbial biofilms. Biofilm formation is initiated when bacteria attach to a surface, or to each other. Subsequently, during the maturation process, the bacteria produce organic polymers, termed the matrix, that act as glue-like materials to futher enhance adhesion (6, 27, 28). The polymers also serve as the scaffolding upon which the three-dimensional architecture of the biofilm is assembled (40). The biopolymers can constitute upto 90% of the dry mass of the biofilm (40). In the context of an infection, biofilm matrixes are crucial since they shield the microbes from contact with the human innate immune system, protect them from reactive oxygen species insult, and decrease the killing efficiency of antimicrobials (56, 83, 163). The latter stages of the biofilm lifecycle are characterized by the periodic detachment and shedding of the biofilm-associated cells, and this process is termed as biofilm dispersion. This process can be genetically programmed in which case the cells initiate the production of proteins that digest the matrix biopolymers, allowing them to be detached (2). Alternately, dispersal can occur under the direction of mechanical shear processes. Regardless of the mechanism, detachment allows the cells the ability to migrate

to alternate sites in the host resulting in disease dissemination (9). Consequently, cells detached from biofilms are often thought to be the etiologic agents of recurrent staphylococcal infections (2, 117). The signals that prompt free-living cells to attach to surfaces or those that elicit biofilm dispersal are an area of active research. Understanding what signals influence these lifestyle choices of *S. aureus* will allow for the rational design of molecules and impart the capacity to guide these processes for therapeutic interventions.

**Does oxygen influence the ability of *S. aureus* to form or disperse from biofilms?**

Oxygen concentrations vary greatly between healthy human tissues (between 19.7 to ~1.5%; normoxia), necrotic tissues, as well as in wounds, where concentrations are estimated to be below 1% (hypoxic) or anoxic (3, 18, 151). Bacteria use oxygen as a TEA to support respiration and consequently sites colonized with bacteria experience a rapid decrease in oxygen tension as infection progresses. Clearly, bacterial pathogens would experience a wide and rapidly changing range of oxygen tensions in the context of infections. In light of these observations it was intriguing to note that biofilm-associated infections caused by *S. aureus* often occur in tissues where the normal oxygen concentrations are low (<6%). Chronic osteomyelitis is an infection of the skeletal tissue wherein *S. aureus* established biofilms upon dead bones (2, 13). The normoxic concentration of oxygen in healthy skeletal tissue is about 6%. Keratitis and conjunctivitis are infections are ocular infections (2). The normoxic

concentration of oxygen in the posterior chamber of the eye and the lens is between 2-3.5%. These observations led me to hypothesize that decreased oxygen tensions could be one environmental factor that prompt *S. aureus* to establish biofilms.

Typically when a patient reaches the hospital and therapeutic intervention can be made, it is likely that infection would have progressed to the point where biofilms have already been established *in vivo*. The infected tissue is also likely to be experiencing hypoxia or anoxia. Hyperbaric oxygen therapy (HBOT) is a treatment in which patients are placed inside a chamber with pressure higher than sea level (138, 141). In the chamber patients inhale 100% oxygen, intermittently (138, 141). HBOT is a medically approved therapy used in managing chronic osteomyelitis. These observations led me to hypothesize that increased oxygen tensions could be one environmental factor that prompt *S. aureus* to detach from biofilms and disperse.

The initial aim of the studies described in this thesis was to test the two hypotheses stated above. I present data in Chapter 2 and Chapter 4 that lent support to both my initial hypotheses. Therefore I expanded my study to determine the mechanistic and regulatory bases by which oxygen influences the ability of *S. aureus* to form biofilms or disperse from them.

In Chapter 2 I report that oxygen influences biofilm formation in its capacity as a TEA. Decreased respiration triggers genetic programming in *S. aureus* that leads to self-rupturing (or cell-lysis) of cells. The biopolymers released upon cellular rupture were utilized to construct the biofilm matrix. Self-

rupturing was achieved by the production of an enzyme that digests the cell wall and decreased synthesis of a cell-wall ribitol-based polymer. In Chapter 2 and Chapter 3, I report that the divergent reprogamming of cellular processes upon changes in oxygen tensions in the environment was achieved using modular regulatory systems, termed as two-component regulatory systems (TCRS) . Changes in the cellular respiratory status served as the stimulus that triggered genetic reprogramming by the two TCRS. Moreover, both the TCRS influenced biofilm formation in the context of an animal model of implant-associated biofilm infection.

In Chapter 4, I report that the detachment of cells from the biofilm matrix was achieved by reversing the cell-rupturing process. The data suggest that when oxygen starved cells are supplied fresh oxygen they decrease the production of a cell-wall digesting enzyme, but produce a protein that is capable of degrading the biofilm matrix. Similar to the findings reported in earlier Chapters, changes in the cellular respiratory status served as the stimulus that triggered biofilm dispersal and this process was also mediated by a TCRS.

# CHAPTER 2

## Impaired respiration elicits SrrAB-dependent programmed cell lysis and biofilm formation in *Staphylococcus aureus*

**Published in the Elife journal, 2017**

**Abstract:**

Biofilms are communities of microorganisms attached to a surface or each other. Biofilm-associated cells are the etiologic agents of recurrent *S. aureus* infections. Infected human tissues are hypoxic or anoxic. *S. aureus* increases biofilm formation in response to hypoxia, but how this occurs is unknown. In the current study we report that oxygen influences biofilm formation in its capacity as a TEA for cellular respiration. Genetic, physiological, or chemical inhibition of respiratory processes elicited increased biofilm formation. Impaired respiration led to increased cell lysis via divergent regulation of two processes: increased expression of the AtlA murein hydrolase and decreased expression of wall-teichoic acids. The AltA-dependent release of cytosolic DNA contributed to increased biofilm formation. Further, cell lysis and biofilm formation were governed by the SrrAB TCRS. Data presented support a model wherein SrrAB-dependent biofilm formation occurs in response to the accumulation of reduced menaquinone.

**Introduction:**

*S. aureus* is a commensal bacterium that is estimated to colonize between 20-50% of the healthy human population (38, 51, 108, 114, 164). Colonization typically occurs in the nares, throat, or on the skin (53, 114, 164). Under select conditions, *S. aureus* is capable of causing both invasive as well as non-invasive infections (78, 150, 159). The dominant fraction of invasive infections caused by this bacterium occur in the context of bacteremia (78). In addition, *S. aureus* can infect and cause diseases of the lungs (penumonia), skin (cellulitis), skeletal tissues (ostoemyelitis), heart tissue (endocarditis) and septic shock (78, 150). In the United States, pneumonia and septic shock are rapidly progressing infections and often fatal with mortality rates of 30-55% (78). While bacteremia and endocarditis infections have a lower degree of mortality, they are associated with a higher degree of recurrence, suggestive of therapeutic recalcitrance (78). A recent epidemiological analysis of ~8,700 cases in the US, of invasive *S. aureus* infections, found that nearly 92% cases required hospitalization (78).

Historically, *S. aureus* infections were nosocomial in origin; however, their onset or occurrence increasingly transpires in community settings (78, 148). In the United States, pulsed-field type USA300 methicillin-resistant *S. aureus* (MRSA) has emerged as the dominant etiologic agent of community-associated invasive infections (78). Treatment of *S. aureus* infections is often problematic due to the increasing prevalence of antibiotic resistance. *S. aureus* strains have been isolated that are resistant to nearly all clinically available antibiotics, including the last-line antibiotics linezolid and daptomycin (20, 129, 130).

Biofilms are architecturally complex, multicellular communities of microorganisms of either mono- or poly-microbial compositions (25, 26). It has been theorized, based upon studies using direct techniques, such as microscopy, that ~99% of bacteria establish biofilms in their natural environments (26). A number of persistent and chronic bacterial infections in humans, such as periodontis and cystic fibrosis, are associated with the ability of the bacterium to establish biofilms (28, 137). In addition, biofilms of infectious agents are well characterized to form upon biomedical devices such as prosthetics, heart valves, catheters, and contact lenses (6, 27, 28). A number of staphylococcal infections, such as osteomyelitis, are also intimately connected to the ability of the bacterium to form biofilms (70, 117). Reflective of their clinical significance, biofilms are considered to be the etiologic agents of recurrent staphylococcal infections (70, 117).

*S. aureus* biofilms are typically composed of one or more extracellular polymeric molecules (DNA, proteins, or polysaccharides) that provide structural integrity and may also facilitate intercellular adhesion (9, 29, 126, 136). The polymers interact to facilitate the formation an extracellular matrix. This matrix provides bacterial cells protection from environmental stress, innate immunity, as well as therapeutic agents (31). The polymer(s) utilized to facilitate biofilm formation can vary between staphylococcal isolates with some favoring DNA and/or proteins and others polysaccharides (9, 29, 126, 136). The complexity of biofilm formation results in this process being highly regulated and deterministic.

Biofilm formation in *S. aureus* is responsive to diverse signals including nutrient limitation and quorum sensing (9, 70, 92, 117).

Oxygen concentrations vary greatly between healthy human tissues (between 19.7 to ~1.5%; normoxia) (18). Oxygen concentrations also vary between healthy and infected or necrotic tissues, as well as in wounds, where concentrations are estimated to be below 1% (hypoxic) or anoxic (3, 18, 151). A recent study found that *S. aureus* infections in skeletal tissues (osteomyelitis) cause an ~3-fold decrease in oxygen concentrations resulting in increasing hypoxia as infection proceeds (158).

Multiple studies have focused upon the human systems that are active under hypoxia or anoxia and aid in combating bacterial infections. However, relatively little is known about how *S. aureus* mount a response to hypoxia or anoxia. A study by Cramton *et al.* found that decreased oxygen concentrations result in increased biofilm formation in *S. aureus* (30). An alternate study found that *S. aureus* growing in biofilms are starved for oxygen and that the rate of oxygen depletion is proportional to the rate of biofilm maturation (166). Cramton *et al.* also found that decreased oxygen concentrations lead to increased production of the polysaccharide intercellular adhesin (PIA); a polymer used by some *S. aureus* isolates to facilitate intercellular adhesion (30). However, the role or requirement of PIA in low oxygen biofilms is unclear since biofilm formation in a PIA deficient strain was not examined (30). It is also unclear how the lack of oxygen, a cell permeable molecule, translates into increased biofilm formation.

TCRS are modular signal transduction pathways that facilitate the integration of multiple stimuli into cellular signaling circuits, allowing for a rapid and robust response to environmental alterations (145, 146). TCRS consist of a histidine kinase (HK) and a response regulator (RR). The system input occurs at the level of the HK which is the protein that interacts with the stimuli. The stimuli can be either intracellular or extracellular, and the HK itself can be either membrane associated or cytosolic. HKs can have one or more of the following functionalities: they can undergo autophosphorylation, transfer phosphoryl groups to the RR or remove phosphoryl groups from the RR. Interaction with a signal molecule alters the functionality of the HK thereby effecting changes in the levels of the phosphoryl group upon the RR. The levels of phosphoryl groups upon the RR at any given point determine whether system output is increased or decreased. In the case of DNA binding RR's, changes in the phoshporyl levels alter the affinity of the protein for DNA leading to changes in gene transcription and a tailored physiological response (145, 146).

The goal of this study was to examine the mechanisms by which oxygen affects *S. aureus* biofilm formation. Data presented show that oxygen impacts biofilm formation in its capacity as a TEA in cellular respiration. Consequently, growth conditions that diminish respiration elicit increased biofilm formation. Impaired respiration leads to increased cell lysis via increased expression of the AltA murein hydrolase and a concomitant decrease in the expression of wall-teichoic acids. The regulatory tuning of these two processes in a divergent manner effects cell lysis. Increased biofilm formation and cell lysis is a

programmed mechanism that is governed by the SrrAB TCRS. Genetic evidence suggests that SrrAB-dependent biofilm formation occurs in response to the accumulation of reduced menaquinone.

**Results:**

***S. aureus* forms robust biofilms in the absence of oxygen**. The influence of anaerobiosis upon biofilm formation of *S. aureus* was examined. Regulatory networks integral to staphylococcal physiology differ between *S. aureus* isolates (61, 106). Biofilm formation was examined in diverse *S. aureus* isolates that vary in their ability to form biofilms (LAC, SH1000, MW2, N315). Strains were cultured aerobically, with a seal that allows free diffusion of gases, or anaerobically (in a COY anaerobic chamber equipped with an oxygen scavenging catalyst, $O_2$ <1 ppm) prior to quantifying biofilms. Biofilm formation increased substantially for each strain during anaerobic growth (between ~4-30 fold) (Figure 2.1A and 2.1B). Unless specifically mentioned, the experiments described henceforth were conducted using the community-associated MRSA strain LAC (hereafter wild-type; WT).

**Oxygen influences biofilm formation in its capacity as a terminal electron acceptor for cellular respiration.** The principal influence of oxygen upon staphylococcal physiology is achieved in its capacity as a TEA for respiration. Increased biofilm formation during anaerobic growth occurred upon culture in a medium lacking a TEA (fermentative growth). We tested the hypothesis that

impaired respiration is a signal that elicits biofilm formation. In addition to oxygen, *S. aureus* can utilize nitrate as a TEA. Anaerobic biofilm formation decreased, as the concentration of nitrate provided in the medium was increased (Figure 2.1C). The addition of nitrate to aerobic cultures did not significantly alter biofilm formation (Figure 2.1C).

We reasoned that strains incapable of respiration would display increased biofilm formation. Heme auxotrophs have non-functional terminal oxidases and are unable to respire. They form small colonies when cultured in the presence of oxygen, and therefore are termed small colony variants (SCV) (54). A *hemB::Tn* strain formed considerably more biofilm than the WT when cultured aerobically, but displayed biofilm formation similar to the WT when cultured fermentatively (Figure 2.1D). Likewise, nitrate supplementation did not decrease anaerobic biofilm formation in a nitrate reductase (*narG::Tn*) mutant, which is unable to utilize nitrate as a TEA (Figure 2.1E) (14, 134). To further test our premise, biofilm formation was examined in the WT cultured aerobically with varying amounts of the respiratory poison sodium azide. Biofilm formation increased in synchrony with the concentration of sodium azide in the growth medium (Figure 2.1F).

From Figure 2.1 we concluded that decreased cellular respiration results in increased biofilm formation. Further, biofilm formation was responsive to the concentration of a TEA or the ability of cells to respire.

**Impaired respiration leads to AtlA dependent release of DNA and cytosolic proteins facilitating biofilm formation.** We sought to understand the mechanisms underlying the formation of fermentative biofilms. We examined the dependence of fermentative biofilms upon one or more of the described structural polymers: PIA, high-molecular weight extracellular DNA (eDNA), or proteins (9, 29, 41, 126, 136). The *icaABCD* operon encodes for proteins required to biosynthesize PIA (29). Strains lacking functional IcaA, IcaB, or IcaC were not attenuated in fermentative biofilm formation, suggesting that PIA is dispensable for this phenotype (Figure 2.S1). However, supplementation of the growth medium with DNase, which degrades DNA, substantially attenuated biofilm formation suggesting that DNA is an integral component of fermentative biofilms (Figure 2.2A). Consistent with this theory, the accumulation of eDNA increased appreciably in the matrix of fermenting biofilms (Figure 2.2B).

Prevailing models suggest that eDNA in staphylococcal biofilms arises as a consequence of a self digestive cell-lysis process (autolysis), which results in the release of eDNA (41, 126). Polyanethole sulfonate (PAS) inhibits *S. aureus* autolysis (155, 160). Supplementing growth media with PAS diminished fermentative biofilm formation (Figure 2.S2).

Peptidoglycan (murein) cleavage would be necessary for autolysis. The *S. aureus* genome encodes multiple murein hydrolases (43, 110). Fermentative biofilm formation was examined in a set of strains that each lacked one predicted murein hydrolase. One strain, with a disruption in the gene encoding for the AtlA murein hydrolase (*atlA::Tn*), was attenuated in biofilm formation (Figure 2. S3).

AtlA has been previously implicated to be required for biofilm formation during aerobic growth (8, 12, 64). The *atlA::Tn* strain displayed decreased biofilm formation in the presence of oxygen (~1-fold decrease) and this phenotype was exacerbated (~10-fold decrease) in fermenting cultures (Figure 2.2C) suggesting that the role of AtlA in biofilm formation is increased during fermentative growth. Moreover, eDNA accumulation was greatly decreased in the biofilm matrix of the fermentatively cultured *atlA::Tn* strain (Figure 2.2D).

A recent study found that cytosolic proteins form a significant portion of staphylococcal biofilm matrixes (41). AtlA has been implicated in the release of cytosolic proteins into the extracellular milleu (120). The supplementation of media with proteinase K, which degrades proteins, attenuated fermentative biofilm formation, suggesting that in addition to eDNA, proteins also form an integral part of the biofilm matrix in fermenting cells (Figure 2.2E). To further examine this, the activity of catalase (Kat), an abundant intracellular protein (24), was measured in the spent media supernatants (104). The spent media supernatant from fermenting WT had ~5-fold increased Kat activity relative to aerobically cultured WT (Figure 2.S4). Kat activity was decreased by ~5-fold in the spent media supernatant from the fermentatively cultured *altA::Tn* strain (Figure 2.2F). These data were normalized to intracellular Kat activity to negate for potential changes in Kat expression.

From Figures 2.2 and Figure 2.S 1-4 we concluded that fermenting cells release an increased quantity of DNA and cytoplasmic proteins, into their

extracellular milleu, in an AtlA-dependent manner. The eDNA and proteins are incorporated into the biofilm matrix and contribute to biofilm formation.

**Impaired respiration elicits increased expression of AtlA and alterations that make cells more amenable to cleavage by AtlA.** Three scenarios could underlie the increased role of AtlA in fermentative biofilm formation. First, the expression of AtlA is increased leading to increased autolysis. Second, cell walls are altered in order to make them more amenable to AtlA-dependent lysis. Third, a combination of scenarios one and two. To discern which of these scenarios is operative in fermenting cells, the abundance of the *atlA* transcript was assessed in WT cultured aerobically or fermentatively. The *atlA* transcript was increased ~5-fold upon fermentative culture (Figure 2.3A). Subsequently, AtlA activity was examined within the context of intact whole cells using autolysis assays (12). Fermentatively cultured WT cells underwent autolysis faster than those cultured aerobically. The *atlA::Tn* strain, cultured aerobically or fermentatively, was severely deficient in undergoing autolysis suggesting that AtlA was the dominant murein hydrolase contributing to autolysis under the growth conditions examined (Figure 2.3B).

Murein hydrolase assays were used to quantify AtlA-dependent bacteriolytic activity. The WT and *atlA::Tn* strains were cultured aerobically or fermentatively, cell-wall associated proteins were detached (hereafter CW-extracts), and bacteriolytic activity was examined using heat-killed *Micrococcus luteus* as a substrate. CW-extracts from fermenting WT lysed *M. luteus* more

rapidly than CW-extracts from WT cultured aerobically (Figure 2.3C). Bacteriolytic activity was nearly undetectable when using CW-extracts from the *atlA::Tn* strain cultured aerobically or fermentatively. These data confirmed that AtlA was the dominant murein hydrolase in the extracts and increased AtlA activity was associated with the WT cultured fermentatively (Figure 2.3C).

We next examined whether cell walls were altered in order to make them more amenable to AtlA. The WT strain was cultured aerobically or fermentatively, heat-killed to inactivate native autolysins, and the cells were subsequently provided as substrates for murein hydrolase assays. AtlA is a bifunctional enzyme that is proteolytically cleaved into a N-acetylmuramyl-L-alanine amidase (AM) and endo-β-N-acetylglucosaminidase (GL) ((116) and illustrated in Figure 2.S5). The use of *M. luteus* and *S. aureus* cells as substrates allows for differentiation between AM and GL activities (116, 153). GL displays poor activity against *S. aureus*, but is capable of cleaving *M. luteus*. Murein hydrolase assays were conducted using CW-extracts obtained from a Δ*atlA* strain carrying empty vector or plasmids encoding for full length AtlA (p*atlA*), AM only (p$atlA_{AM}$) and GL only (p$atlA_{GL}$) (12). Lysis of heat-killed *S. aureus*, as well as *M. luteus*, was undetectable with CW-extracts from the Δ*atlA* strain carrying empty vector verifying that bacteriolytic activity under the conditions examined was dependent upon AtlA, AM, or GL (Figure 2.3D). CW-extracts from the Δ*atlA* strain carrying p$atlA_{GL}$ did not lyse *S. aureus*, but proficiently lysed *M. luteus*, confirming that *S. aureus* are poor substrates for GL (Figure 2.3E). CW-extracts from the Δ*atlA* strain carrying p*atlA* or p$atlA_{AM}$ lysed fermentatively cultured heat-killed WT at a

faster rate than aerobically cultured WT, suggesting fermenting *S. aureus* cells are more amenable to cleavage by AtlA and AM (Figure 2.3F-G).

**Decreased expression of wall-teichoic acids in fermenting cells increases their amenability towards cleavage by AtlA.** Wall-teichoic acids (WTA) are cell-surface glycopolymers that are covalently attached to peptidoglycan. The biosynthetic pathway for WTA in *S. aureus* is illustrated in Figure 2.4A. WTA negatively modulate AtlA activity (7, 133). Decreased expression of WTA during fermentative growth could result in cells that are more amenable to AtlA-dependent lysis. Consistent with this logic, the transcription of genes encoding for proteins in the WTA biosynthetic pathway (*tarA*, *tarO*, *tarB*, *tarH*) was decreased during fermentative growth (between 6-50 fold) (Figure 2.4B).

Tunicamycin is an inhibitor of TarO and MnaA, which are necessary for WTA biosynthesis (Figure 2.4A) (16, 55, 96). *S. aureus* cultured in the presence of tunicamycin do not synthesize WTA (16). WT was cultured aerobically or fermentatively in the presence or absence of tunicamycin, the cells were heat-killed, and used as substrates in murein hydrolase assays. WT cells cultured aerobically with tunicamycin were lysed at a rate similar to that of fermentatively cultured cells by CW-extracts from a Δ*atlA* strain carrying either p$atlA_{AM}$ or p*atlA*. This confirmed that changes in WTA expression alter the amenability of fermenting cells to cleavage by AtlA and AM (Figure 2.S6A and 2.S6B).

Two models have been proposed to explain the influence of WTA upon AtlA activity. Schlag *et al.* found that the presence of WTA interferes with the

binding of AtlA to the cell surface (133). Biswas *et al.* found that WTA contributes to proton binding on the cell surface. AtlA activity decreases substantially below pH 6.5 (7), and therefore, it was proposed that binding of protons by WTA leads to a decrease in the local pH of the cell surface thereby inhibiting AtlA activity (7). We examined the contribution of these two mechanisms in the lysis of fermenting *S. aureus*.

First, the effect of proton binding by WTA upon AtlA activity was examined by decreasing the pH of the murein hydrolase and autolysis assays. We reasoned that an increased concentration of protons would exacerbate the effect of proton binding by WTA. Under this scenario, cells containing an increased abundance of WTA would be expected to be resistant towards AtlA dependent cleavage at decreased pH. Consistent with this premise, AtlA-dependent lysis of heat-killed WT was dramatically decreased in murein hydrolase assays conducted at a pH of 5 (Figures 2.4C and Figure 2.S6A and 2.S6B). Importantly, lysis of fermenting WT cells was still observed while it was nearly absent for those cultured aerobically (Figure 2.4C). In contrast, lysis rates for tunicamycin treated WT were unaltered upon decreasing the pH (Figures 2.4C, Figure 2.S6 and Figure 2.S7), confirming that the influence of pH upon AtlA activity was observed entirely as a result of alterations in WTA expression. The results from autolysis assays conducted at pH 5 lent further support to the findings of the murein hydrolase assays (Figure 2.4D). Strikingly, autolysis was abrogated in aerobically cultured WT, while fermentatively cultured cells or those cultured in

the presence of tunicamycin underwent proficient AtlA-dependent autolysis (Figure 2.4D).

Second, we examined whether fermenting WT bind an increased amount of AtlA and whether this is dependent upon WTA expression (42). Various heat-killed cells were incubated at pH 5 with CW-extract from a Δ*atlA* strain carrying a plasmid encoding for full length AtlA (p*atlA*). The cells were subsequently removed, and the bacteriolytic activity remaining in the supernatants was quantified using heat-killed *M. luteus* cells as substrate. Aerobically or fermentatively cultured heat-killed WT cells did not bind bacteriolytic enzymes while tunicamycin treated cells bound a majority of the bacteriolytic enzymes (Figure 2.4E). We concluded that the complete loss of WTA expression does indeed increase binding of AtlA to the cell surface confirming and extending the findings of Schlag *et al.* (133). However, altered AtlA binding to WTA was unlikely to underlie the increased lysis of fermenting cells.

From Figures 2.3, 2.4, and Figure 2.S6 and 2.S7, we concluded that fermenting *S. aureus* had increased expression of AtlA and concomitantly decreased expression of WTA. The combination of these two divergent responses facilitates increased autolysis. Since the changes in expression were accompanied by similar changes in transcription we concluded that impaired respiration elicits programmed cell lysis (PCL).

**Programmed cell lysis and biofilm formation in fermenting cells are governed by the SrrAB two-component regulatory system.** Respiration is predominantly mediated by membrane-associated factors. Regulatory system(s) that perceive respiratory status were likely to be membrane associated. *S. aureus* encodes for 16 TCRS. Of these, 14 are predicted to employ a membrane-associated HK. Fermentative biofilm formation was examined in strains that each lacked one individual TCR system (except WalKR, which is essential) (35, 119). A strain lacking the staphylococcal respiratory regulatory system (SrrAB) was attenuated in fermentative biofilm formation (Figure 2.5A). Reintroduction of *srrAB* into the Δ*srrAB* strain upon an episome restored fermentative biofilm formation (Figure 2.5A). Consistent with SrrAB mediated changes in biofilm formation occurring as a result of altered respiratory status, the introduction of a Δ*srrAB* mutation into a *hemB::Tn* strain attenuated the increased biofilm formation of the *hemB::Tn* strain during aerobic growth (Figure 2.5B). Unlike the WT, anaerobic biofilms formed by the Δ*srrAB* strain were largely unaltered when the growth medium was supplemented with nitrate (Figure 2.S8).

The influence of SrrAB upon the transcription of genes encoding for factors involved in PCL and biofilm formation was examined. The abundance of the *atlA* transcript was decreased (~5 fold) in the Δ*srrAB* strain (Figure 2.5C). In contrast, the abundances of transcripts corresponding to genes required for WTA biosynthesis were increased in the Δ*srrAB* strain (~2.5-5 fold).

A strain lacking SrrAB displayed phenotypes consistent with decreased expression of AtlA. The fermentative biofilm formation phenotype of the Δ*srrAB*

*atlA::Tn* strain was similar to that of the *atlA::Tn* strain, suggesting that SrrAB influences biofilm formation, in part, via AtlA (Figure 2.5D). Moreover, the Δ*srrAB* strain was deficient in autolysis (Figure 2.5E) and had decreased accumulation of eDNA in its biofilm matrix when cultured fermentatively (Figure 2.5F). To further examine the influence of AtlA upon SrrAB-dependent biofilm formation we introduced multicopy plasmids with alleles encoding for either full length AtlA (p*atlA*) or an enzymatically inactivated AM (p$atlA_{AM\ H263A}$) into the Δ*srrAB* strain and examined biofilm formation. The presence of p*atlA* partially suppressed the fermentative biofilm formation defect of the Δ*srrAB* strain when compared to the strain carrying p$atlA_{AM\ H263A}$ (Figure 2.5G). Additionally, fermentatively cultured, heat-killed, Δ*srrAB* cells were lysed at a slower rate by CW-extracts from the Δ*atlA* strain carrying p*atlA*, consistent with increased expression of WTA in the Δ*srrAB* strain (Figure 2.5H).

**Genetic evidence suggests that SrrAB-dependent biofilm formation is responsive to the redox status of the menaquinone pool.** The cellular molecule(s) that influence SrrAB activity are unidentified. *S. aureus* synthesizes menaquinone and strains lacking menaquinone are unable to respire (154). Upon analyzing previous studies we observed that the transcription of genes positively regulated by SrrAB were reduced in a menaquinone auxotroph (77, 80, 121, 162). A *hemB* mutant is also unable to respire (54) and data presented in Figure 2.5B suggest that SrrAB activity, with respect to biofilm formation, is stimulated in

a *hemB::Tn* strain. These seemingly conflicting pieces of information could be readily explained if menaquinone is necessary for SrrAB stimulation.

We reasoned that if SrrAB activity is diminished in the absence of menaquinone then a *hemB::Tn menF::Tn* strain should phenocopy a Δ*srrAB hemB::Tn* strain for biofilm formation. Biofilm formation was examined during aerobic growth in a *hemB::Tn menF::Tn* double mutant, a Δ*srrAB hemB::Tn menF::Tn* triple mutant, as well as their parental strains. The *hemB::Tn* strain displayed increased biofilm formation relative to the *menF::Tn* strain (Figure 2.6A). Importantly, the Δ*srrAB hemB::Tn, hemB::Tn menF:Tn*, and Δ*srrAB hemB::Tn menF::Tn* strains phenocopied the biofilm formation of the *menF::Tn* strain (Figure 2.6A). These data confirmed that the presence of menaquinone is necessary for SrrAB-dependent biofilm formation in a *hemB::Tn* strain.

Menaquinone functions as both an electron acceptor and an electron donor in the electron transfer chain (80). Inactivation of heme biosynthesis results in defective terminal oxidases (122) and the accumulation of reduced menaquinone. We examined whether a strain enriched for oxidized menaquinone also displayed an increase in the formation of SrrAB-dependent biofilms. *S. aureus* encodes for two NADH::menaquinone oxidoreductases (NdhC and NdhF) and one succinate dehydrogenase (Sdh) (44, 135). A Δ*ndhC ndhF::Tn sdh:Tn* strain is deficient in the passage of electrons to menaquinone and consequently enriched in oxidized menaquinone. The Δ*ndhC ndhF::Tn sdh:Tn* strain displayed a negligible increase in aerobic biofilm formation (~1.4 fold increase), which was phenocopied by the Δ*srrAB* Δ*ndhC ndhF::Tn sdh:Tn* strain (Figure 2.6B).

Taken together, the data in Figure 2.6 led us to infer that with respect to biofilm formation 1) menaquinone influences SrrAB activity, 2) the absence of menaquinone results in SrrAB being non-responsive, 3) SrrAB activity is increased upon enrichment of reduced menaquinone, and 4) SrrAB is non-responsive to the enrichment of oxidized menaquinone.

**Discussion:**

Biofilms are the etiologic agents of recurrent staphylococcal infections. Previous work found that hypoxic growth results in increased biofilm formation of *S. aureus*. However, the molecular and regulatory mechanism(s) translating the lack of oxygen into biofilm formation were unknown. We report that oxygen impacts biofilm formation in its capacity as a TEA for cellular respiration. Consistent with this premise, supplementing the growth medium with the alternate TEA nitrate decreased biofilm formation during anaerobic growth. Moreover, genetic or chemical inhibition of respiratory processes resulted in increased biofilm formation even in the presence of a TEA. TEA availability in the natural microenvironments of *S. aureus* varies leading to the supposition that biofilm formation would be responsive to the concentration of TEA. Consistent with this logic, biofilm formation was titratable with respect to the concentration of a TEA or a molecule that inhibits respiration.

Fermenting biofilms were dependent upon the presence of high molecular weight DNA. High molecular weight DNA in *S. aureus* biofilm matrixes (eDNA) has been shown to originate from genomic DNA, and thus, its presence suggested that fermenting cells undergo increased autolysis (126). Lending support to this concept, fermentative biofilm formation was attenuated upon chemical inhibition of autolysis or genetic inactivation of the AtlA murein hydrolase. Fermenting cells underwent increased autolysis in a AtlA-dependent manner and the matrix from the *atlA::Tn* strain had nearly undetectable levels of eDNA. *S. aureus* biofilms incorporate cytosolic proteins into their matrixes and

AtlA has been implicated in the release of cytosolic proteins via a process that is not completely understood (41, 120). We found that fermenting cells had increased activity for a cytosolic protein in the extracellular milleu and an *atlA::Tn* strain was deficient in the release of this protein. Fermenting biofilms were also readily disrupted upon supplementing media with proteinase K suggesting that, in addition to eDNA, proteins are integral components of the fermentative biofilm matrix.

The increased role of AtlA in fermenting biofilms was due to a combination of two divergent cellular responses. First, fermenting cells increased the transcription of *atlA* and autolysis and murein hydrolase assays confirmed that this was translated into increased AtlA activity. Second, fermenting WT cells that had been heat-killed displayed an increased amenability to AtlA-dependent cleavage when used as substrates in murein hydrolase assays. These findings suggested that the cell surface was being altered to facilitate cell lysis. Wall-teichoic acids are cell surface glycopolymers that are covalently attached to peptidoglycan and negatively impact AtlA activity (7, 133). The transcription of WTA biosynthesis genes was decreased during fermentative growth. Autolysis and murein hydrolase assays, as well as the WTA synthesis inhibitor tunicamycin, confirmed that WTA expression was decreased during fermentative growth. Since two cellular processes are divergently modulated at the transcriptional level in response to an environmental stimulus (TEA availability) to affect autolysis, we propose that this process be termed as programmed cell lysis, which is illustrated in our working model shown in Figure 2.7.

The cell walls of gram-positive bacteria have been long recognized to serve as proton reservoirs (15, 79). The walls of respiring cells have a low pH and calculations estimate that the local pH can decrease by 3-4 units (15, 79). Further, energy-limiting conditions, such as fermentative growth, or proton trapping, influence bacterial autolysis (69, 74). Thus, it has been clear that cell wall composition, the localized pH of the cell wall, and cellular autolysis are interconnected. However, the mechanisms underlying these interconnections have remained elusive. A recent study by Biswas *et al*. shed light on these processes in *S. aureus* (7). Biswas *et al*. found that WTA traps protons at the cell surface and they proposed that this results in decreased pH of the microenvironment, and thereby, inhibits AtlA activity (7). We found that the influence of pH upon AtlA activity, in both murein hydrolase, as well as autolysis assays, was almost entirely as a result of alterations in WTA expression. These findings both confirm and extend the model put forth by Biswas *et al.* (7). An alternate study by Schlag *et al.* proposed that WTA negatively affects AtlA activity by interfering with its binding to the cell surface (133). We found that at a pH of 5, tunicamycin treated cells bound a majority of the bacteriolytic activity corresponding to AtlA. In contrast, binding was absent in cells not treated with tunicamycin, regardless of whether they were cultured aerobically or fermentatively. Thus, our findings also confirmed and extended the findings of Schlag *et al*. However, the complete absence of WTA synthesis is unlikely to be a phenomenon that would be physiologically encountered. Therefore, in fermenting *S. aureus*, where the final pH of the culture medium is ~5, we propose

that the model of Biswas *et al*. would dominate with respect to autolysis and biofilm formation.

Acidic pH has long been recognized to elicit biofilm formation in *S. aureus* (124). However, the mechanisms underlying this phenotype have been unclear. Recently, Foulston *et al.* found that cytoplasmic proteins released into the extracellular mileu associate with the exterior of cells, in a pH-dependent and reversible manner, facilitating matrix formation (41). The association of the proteins with the cells increases with decreasing pH (41). However, Foulston *et al.* conducted their study in a medium that leads to a decrease in pH over growth (41). Thus, it was unclear whether low pH was necessary for the release of the cytoplasmic proteins. Our data suggest that low pH optimizes AtlA activity and thereby effects the release of the cytoplasmic proteins, extending the findings of Foulston *et al.* Further, the physiological condition(s) under which this mechanism would be relevant was not entirely clear. In the present study we demonstrate that this mechanism is pertinent in the context of an environmental signal (oxygen) that is crucial in infection progression. Finally, we note that the pH in the nares and skin, which are sites colonized by *S. aureus,* is lower than the homeostatic 7.4 (157). However, to our knowledge, it is unknown if low pH contributes to *S. aureus* colonization *in vivo*.

Respiration is a process mediated predominantly by membrane associated cellular factors. A strain lacking the SrrAB TCRS, consisting of a transmembrane HK (SrrB) (121), was attenuated in biofilm formation. A strain lacking SrrAB had decreased transcription of *atlA*, increased transcription of

WTA biosynthesis genes, and displayed multiple phenotypes consistent with the transcriptional data. Further, the biofilm deficient phenotype of the Δ*srrAB* strain was partially suppressed by the introduction of *atlA* in multicopy. These data suggest that SrrAB influences PCL and biofilm formation by divergently influencing AtlA and WTA expression.

SrrAB output was previously shown to be altered under conditions of hypoxia and nitric oxide stress (77). However, the cellular molecule(s) that influence SrrAB activity are unidentified. We found that SrrAB-dependent biofilms increased as a function of decreased respiratory activity. SrrAB-dependent biofilms were formed upon accumulation of reduced, but not oxidized menaquinone, and SrrAB output was abrogated in the absence of menaquinone. These findings suggest that 1) menaquinone is necessary for stimulus transmission to SrrAB, and 2) the oxidation state of the cellular menaquinone pool influences SrrAB output. We also considered the possibility of two alternate signals that could affect SrrAB output: culture pH and decreased proton motive force. Fermentative growth of *S. aureus* upon TSB results in the release of acidic by-products, which decrease pH of the extracellular milleu (143). Diminished respiration also decreases the proton motive force. However, heme and menaquinone auxotrophs are both deficient in respiration and the concentration of fermentative by-products and the pH in the spent media is similar in these strains ((54) and data not shown). These strains also display a similar decrease in membrane potential (54). Yet, only a heme auxotroph forms SrrAB-dependent

biofilms. Thus, we deem it unlikely that pH or alterations in proton motive force alter SrrAB activity with respect to biofilm formation.

It is worth noting the similarities that exist between the *Escherichia coli* ArcAB TCRS and SrrAB. Although these TCRS do not display significant homology, the stimuli influencing their activity are similar. ArcB is proposed to donate electrons from conserved cysteine residues to oxidized quinones resulting in silencing of kinase activity (94). Similar to ArcB, SrrB contains three conserved cysteine residues, which may facilitate redox interactions with the menaquinone pool. While this leads to the supposition that the molecular mechanism of SrrB signaling may be similar to ArcB, further biochemical analyses are required to make this conclusion. The *Bacillus subtilis* TCRS ResDE displays similarities to SrrAB and it also responds to changes in the respiratory status. However, unlike SrrB, ResE does not contain cysteine residues and studies have deemed it unlikely that the menaquinone pool influences ResDE activity (47).

Similar to *S. aureus*, *B. subtilis* increases biofilm formation under hypoxic growth and this phenotype is reversed upon supplementation with the alternate TEA nitrate (81). Biofilm formation in *B. subtilis* coincided with increased transcription of genes required for matrix production, which was mediated via the membrane-associated kinases KinA and KinB (81). *B. subtilis* ResD binds to the promoter regions or within the coding regions of *lytF* and *cwlO*, which encode for two major bacillus autolysins, suggesting it modulates the transcription of these genes (60, 66, 115, 161). Further, the binding of ResD to these DNA regions was

limited to fermentative growth (60). However, to our knowledge, it is currently unknown whether ResDE has a role in respiration dependent biofilm formation. The gram-negative bacterium *Pseudomonas aeruginosa* also increases biofilm formation under hypoxic growth and this phenotype is also reversed upon supplementation with the alternate TEA nitrate (32, 33). However, the regulatory mechanisms driving respiration dependent biofilm formation in *P. aeruginosa* are unknown. Thus, it seems likely that increased biofilm formation in response to TEA limitation is conserved among diverse bacteria. However, the genetic and regulatory bases underlying biofilm formation may differ.

Clinical isolates of *S. aureus* that are incapable of respiration, termed as SCV, display increased resistance towards antibiotics and cause persistent infections (105, 122). The SCV phenotype often, but not always, arises as a result of mutations in genes necessary for heme biosynthesis resulting in non-functional terminal oxidases (54, 122). Our finding that a heme auxotroph forms SrrAB-dependent biofilms lends considerable insight into the mechanisms that may predominate within clinical SCV strains.

While we suggest the usage of the term PCL in the context of the mechanisms outlined herein, we note that this should not be confused with the process of programmed cell death (PCD) in bacteria or in eukaryotes (75, 84, 125). Mechanistically, these are distinctly unique processes. Moreover, the morphological and biochemical markers determined in our study do not satisfy the criteria set forth by the committee on cell death (84). However, in the holistic view there are certainly intriguing parallels that are apparent between *S. aureus*

PCL and eukaryotic PCD. PCD occurs as a homeostatic measure in multicellular organisms, whereby a genetically programmed mechanism of cellular catabolism eliminates select quantities and types of cells (75, 84). PCD is crucial to a variety of processes ranging from proper cell turnover and embryonic development to the functioning of the immune system (75, 84). While PCD occurs at the cellular level and typically in a localized environment, it provides benefits at the organism level (75). Similar to PCD, our data suggest that PCL may provide bacteria with a population-level advantage by facilitating biofilm establishment, thereby imparting protection from the immune system and therapeutic agents.

Respiration in eukaryotic cells relies upon using oxygen as a substrate. Similar to PCL, hypoxia or anoxia trigger PCD in eukaryotes (140, 156). PCD occurs as one of two distinct biochemical modalities: apoptosis or necrosis. Hypoxia triggered PCD manifests as a mixture of apoptosis and necrosis (140). Anoxia triggered PCD is largely an apoptotic process (156). Interestingly, anoxia-triggered PCD is dependent upon mitochondrial membrane permeabilization by the pro-apoptotic Bcl-2 family proteins Bax and Bak (86, 156). Recent evidence suggests that Bax and Bak function as holin-like proteins and facilitate the formation of oligomeric membrane pores (86, 118). *S. aureus* also encodes for two holin-like proteins termed CidA and LrgA (123). The *cid* operon genes, *cidA* and *cidB* have been implicated in programmed cell death in aerobically cultured cells (21). CidA was previously proposed to have role in cell lysis (126). This role was predicated upon the phenotype of a *cidA* mutant; however, recent studies suggest that this was likely an outcome of a secondary mutation (21, 126). In our

hands, *cidA::Tn*, *cidB::Tn*, and *lrgA::Tn* strains were not attenuated in fermentative biofilm formation, suggesting a functional separation of the *S. aureus* PCD and PCL pathways, with respect to biofilm formation (data not shown).

In summary, we report that oxygen impacts *S. aureus* biofilm formation in its capacity as a TEA. Decreased respiration results in PCL via increased expression of AtlA and decreased expression of WTA. These processes are governed by the SrrAB TCRS and evidence suggests this occurs in response to the accumulation of reduced menaquinone. The AtlA-dependent release of cytosolic components facilitates biofilm formation.

**Material and Methods:**

**Materials**. Restriction enzymes, quick DNA ligase kit, deoxynucleoside triphosphates, and Phusion DNA polymerase were purchased from New England Biolabs. The plasmid mini-prep kit, gel extraction kit and RNA protect were purchased from Qiagen. DNase I was purchased from Ambion. Lysostaphin was purchased from Ambi products. Oligonucleotides were purchased from Integrated DNA Technologies and sequences are listed in Table 2.S1. Trizol and High-Capacity cDNA Reverse Transcription Kits were purchased from Life Technologies. Tryptic Soy broth (TSB) was purchased from MP biomedical. Unless otherwise specified all chemicals were purchased from Sigma-Aldrich and were of the highest purity available.

**Bacterial growth conditions.** Unless otherwise stated, the *S. aureus* strains used in this study (Table 2.1) were constructed in the community-associated *S. aureus* USA300 LAC strain that was cured of the native plasmid pUSA03 that confers erythromycin resistance (10). Overnight cultures of *S. aureus* were grown at 37 °C in 10 mL culture tubes containing 1 mL of TSB or 30 mL culture tubes containing 5 mL TSB. Difco BiTek agar was added (15 g $L^{-1}$) for solid medium. When selecting for or against plasmids, antibiotics where added to the following concentrations: 150 μg $mL^{-1}$ ampicillin; 30 μg $mL^{-1}$ chloramphenicol (Cm); 10 μg $mL^{-1}$ erythromycin (Erm); 3 μg $mL^{-1}$ tetracycline (Tet); kanamycin, 125 μg $mL^{-1}$ (Kan); anhydrotetracycline 150 ng $mL^{-1}$.

*Growth model to assess biofilm formation.* Aerobic, overnight cultures, were diluted into fresh TSB and incubated statically at 37 °C. For aerobic growth, the cultures were grown in 96-well microtiter plates containing 200 µL in each well or six-well plates containing 6 mL in each well and were covered with an Aera seal (Excel scientific), which allowed for uniform gas exchange. For anaerobic growth, cultures were inoculated aerobically followed immediately by passage through an airlock (3 vacuum/gas exchange cycles) into a COY anaerobic chamber equipped with a catalyst to maintain oxygen concentrations below one ppm. Anaerobic growth in the presence of a TEA was achieved by supplementing the media with sodium nitrate (prepared fresh daily).

**Recombinant DNA and genetic techniques.** *E. coli* DH5α was used as a cloning host for plasmid construction. All clones were passaged through RN4220 (82) and subsequently transduced into the appropriate strains using bacteriophage 80α (111). All *S. aureus* mutant strains and plasmids were verified using PCR, sequencing of PCR products or plasmids (Genewiz, South Plainfield, NJ), or genetic/chemical complementation of phenotypes.

**Construction of mutant strains and plasmids.** The erythromycin resistance cassette in a *menF::Tn* (*ermB*) strain was exchanged to a tetracycline resistance cassette as described earlier, with minor changes (11). The *menF::Tn* (*ermB*) strain was transduced with the pTnTet plasmid and Tet resistance was selected at 30°C. A single colony was used to inoculate 5 mL of TSB medium and cultured

with shaking overnight at 30 °C in the presence of Cm. To initiate recombination, cells from the overnight culture were spread onto a TSB agar plate containing Tet and incubated at 42 °C (replication non-permissive). Single recombinants were inoculated into 5 mL of TSB and incubated at 30 °C in the absence of antibiotic to promote recombination and plasmid loss. These overnights were re-diluted 1:1000 fold into TSB medium containing 30 ng $mL^{-1}$ of Atet and cultured overnight at 30 °C. The overnight culture was diluted of 1:50,000 before plating 20-100 µL onto TSA containing Atet to select against plasmid containing cells. Colonies were screened by replica plating for Cm sensitivity and Tet resistance. The resultant strain, once reconstructed, was verified to be deficient in menaquinone biosynthesis by chemical complementation using menaquinone-4 (MK4). Where mentioned, strains interrupted in *hemB* were verified using chemical complementation by supplementing growth medium with hemin.

The Δ*ndhC::tetM* strain was constructed as described earlier (102). The pJB38_Δ*srrAB::tet* plasmid was created by using PCR to amplify the *tetM* allele from strain JMB1432 using primers G+tetMluI and G+tetNheI. The PCR product was digested with MluI and NheI and ligated into similarly digested pJB38_Δ*srrAB* (pJB38_Δ*srrAB::tetM*) (71). The Δ*srrAB*::*tetM* strain was created as outlined above.

The pLL39_*srrAB* plasmid, containing *srrAB* under the transcriptional control of their native promoter, was constructed using yeast recombinational cloning as previously described (71, 100, 103). Amplicons were generated using the following primer pairs: pLL39_yeastF and yeast_srrProR, yeast_srrProF and

srrAB_pLL39R. The *srrAB* alleles and the upstream promoter region were amplified from the LAC chromosome and the pLL39 vector was linearized using SalI. The resultant pLL39_*srrAB* plasmid was integrated as an episome into the chromosome of the Δ*srrAB* strain (JMB1467).

**Static model of biofilm formation.** Biofilm formation was examined as described earlier, with minor changes (99). Overnight cultures were diluted into fresh TSB to a final optical density of 0.05 ($A_{590}$). 200 µL aliquots of diluted cultures were added to the wells of a 96-well microtitre plate (Corning 3268) and the plate was subsequently incubated statically at 37 °C for 22 hours. Prior to harvesting the biofilm, the optical density ($A_{590}$) of the cultures was determined. The plate was subsequently washed twice with water, biofilms were heat fixed at 60 °C, and the plates were allowed to cool to room temperature. The biofilms were stained with 0.1% crystal violet, washed thrice with water, destained with 33% acetic acid and the absorbance of the resulting solution was recorded at 570 nm, standardized to an acetic acid blank, and subsequently to the optical density of the culture upon harvest. Finally, the data were normalized with respect to the WT or as described in the figure legends to obtain relative biofilm formation.

**Quantitative real-time PCR assays.** Biofilms were cultured in the presence or absence of oxygen for eight hours. At point of harvest the spent medium was discarded and the remaining culture was immediately resuspended in RNAProtect reagent (Qiagen) and treated according to manufacturer instructions. The treated culture was subjected to centrifugation, the supernatant was discarded, and the cell pellet was resuspended in RNase free 50 mM Tris, pH 8. Cell-free extracts were generated using bead beating. RNA was extracted using Trizol, as per manufacturer instructions. Downstream treatments of the purified RNA and construction of cDNA libraries was as described earlier (102). Primers for PCR were designed manually or using the Primer Express 3.0 software from Applied Biosystems. Quantitative real time PCR reactions (Table 2.S1) were conducted as described earlier (102).

**Quantification of high-molecular weight extracellular DNA.** eDNA was analyzed as described earlier with some changes (73). Overnight cultures were diluted into TSB to a final optical density of 0.05 ($A_{600}$) in a final volume of 6 mL per well of a six-well plate. The cultures were incubated statically at 37 °C for 22 hours. At point of harvest, the spent media supernatant was aspirated out of each well. One mL of 1X phosphate buffered saline (PBS) was immediately added to the wells and a cell scraper was used to transfer the contents to an eppendorf tube. The biomass was pelleted by centrifugation and the supernatant was removed by aspiration. The pellets were thoroughly resuspended in 1X PBS and vortexed for 5 minutes using a Vortex Genie 2 (Scientific Industries) at the

highest speed possible using a vertical micro-tube adapter. Aliquots were removed for determination of the viable cell count (colony forming units) and samples were pelleted by centrifugation. Control experiments verified that the viable cell counts were not affected by the vortexing procedure (data not shown). Equal volumes of the supernatants were assessed for the presence of high molecular weight DNA (>10 kilobases) using agarose gel electrophoresis. To assess the eDNA in a semi-quantitative manner, the gels were photographed and the bands were subjected to density analysis using Image J software. For each sample, the spot densities were normalized to the viable cell count (colony forming units) and subsequently as mentioned in the figure legends.

**Cytoplasmic protein release assays.** Strains were cultured as described under eDNA analyses. The samples were vortexed briefly, biomass was transferred into a microcentrifuge tube, and cell pellets and spent media supernatants were partitioned by centrifugation. The spent media supernatant was retained for further analyses. The cell pellets were resuspended in lysis buffer (50 mM Tris, 150 mM NaCl, 4 µg lysostaphin, 8 µg DNAse, pH 7.5) and incubated at 37 °C until confluent lysis was observed. Cell lysates were clarified using centrifugation to obtain cell-free extracts. Catalase (Kat) activity was assayed, in both the cell-free extracts as well as spent medium supernatants as described elsewhere (4, 99). The ratio of extracellular to intracellular Kat activity was utilized to determine protein release. In control experiments, Kat activity was undetectable in a *katA::Tn* strain (data not shown).

**Whole cell autolysis assays.** Overnight cultures were diluted into TSB to a final optical density of 0.05 ($A_{600}$) and cultured for four hours. Whole cell autolysis assays were conducted as described elsewhere with minor changes (12). Briefly, the cultures were harvested by centrifugation, cell pellets were washed twice, and resuspended in autolysis buffer (50 mM HEPES, 150 mM NaCl, 0.05% Triton X-100, pH 7.5). For analyses conducted at pH 5, HEPES was replaced with 0.2 M sodium acetate buffer and all other components remained unaltered. The cell suspensions were then incubated at 37 °C with shaking and optical densities were recorded periodically.

**Murein hydrolase assays.** Biofilms were cultured for four hours and cells were harvested as mentioned under eDNA analyses. Thereafter, CW-extracts were prepared and murein hydrolase activity determined as described elsewhere with minor changes (95). Briefly, cell pellets were washed and CW-extracts were prepared by resuspension in 3 M lithium chloride and incubation for 25 minutes (95). Protein concentrations of the extracts were determined and between 0.1-0.5 µg of an individual extract was combined with heat-killed cell substrates (0.35 optical density ($A_{600}$)) in assay buffer (50 mM Hepes, 150 mM NaCl, 0.01% Triton X-100, pH 7.5). For analyses conducted at pH 5, HEPES was replaced with 0.2 M sodium acetate and all other components remained unaltered. Samples were incubated with shaking at 37 °C and optical densities were recorded periodically. Binding assays were conducted as earlier (42).

**Figure 2.1**

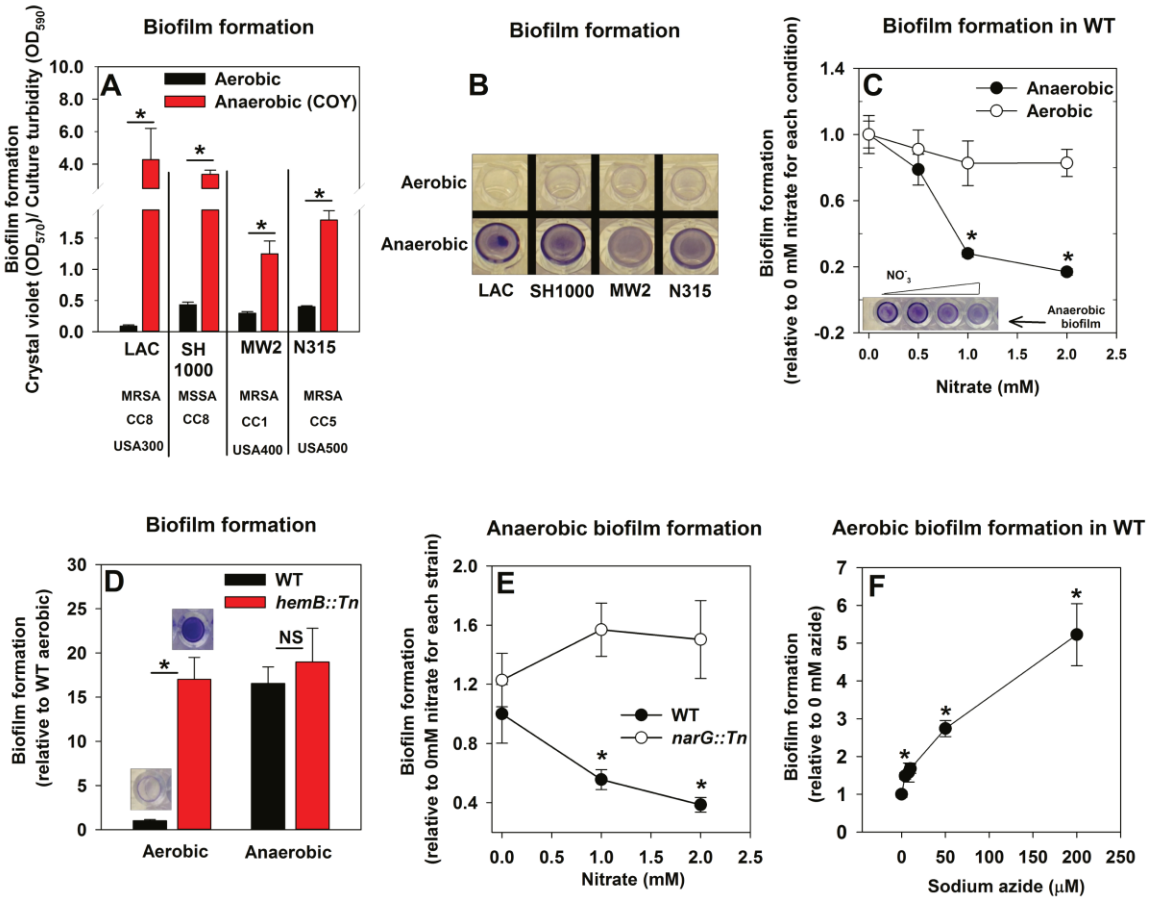


**Figure 2.1. Oxygen impacts biofilm formation in its capacity as a terminal electron acceptor.** Panels A and B; Anaerobic growth elicits increased biofilm formation in multiple *S. aureus* isolates. Biofilm formation of the LAC (JMB1100; hereafter wild-type (WT)), SH1000 (JMB 1323), MW2 (JMB1324) and N315 (JMB 7570) isolates following aerobic or anaerobic growth is displayed. MRSA denotes methicillin resistance, MSSA denotes methicillin sensitivity, CC denotes clonal complex type and the USA number denotes the pulsed-field gel electrophoeresis type. Panel C; Supplementing growth media with the alternate TEA nitrate results

in decreased biofilm formation during anaerobic growth. Biofilm formation for WT following aerobic or anaerobic growth and in media containing between 0-2 mM sodium nitrate is displayed. Panel D; A strain incapable of respiration upon oxygen forms increased biofilms when cultured aerobically, but not fermentatively. Biofilm formation for the WT and *hemB::Tn* (JMB6037) strains following aerobic or anaerobic growth is displayed. Panel E; Nitrate supplementation does not decrease anaerobic biofilm formation in a nitrate reductase mutant. Biofilm formation for the WT and *narG::Tn* (JMB7277) strains following anaerobic growth and in media containing between 0-2 mM sodium nitrate. Panel F; Chemical inhibition of respiration elicits increased biofilm formation during aerobic growth. Biofilm formation for the WT following aerobic growth in media supplemented with 0-250 µM sodium azide. The data represent the average values of eight wells (Panels A, C-E) or quadruplicates (Panel F) and error bars represent standard deviations. Representative photographs of biofilms formed upon the surface of a 96-well microtiter plate and stained with crystal violet are displayed in Panel B or insets in Panel C and D. Error bars are displayed for all data, but on occasion may be too small to see. Statistical significance was calculated using a two-tail Student's t-test and p-values >.05 were considered to be not significant while * indicates p-value of <.05.

**Figure 2.2**

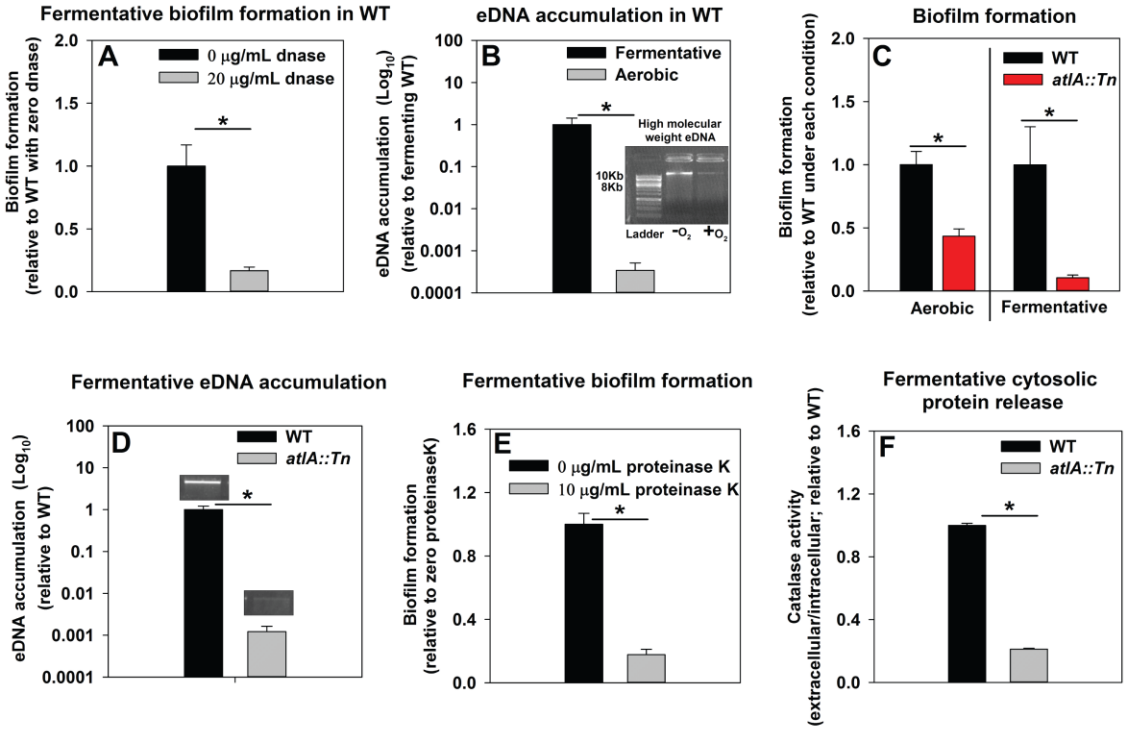


**Figure 2.2. Impaired respiration results in AtlA-dependent release of high molecular weight DNA, cytoplasmic proteins and an increase in biofilm formation.** Panel A; Fermentative biofilm formation is attenuated upon supplementation of growth medium with DNase. Biofilm formation of the WT (JMB 1100) following fermentative growth in media with or without 20 µg/mL DNase is displayed. Panel B; High molecular weight DNA (eDNA) accumulation is increased in the biofilm matrix of fermenting cells. Biofilms of the WT were cultured aerobically or fermentatively, eDNA was extracted, and analyzed using agarose gel electrophoeresis (inset photograph). The data were normalized to the viable cell count, and thereafter, to eDNA accumulation in fermenting WT. Panel C; Fermentative biofilm formation is dependent upon the AtlA murein

hydrolase. Biofilm formation for the WT and the *atlA::Tn* (JMB 6625) strains cultured aerobically or fermentatively is displayed. Panel D; eDNA accumulation in fermenting biofilms is dependent upon AtlA. Biofilms of the WT and *atlA::Tn* strains were cultured fermentatively and eDNA accumulation assessed. The data were normalized to the viable cell count, and thereafter, to eDNA accumulation in WT. Panel E; Fermentative biofilm formation is attenuated upon supplementation of growth medium with Proteinase K. Biofilm formation for the WT following fermentative growth in media with or without 10 µg/mL Proteinase K is displayed. Panel F; Fermentative growth results in AtlA-dependent release of a cytosolic protein into the extracellular milleu. Biofilms of the WT and *atlA::Tn* strains were cultured fermentatively and the activity of the cytosolic protein catalase (Kat) was measured in the spent media supernatant. The data were normalized to intracellular Kat activity, and thereafter to WT levels. The data represent the average values of eight wells (Panels A, C and E), sextuplets (Panel B) or triplicates (Panels D and F) and error bars represent standard deviations. Representative photographs of eDNA are displayed in Panel B or inset in Panel D. Error bars are displayed for all data, but might be too small to see on occasion. Statistical significance was calculated using a two-tail Student's t-test and p-values >.05 were considered to be not significant while * indicates p-value of <.05.

## Figure 2.3

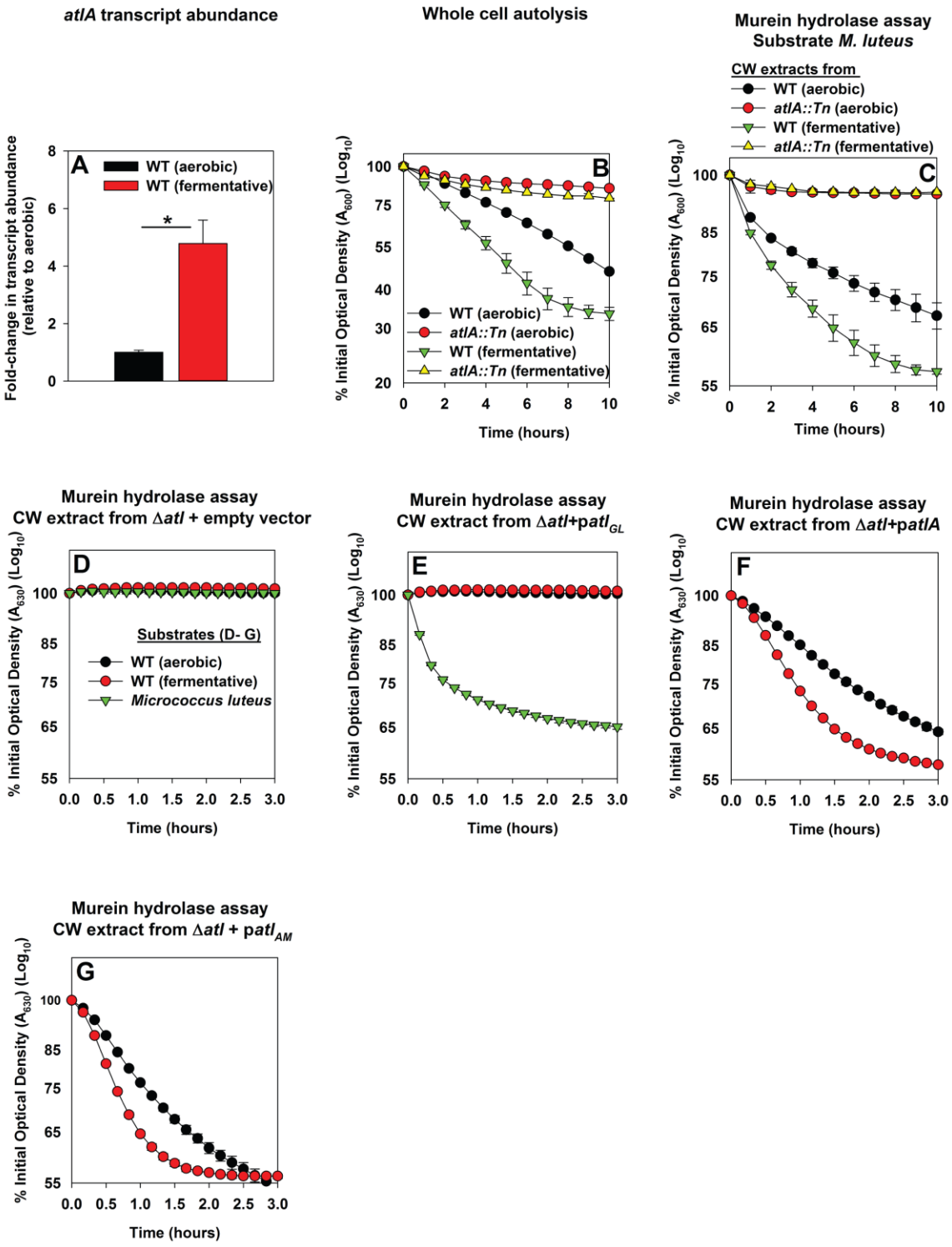
atlA transcript abundance
A
WT (aerobic)
WT (fermentative)
*
Fold-change in transcript abundance (relative to aerobic)
Whole cell autolysis
B
% Initial Optical Density (A600) (Log10)
Time (hours)
WT (aerobic)
atlA::Tn (aerobic)
WT (fermentative)
atlA::Tn (fermentative)
Murein hydrolase assay
Substrate M. luteus
CW extracts from
C
Murein hydrolase assay
CW extract from Δatl + empty vector
D
Substrates (D- G)
Micrococcus luteus
% Initial Optical Density (A630) (Log10)
Murein hydrolase assay
CW extract from Δatl+patlGL
E
Murein hydrolase assay
CW extract from Δatl+patlA
F
Murein hydrolase assay
CW extract from Δatl + patlAM
G

**Figure 2.3. Impaired respiration elicits increased expression of AtlA and alterations that make cells more amenable to cleavage by AtlA.** Panel A; The *atlA* transcript is increased upon fermentative growth. Biofilms of the WT (JMB 1100) were cultured aerobically or fermentatively, mRNA was extracted, and the abundance of the *atlA* transcript was quantified. The data were normalized to 16S rRNA levels, and thereafter, to levels observed aerobically. Panel B; Fermenting cells undergo increased autolysis in an AtlA-dependent manner. The WT and *atlA::Tn* (JMB 6625) strains were cultured aerobically or fermentatively and autolysis was examined in intact whole cells. Panel C; AtlA-dependent bacteriolytic activity is increased in fermenting cells. Murein-hydrolase activity in CW-extracts detached from the WT or *atlA::Tn* strains cultured aerobically or fermentatively is displayed (pH of 7.5). Heat-killed *Micrococcus luteus* was used as a substrate. Panel D-G; Fermenting cells are more amenable to AtlA and AM-dependent cleavage. Murein-hydrolase activity using CW-extracts detached from a Δ*atlA* strain (KB 5000) carrying plasmids encoding for empty vector control (Panel D), GL only (p$atlA_{GL}$) (Panel E), full-length AtlA (p*atlA*) (Panel F), or AM only (p$atlA_{AM}$) (Panel G) upon heat-killed cells of the WT cultured aerobically or fermentatively or *M. luteus* as substrates is displayed (pH of 7.5). The data in Panel A represent the average values of triplicates. Statistical significance was calculated using a two-tail Student's t-test and * indicates p-value of <.05. The data in Panels B-G represent the average value of technical duplicates from one set of substrate preparation, autolysis experiments, or CW extract preparations. Autolysis experiments or the preparation of heat-killed substrates or CW-extracts

were conducted on least three separate occasions and similar results were obtained. Error bars in all panels represent standard deviations. Error bars are displayed for all data, but might be too small to see on occasion.

## Figure 2.4

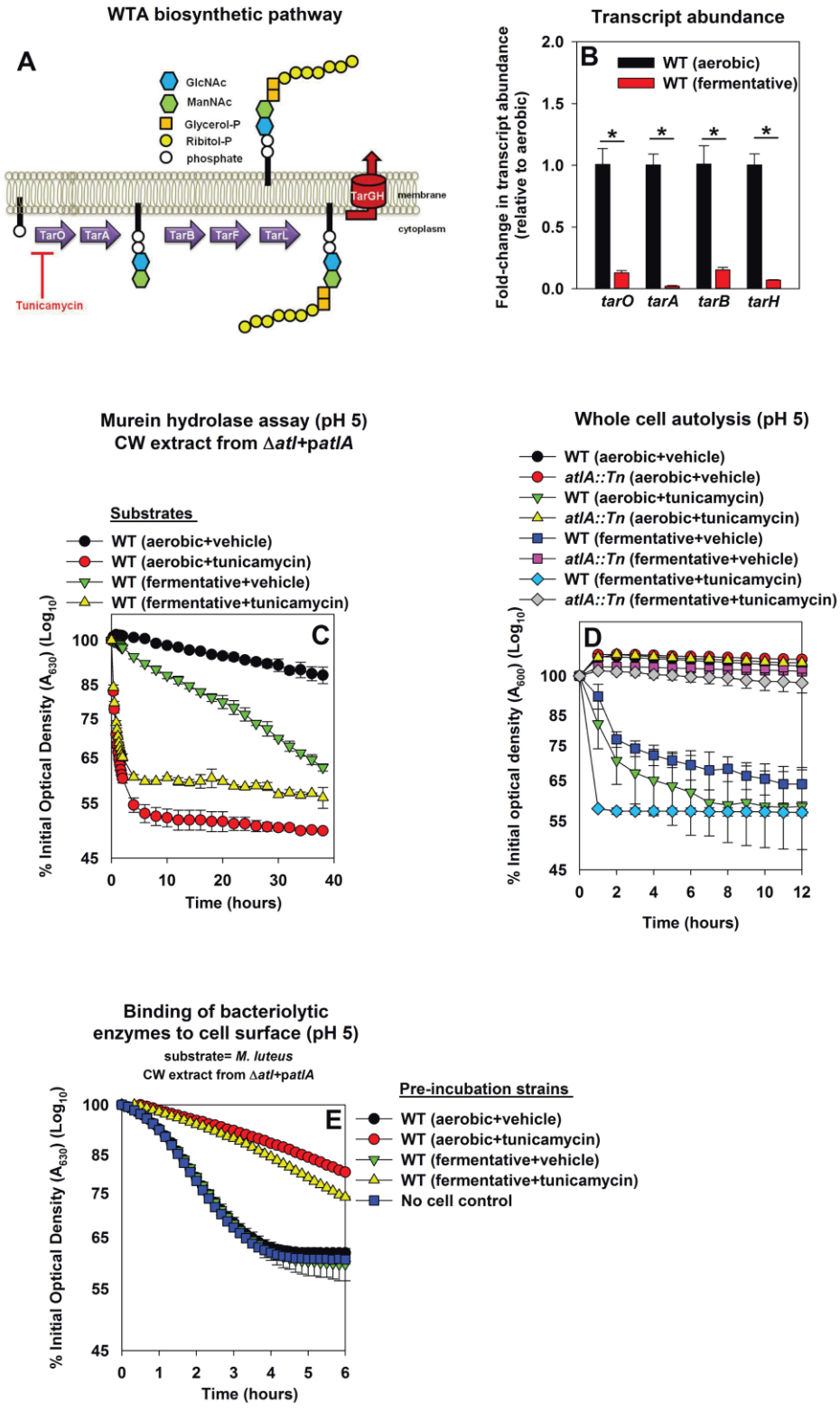
WTA biosynthetic pathway
A
GlcNAc
ManNAc
Glycerol-P
Ribitol-P
phosphate
TarGH
membrane
cytoplasm
TarO
TarA
TarB
TarF
TarL
Tunicamycin
Transcript abundance
B
WT (aerobic)
WT (fermentative)
Fold-change in transcript abundance (relative to aerobic)
2.0
1.5
1.0
0.5
0.0
*
tarO
tarA
tarB
tarH
Murein hydrolase assay (pH 5)
CW extract from Δatl+patlA
Substrates
WT (aerobic+vehicle)
WT (aerobic+tunicamycin)
WT (fermentative+vehicle)
WT (fermentative+tunicamycin)
C
% Initial Optical Density (A630) (Log10)
100
85
75
65
55
45
0
10
20
30
40
Time (hours)
Whole cell autolysis (pH 5)
WT (aerobic+vehicle)
atlA::Tn (aerobic+vehicle)
WT (aerobic+tunicamycin)
atlA::Tn (aerobic+tunicamycin)
WT (fermentative+vehicle)
atlA::Tn (fermentative+vehicle)
WT (fermentative+tunicamycin)
atlA::Tn (fermentative+tunicamycin)
D
% Initial optical density (A600) (Log10)
100
85
75
65
55
45
0
2
4
6
8
10
12
Time (hours)
Binding of bacteriolytic enzymes to cell surface (pH 5)
substrate= M. luteus
CW extract from Δatl+patlA
Pre-incubation strains
WT (aerobic+vehicle)
WT (aerobic+tunicamycin)
WT (fermentative+vehicle)
WT (fermentative+tunicamycin)
No cell control
E
% Initial Optical Density (A630) (Log10)
100
85
75
65
55
45
0
1
2
3
4
5
6
Time (hours)

**Figure 2.4. Decreased expression of wall-teichoic acids during fermentative growth makes *S. aureus* more amenable to cleavage by AtlA.** Panel A; Schematic of wall teichoic acid (WTA) biosynthesis in *S. aureus*. The diagram displays select proteins involved in WTA biosynthesis and is redrawn as initially presented by Campbell *et al.* (17). The initial transformations in the pathway catalyzed by TarO and TarA are non-essential, while the latter steps are essential. Tunicamycin inhibits TarO, as well as the 2-epimerase MnaA, which modulates the substrate levels for TarO (16, 96). MnaA is not displayed. Panel B; Transcript levels corresponding to genes encoding for WTA biosynthesis proteins are decreased upon fermentative growth. Biofilms of the WT (JMB 1100) were cultured aerobically or fermentatively, mRNA was extracted, and the abundances of the *tarO*, *tarA*, *tarB*, and *tarH* transcripts were quantified. The data were normalized to 16S rRNA levels, and thereafter to levels observed aerobically. Panel C; AtlA-dependent cleavage of heat-killed cells at a decreased pH is modulated via WTA. Murein-hydrolase activity at pH of 5 for CW-extracts detached from a Δ*atlA* strain (KB 5000) carrying p*atlA* and incubated with heat-killed cells of the WT cultured aerobically or fermentatively in the presence or absence of 100 ng/mL of tunicamycin as substrates is displayed. Panel D; AtlA-dependent autolysis of intact whole cells at decreased pH is modulated via WTA. The WT and *atlA::Tn* (JMB 6625) strains were cultured aerobically or fermentatively in the presence or absence of 100 ng/mL tunicamycin. Autolysis was examined in intact cells resuspended in a buffer with pH of 5. Panels E; Heat-killed aerobic or fermenting WT bind similar amounts of AtlA. CW-extract

detached from a Δ*atlA* strain (KB 5000) carrying p*atlA* was incubated at pH of 5 with heat-killed WT, cultured aerobically or fermentatively in the presence or absence of 100 ng/mL of tunicamycin, or in the absence of cells (control) for 8 minutes. The cells were separated by centrifugation and bacteriolytic activity in the resultant supernatant assessed upon heat-killed *M. luteus* as a substrate is displayed. Data in Panel B represents the average value of triplicates. Statistical significance was calculated using a two-tail Student's t-test and * indicates p-value of <.05. Data in Panels C-E represent the average value of technical duplicates from one set of substrate preparation or autolysis assays. The heat-killed substrates were prepared or autolysis assays were conducted on least three separate occasions and similar results were obtained. Error bars in all panels represent standard deviations. Error bars are displayed for all data, but might be too small to see on occasion.

## Figure 2.5

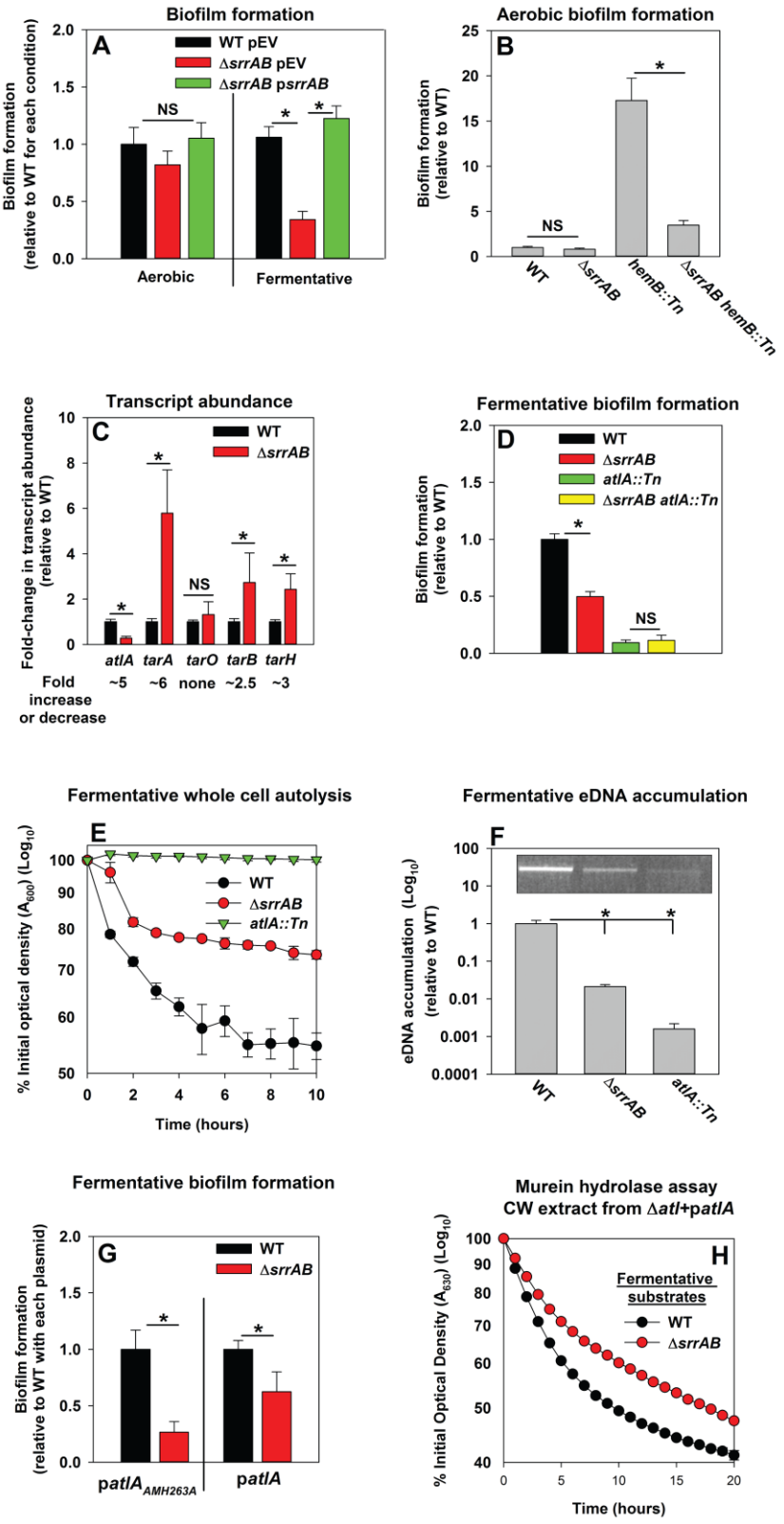
Biofilm formation
A
WT pEV
ΔsrrAB pEV
ΔsrrAB psrrAB
Biofilm formation (relative to WT for each condition)
NS
*
*
Aerobic
Fermentative
Aerobic biofilm formation
B
Biofilm formation (relative to WT)
NS
*
WT
ΔsrrAB
hemB::Tn
ΔsrrAB hemB::Tn
Transcript abundance
C
WT
ΔsrrAB
Fold-change in transcript abundance (relative to WT)
atlA tarA tarO tarB tarH
Fold increase or decrease
~5 ~6 none ~2.5 ~3
Fermentative biofilm formation
D
WT
ΔsrrAB
atlA::Tn
ΔsrrAB atlA::Tn
Biofilm formation (relative to WT)
NS
Fermentative whole cell autolysis
E
WT
ΔsrrAB
atlA::Tn
% Initial optical density (A600) (Log10)
Time (hours)
Fermentative eDNA accumulation
F
eDNA accumulation (Log10) (relative to WT)
WT
ΔsrrAB
atlA::Tn
Fermentative biofilm formation
G
WT
ΔsrrAB
Biofilm formation (relative to WT with each plasmid)
patlA AMH263A
patlA
Murein hydrolase assay
CW extract from Δatl+patlA
H
Fermentative substrates
WT
ΔsrrAB
% Initial Optical Density (A630) (Log10)
Time (hours)

**Figure 2.5. Programmed cell lysis and biofilm formation in fermenting cells are governed by the SrrAB two-component regulatory system.** Panel A; Fermentative biofilm formation is dependent upon SrrAB. Biofilm formation is displayed following aerobic or fermentative growth in the WT (JMB 1100) carrying pLL39 (pEV) or the Δ*srrAB* (JMB 1467) strain carrying either pLL39 (pEV) or pLL39_*srrAB* (p*srrAB*). Panel B; A *hemB* mutant forms SrrAB dependent biofilms aerobically. Biofilm formation following aerobic growth is displayed for the WT, Δ*srrAB*, *hemB::Tn* (JMB 6037), and Δ*srrAB hemB::Tn* (JMB 6039) strains. Panel C; Transcript levels corresponding to genes involved in PCL and biofilm formation are altered in a Δ*srrAB* strain. Biofilms of the WT and Δ*srrAB* strains were cultured fermentatively, mRNA was extracted, and the abundances of the *atlA*, *tarO*, *tarA*, *tarB*, and *tarH* transcripts were quantified. Data were normalized to 16S rRNA levels, and thereafter, to levels observed in the WT. Panel D; The fermentative biofilm formation phenotypes associated with the Δ*srrAB* and *atlA::Tn* mutations are not additive. Biofilm formation is displayed following fermentative growth for the WT, Δ*srrAB*, *atlA::Tn* (JMB 6625), and Δ*srrAB atlA::Tn* (JMB 6624) strains. Panel E; Autolysis of fermenting *S. aureus* is decreased in a strain lacking SrrAB. The WT, Δ*srrAB*, and *atlA::Tn* strains were cultured fermentatively and autolysis was examined (pH of 5). Panel F; eDNA accumulation is decreased in a strain lacking SrrAB. Biofilms of the WT, Δ*srrAB,* and *atlA::Tn* strains were cultured fermentatively and eDNA was quantified. The data were normalized to the viable cell count and thereafter to the levels in the WT. Panel G; *atlA* in multicopy partially suppresses the biofilm formation defect

of the Δ*srrAB* strain. Fermentative biofilm formation is displayed for the WT and Δ*srrAB* strains carrying either p*atlA*$_{AM\ H263A}$ or p*atlA*. Panel H; Heat-killed cells of a Δ*srrAB* strain are less amenable towards AtlA dependent lysis. Murein-hydrolase activity for CW-extracts detached from a Δ*atlA* strain (KB 5000) carrying p*atlA* and combined with fermentatively cultured and heat-killed WT or Δ*srrAB* strains as substrates are displayed. Data presented represent the average value of eight wells (Panels A, B, D-G) or biological triplicates (Panel C and F). Data in Panels E and H represent the average value of technical duplicates from one set of autolysis assays or substrate preparations. The heat-killed substrates were prepared or autolysis assays were conducted on least three separate occasions and similar results were obtained. Error bars in all panels represent standard deviations. Error bars are displayed for all data, but might be too small to see on occasion. Statistical significance was calculated using a two-tail Student's t-test and p-values >.05 were considered to be not significant while * indicates p-value of <.05.

**Figure 2.6**

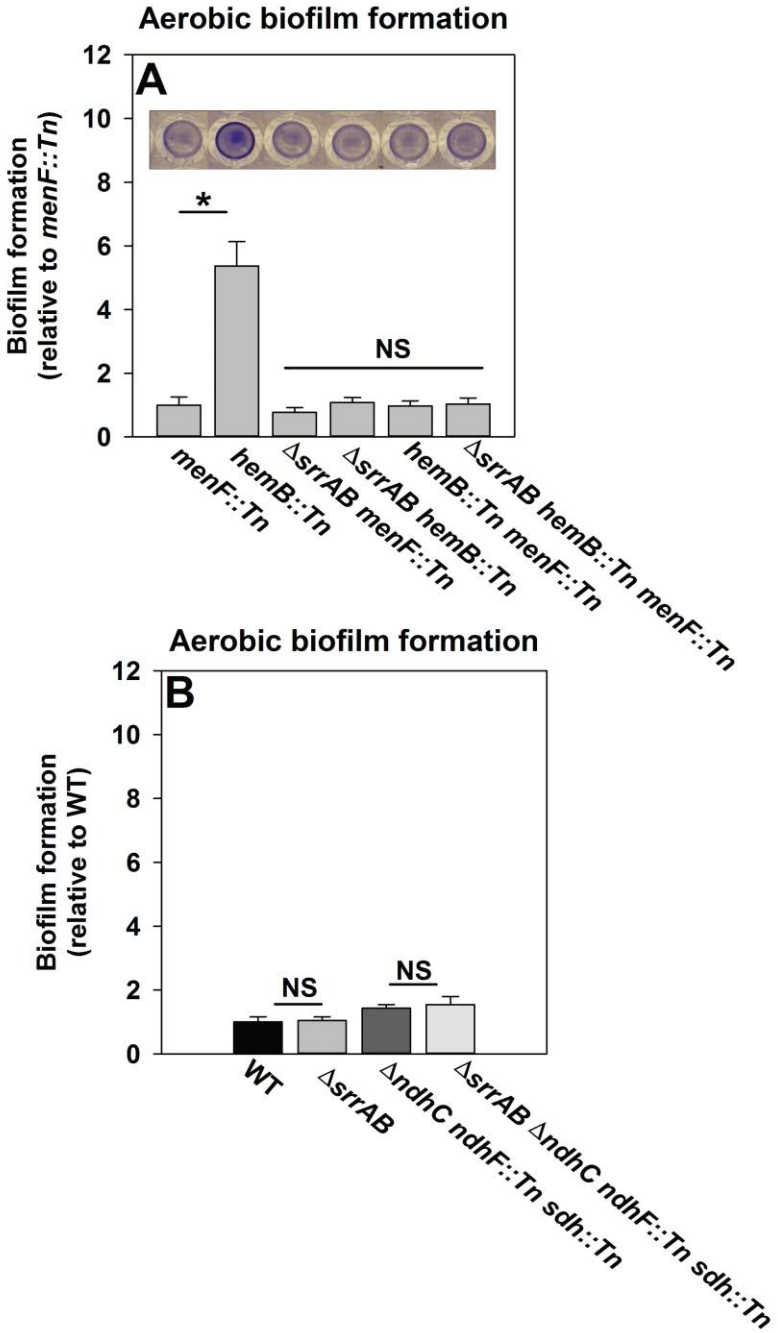
Aerobic biofilm formation
A
Biofilm formation (relative to menF::Tn)
12
10
8
6
4
2
0
*
NS
menF::Tn
hemB::Tn
ΔsrrAB menF::Tn
ΔsrrAB hemB::Tn
hemB::Tn menF::Tn
ΔsrrAB hemB::Tn menF::Tn
Aerobic biofilm formation
B
Biofilm formation (relative to WT)
12
10
8
6
4
2
0
NS
NS
WT
ΔsrrAB
ΔndhC ndhF::Tn sdh::Tn
ΔsrrAB ΔndhC ndhF::Tn sdh::Tn

**Figure 2.6. SrrAB-dependent biofilm formation is responsive to the oxidation state of the cellular menaquinone pool.** Panel A; SrrAB-dependent biofilm formation is inactivated in strains lacking the ability to synthesize menaquinone. Biofilm formation following aerobic growth is displayed for the *menF::Tn* (JMB6219), *hemB::Tn* (JMB6037), Δ*srrAB menF::Tn* (JMB6221), Δ*srrAB hemB::Tn* (JMB6039), *hemB::Tn menF::Tn* (JMB6217), and Δ*srrAB hemB::Tn menF::Tn* (JMB6673) strains. Panel B; SrrAB-dependent biofilm formation is not stimulated in strains enriched for oxidized menaquinone. Biofilm formation following aerobic growth is displayed for the WT (JMB 1100), Δ*srrAB* (JMB 1467), Δ*ndhC ndhF::Tn sdh:Tn* (JMB 6613), and Δ*srrAB* Δ*ndhC ndhF::Tn sdh:Tn* (JMB 6614) strains. Data in both panels represent the average value of eight wells and the errors bars represent standard deviation. Statistical significance was calculated using a two-tail Student's t-test and p-values >.05 were considered to be not significant while * indicates p-value of <.05.

**Figure 2.7**

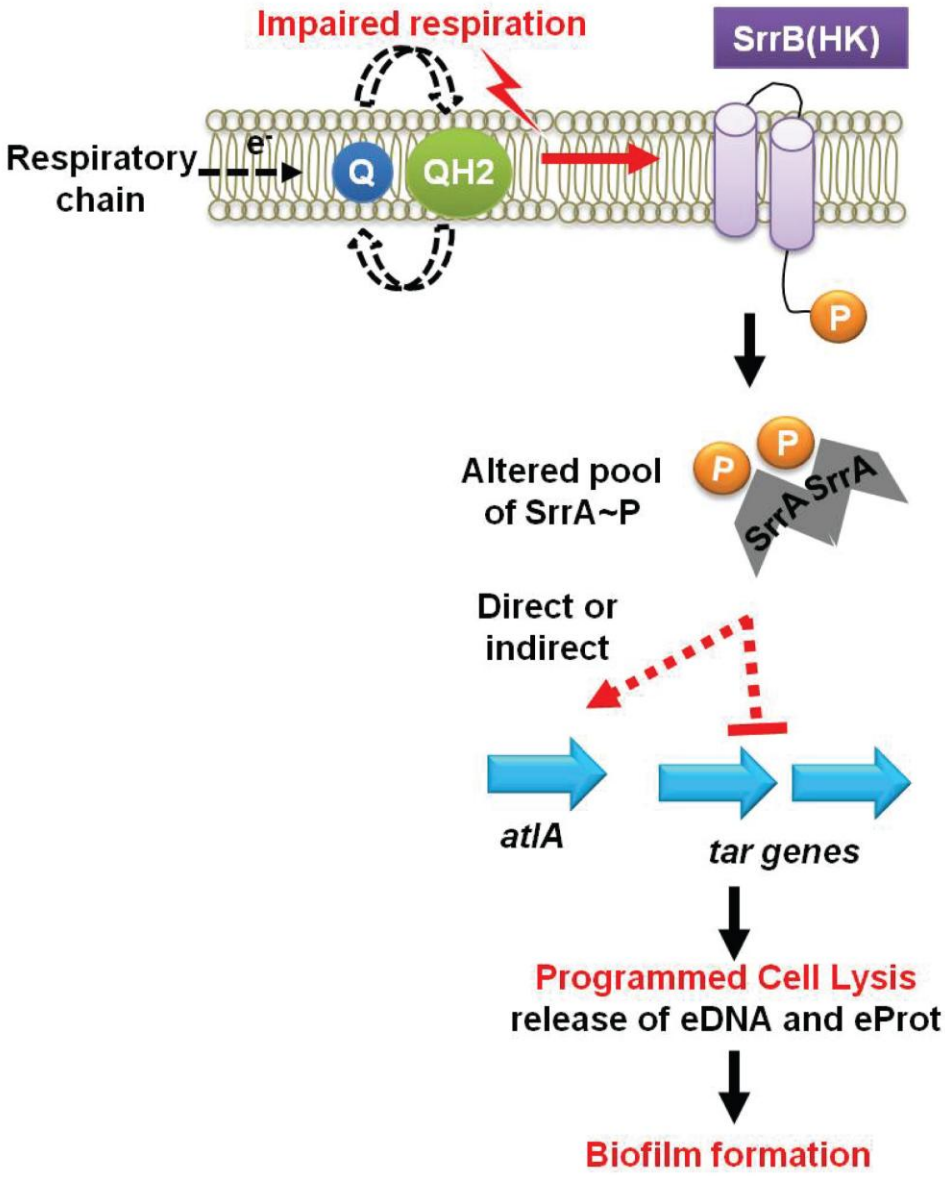


**Figure 2.7. A working model for the influence of respiration upon autolysis and biofilm formation in *S. aureus*.** A decreased capacity to respire results in an enrichment of reduced menaquinone effecting altered activity of the SrrAB TCRS. Altered SrrAB activity leads to increased transcription of *atlA* and

decreased transcription of genes (*tar*) encoding for wall-teichoic acid (WTA) biosynthesis. The consequent decrease in WTA expression and increase in AtlA expression results in the release of DNA and proteins, cell lysis and biofilm formation. Since cell lysis is effected via regulatory tuning of two divergent processes we term this mechanism as programmed cell lysis.

**Table 2.1. Strains and plasmids used in this study.**

| **Strains used in this study** | | | |
|---|---|---|---|
| ***S. aureus* Strains** | **Genotype/Description** | **Genetic Background** | **Source/ Reference** |
| JMB1100 | Wild-type; USA300_LAC (erm sensitive); MRSA; CC8 | LAC | (10) |
| RN4220 | Restriction minus; MSSA; CC8 | NCTC8325 | (82) |
| JMB 1467 | Δ*srrAB* (SAUSA300_1441-42) | LAC | (119) |
| JMB 2047 | Δ*srrAB::tet* | LAC | This work |
| JMB 2078 | *katA::Tn* (ermB) (SAUSA300_1232) | LAC | V. Torres |
| SH1000 | parent; MSSA; CC8 | SH1000 | (62) |
| JMB 1324 | parent, MRSA, USA400, CC1 | MW2 | Alex Horswill |
| JMB 7570 | parent, MRSA, USA100; CC5 | N315 | Ann Stock and (85) |
| JMB 1432 | Δfur::tetM | LAC | (63) |
| JMB 6231 | *sdhA::Tn(ermB)* | LAC | BEI resources and (39) |
| JMB 6232 | Δ*srrAB sdhA::Tn(ermB)* | LAC | This work |
| JMB 6384 | *ndhF::Tn(ermB)* (SAUSA300_0841) | LAC | This work; BEI resources and (39) |
| JMB 2057 | *ΔndhC::tet* (SAUSA300_0844) | LAC | This work |
| JMB 6614 | Δ*srrAB sdhA::Tn(ermB) ΔndhC::tet ndhF::Tn(ermB)* | LAC | This work |
| JMB 6613 | *sdhA::Tn(ermB) ΔndhC::tet ndhF::Tn(ermB)* | LAC | This work |
| JMB 6037 | *hemB::Tn(ermB)* | LAC | BEI resources |

| | | | |
|---|---|---|---|
| | | | and (39) |
| JMB 6039 | Δ*srrAB hemB::Tn(ermB)* | LAC | This work |
| JMB 6029 | *menF::Tn(ermB)* | LAC | BEI resources and (39) |
| JMB 6033 | Δ*srrAB menF::Tn(ermB)* | LAC | This work |
| JMB 6219 | *menF::Tn(tet)* | LAC | This work |
| JMB 6221 | Δ*srrAB menF::Tn(tet)* | LAC | This work |
| JMB 6217 | *hemB::Tn(ermB) menF::Tn(tet)* | LAC | This work |
| JMB 6673 | Δ*srrAB hemB::Tn(ermB) menF::Tn(tet)* | LAC | This work |
| JMB 6625 | *atlA::Tn(ermB)* | LAC | BEI resources and (39) |
| KB5000 | Δ*atlA* | UAMS-1 | (12) |
| JMB 6624 | Δ*srrAB atlA::Tn(ermB)* | LAC | This work |
| JMB 5577 | *icaA::Tn(ermB)* | LAC | This work; BEI resources and (39) |
| JMB 5579 | *icaB::Tn(ermB)* | LAC | This work; BEI resources and (39) |
| JMB 5578 | *icaC::Tn(ermB)* | LAC | This work; BEI resources and (39) |
| JMB 7270 | *hmrA::Tn(ermB)* | JE2 | BEI resources and (39) |
| JMB 7265 | *lytN::Tn(ermB)* | JE2 | BEI resources and (39) |
| JMB 7267 | *lytX::Tn(ermB)* | JE2 | BEI resources and (39) |
| JMB 7266 | *sle1::Tn(ermB)* | JE2 | BEI resources |

| | | | |
|---|---|---|---|
| | | | and (39) |
| JMB 7268 | *lytY::Tn(ermB)* | JE2 | BEI resources and (39) |
| JMB 7269 | *lytZ::Tn(ermB)* | JE2 | BEI resources and (39) |
| JMB 7271 | *lytM::Tn(ermB)* | JE2 | BEI resources and (39) |
| JMB2977 | parent | JE2 | BEI resources and (39) |
| JMB7277 | *narG::Tn (ermB)* | LAC | BEI resources and (39) |
| JMB 1148 | Δ*hptRS* | LAC | (119) |
| JMB 1357 | Δ*lytSR* | LAC | (119) |
| JMB 1330 | *graS::erm* | LAC | (10) |
| JMB 1335 | Δ*saePQRS::spec* | LAC | (113) |
| JMB 1219 | ΔSAUSA300_1219-1220 | LAC | (119) |
| JMB 1383 | Δ*arlSR* | LAC | (119) |
| JMB 1358 | Δ*phoSR* | LAC | (119) |
| JMB 1241 | Δ*airSR* | LAC | (119) |
| JMB 1377 | Δ*vraSR* | LAC | (119) |
| JMB 1333 | Δ*agr::tetM* | LAC | (76) |
| JMB 1223 | Δ*kdpSR* | LAC | (119) |
| JMB 1359 | Δ*hssSR* | LAC | (119) |
| JMB 1145 | Δ*nre*SR | LAC | (119) |
| JMB 1232 | ΔSAUSA300_2558-2559 | LAC | (119) |

**Other Strains**

| | |
|---|---|
| *Escherichia coli* PX5 | Protein Express |
| *Sacchromyces cerevisiae FY2* | William Belden |

**Plasmids used in this study**

| **Plasmid name** | **Insert Locus/function** | **Source/Reference** |
|---|---|---|
| pJB38 | Insertless vector for cloning chromosomal gene deletions | (11) |
| pJB38_*srrAB::tet* | Construction of *srrAB::tet* allele | This work |
| pCM28 | Insertless cloning vector | A. Horswill |
| pCM28_*srrAB* | *srrAB* complementing vector | (101) |
| pLL39 | Cloning vector for genetic complementation | (88) |
| pLL39_*srrAB* | *srrAB* complementing vector | This work |
| pJB141 | *atlA* complementing vector | (12) |
| pJB135 | $atlA_{GL}$ complementing vector | (12) |
| pJB122 | $atlA_{AMH263A}$ complementing vector | (12) |
| pJB128 | Insertless cloning vector | (12) |
| pJB111 | $atlA_{AM}$ complementing vector | (12) |
| pTnTet | Construction of *menF::Tn* (Tet) | (11) |

# CHAPTER 3

## SaeRS is responsive to the cellular respiratory status and regulates fermentative biofilm formation in *Staphylococcus aureus*

**Submitted to Infection and Immunity**

**Abstract:**

Biofilms are multicellular communities of bacterial cells living as a quorum rather than as individual cells. Infected human tissues are hypoxic or anoxic. We have recently described that impaired respiration elicits a programmed cell lysis phenomenon in the human pathogen *S. aureus*. PCL is dependent upon the AtlA murein hydrolase and the SrrAB TCRS, culminating in increased biofilm formation. In the current study we report that the SaeRS TCRS also governs fermentative biofilm formation by positively influencing AtlA activity. The SaeRS modulated factor fibronectin binding protein A (FnBPA) also contributed to the fermentative biofilm formation phenotype. Moreover, data presented suggest that SaeRS-dependent biofilm formation occurs in response to changes in the respiratory status of the cell. Genetic evidence suggests that a high cellular titer of phosphorylated SaeR is required for biofilm formation. Epistasis analyses found that SaeRS and SrrAB influence biofilm formation independent of one another. Analyses using a mouse model of orthopedic implant associated biofilm formation found that both SaeRS and SrrAB govern host colonization. Of these

two TCRS, SrrAB is the dominant system driving biofilm formation *in vivo*. We propose a model wherein impaired cellular respiration stimulates SaeRS, via an as yet undefined signal molecule(s), effecting increased biofilm formation via increased expression of AtlA and FnBPA.

**Introduction:**

*S. aureus* is a commensal organism, colonizing between 20-50% of the human population (38, 51, 108, 114, 164). *S. aureus* is also capable of causing aggressive infections (78). A recent study found that nearly 92% of cases acquiring *S. aureus* infections required hospitalization (78). Treatment of *S. aureus* infections is problematic due to the increasing prevalence of multi-antibiotic resistance. *S. aureus* strains have been isolated that are resistant to nearly all known antibiotics, including the last-line antibiotics linezolid and daptomycin (20, 129, 130).

Persistent bacterial infections in humans are associated with the ability of the bacterium to establish biofilms (28, 137). Biofilms are architecturally complex communities wherein bacteria are attached to a surface, or each other, and embedded in a polymeric matrix (6, 27, 28). The matrix provides protection to the bacteria from innate immunity and imparts therapeutic recalcitrance (6, 27, 28). When living in biofilms bacteria make lifestyle choices as a quorum, in a manner reminiscent of multi-cellular organisms (6, 27, 28). Biofilms of infectious agents are well characterized to form upon the majority of biomedical devices such as prosthetic heart valves, catheters and contact lenses (6, 27, 28). The ability of *S.*

*aureus* to cause infections in the context of medical devices is intimately connected to its ability to form biofilms (70, 117). *S. aureus* is also capable of attaching to and colonizing human tissues and causing diseases such as osteomyelitis (70, 117). Reflective of their clinical significance, biofilms are considered to be the etiologic agents of recurrent staphylococcal infections (70, 117). Biofilm formation in *S. aureus* is multi-factorial and consequently is a highly regulated and deterministic process. Biofilm formation is responsive to signals as varied as nutrient limitation to quorum sensing (70, 117).

Oxygen concentrations vary between healthy and infected or necrotic tissues, as well as in wounds, where they are estimated to be below 1% (hypoxic) or anoxic (complete lack of oxygen) (3, 18, 151). Oxygen is the primary TEA supporting respiratory growth of *S. aureus*. In the absence of oxygen or upon its limitation *S. aureus* utilizes fermentative pathways to generate energy (19, 54).

A study by Cramton *et al.* found that decreased oxygen concentrations result in increased biofilm formation in *S. aureus* (30). However, the mechanisms underlying the influence of oxygen upon biofilm formation are yet to be fully described. We have recently found that oxygen impacts *S. aureus* biofilm formation in its capacity as a TEA for cellular respiration (104). Decreased oxygen concentrations lead to diminished respiration, which serves as a signal that elicits PCL culminating in increased biofilm formation. Consistent with this logic chemical or physiological conditions that diminish the ability of cells to respire prompt an increased biofilm formation response. Likewise, heme

(*hemB::Tn*) and menaquinone auxotrophs (*menF::Tn*) that are incapable of respiration form increased biofilms aerobically. PCL occurs via increased expression of a peptidoglycan hydrolase (AtlA) and decreased expression of the AtlA inhibiting cell-surface glycopolymer wall-teichoic acid. The AltA-dependent cell lysis results in the release of high molecular weight DNA and cytosolic proteins into the extracellular milieu. The DNA and proteins that are released are incorporated into the biofilm matrix and serve as integral structural elements (104).

TCRS are widespread regulatory systems utilized by organisms to adapt to their environments (145, 146). TCRS consist of two proteins; 1) a HK, and 2) a DNA binding RR. The HK is the component that senses the stimulus. Upon stimulation, the HK changes the levels of the phosphoryl groups upon the RR which then leads to alterations in the system output (145, 146). In the case of DNA binding RR's, the levels of phosphorylated RR dictates the affinity and in cases the seequences that the protein binds to, thereby efecting a tailored physiological response. In a previous study, we found that PCL and biofilm formation is a programmed mechanism that is governed, in part, by the SrrAB TCRS (104). Further, SrrAB-dependent biofilm formation occurs in response to the accumulation of reduced menaquinone. SrrAB-dependent biofilm formation is silenced in the absence of menaquinone, however a *menF::Tn* strain still forms increased biofilms in the presence of oxygen in an as yet undefined manner (104).

The *S. aureus* SaeRS TCRS is a critical modulator of toxin and exo-protein expression and has crucial roles in modulating innate immunity and in pathogenesis (23, 49, 152). SaeS is the HK and SaeR is the RR. SaeRS activity is responsive to multiple host, as well as non-host signals (45, 93, 112). SaeRS are encoded by the *saePQRS* operon and *saeR* and *saeS* are co-transcribed, from an auto-regulated promoter (68, 112, 113). SaeR is a member of the OmpR family of RR and binds to DNA in its phosporylated state. Phosphorylated SaeR (SaeR~P) displays a variable affinity for its target promoter regions and therefore the SaeRS regulon consists of 2 classes of genes: Class I genes are low affinity targets that are activated in the presence of a high pool of SaeR~P while Class II genes are high affinity targets that are activated even when levels of SaeR~P are low (91). SaeS displays polymorphisms between isolates of *S. aureus*. In the Newman strain, SaeS contains a Pro18 ($SaeS^{P18}$) instead of the Leu18 ($SaeS^{L18}$), which is found in most *S. aureus* strains (1, 91, 144). $SaeS^{P18}$ imparts constitutive kinase activity leading to an increased pool of SaeR~P, and thereby results in the activation of Class I genes (1, 91, 144). SaeP and SaeQ form a membrane-associated complex that activates the phosphatase activity of SaeS, aiding the return of SaeS to a pre-stimulus state, and thus negatively influence the SaeRS regulon (67).

The goal of the current study was to expand our understanding of the molecular and regulatory mechanism(s) driving fermentative biofilm formation. We report that SaeRS positively governs fermentative biofilm formation. Data presented suggest that the influence of SaeRS upon biofilm formation is exerted

via increased expression of the AltA murein hydrolase and fibronectin binding protein A. Further, SaeRS-dependent biofilm formation occurs in response to alterations in the respiratory status and during conditions of high cellular levels of SaeR~P. Epistatic analyses found that SrrAB and SaeRS govern biofilm formation independently of one another. We also report that SrrAB and SaeRS influence staphylococcal pathogenesis in the context of an animal model of biofilm-associated infection.

**Results:**

**Fermentative biofilm formation is dependent upon the SaeRS two-component system.** Cellular respiration is dependent upon membrane-associated factors. We reasoned that regulatory system(s) utilized by the cell to perceive the respiratory status were likely to be membrane associated. *S. aureus* encodes for 16 TCRS; of which, the HK for 14 are predicted to be membrane associated or spanning. Fermentative biofilm formation was examined in strains that each lacked one individual TCRS (except WalKR, which is essential). The Δ*srrAB* and Δ*saePQRS* mutant strains were also attenuated in fermentative biofilm formation (Figure 3.1A). Reintroduction of *saePQRS* into the Δ*saePQRS* strain upon a multi-copy plasmid restored fermentative biofilm formation (Figure 3.1B). The phenotype of the Δ*srrAB* mutant was previously described (104).

Proteins are integral matrix components in fermenting biofilms. SaeRS negatively modulates expression of the secreted protease aureolysin (Aur) and Aur is the most abundant protein in the exo-proteome of a LAC *sae* mutant (19).

The introduction of a *aur*::*Tn* mutation into the Δ*saePQRS* strain did not alter the fermentative biofilm formation phenotype of the Δ*saePQRS* strain, suggesting that increased Aur expression does not contribute to the decreased biofilm phenotype of this strain (Figure 3.1C).

**SaeRS influences fermentative biofilm formation via the AtlA murein hydrolase and fibronectin binding protein A.** AtlA is a dominant factor required for the formation of fermentative biofilms (104). Phosphorylated SaeR binds a direct repeat sequence GTTAAN$_6$GTTAA (113). The guanine in the binding sequence is dispensable (113, 147). A putative SaeR binding site was present ~240 base pairs upstream of the predicted transcriptional start site for *atlA*, suggesting SaeR modulates *atlA* transcription (Figure 3.S1). The binding site differed from the consensus sequence only by the dispensable base, guanine (147). Consistent with the *in silico* prediction, *atlA* transcript levels were decreased in the Δ*saePQRS* strain during fermentative growth (Figure 3.2A).

A strain lacking SaeRS displayed phenotypes consistent with decreased expression of AtlA. The activity for AtlA was measured within the context of intact whole cells using autolysis assays (12). Fermentatively cultured Δ*saePQRS* and *atlA::Tn* (positive control) strains were deficient in autolysis (Figure 3.2B). One outcome of *S. aureus* autolysis is the release of high-molecular weight genomic DNA into the extracellular milieu (41, 126). Fermentatively cultured Δ*saePQRS* and *atlA::Tn* (positive control) strains displayed decreased accumulation of high molecular weight DNA in their biofilm matrixes (Figure 3.2C). AtlA has also been

implicated in the release of cytosolic proteins into the extracellular milleu (120). The activity of catalase (Kat), an abundant intracellular protein (24, 99), was decreased by ~4-fold in the spent media supernatant from the fermentatively cultured Δ*saePQRS* strain (Figure 3.S2). These data were normalized to intracellular Kat activity to negate for potential changes in Kat expression.

AtlA is a bifunctional enzyme that is proteolytically cleaved into a N-acetylmuramyl-L-alanine amidase and endo-β-N-acetylglucosaminidase (116). Full-length AtlA or AM are required for cleavage of *S. aureus* cells, while GL is dispensable for this activity (12). To further examine the influence of AtlA upon SaeRS-dependent biofilm formation we introduced multicopy plasmids with alleles encoding for either full-length AtlA (p*atlA*) or an enzymatically inactivated AM (p$atlA_{AM\ H263A}$) into the Δ*saePQRS* strain and examined fermentative biofilm formation. The presence of p*atlA* suppressed the fermentative biofilm formation defect of the Δ*saePQRS* strain when compared to the strain carrying p$atlA_{AM\ H263A}$ (Figure 3.2D).

Transcription of *fnbpA*, which encodes for the fibronectin binding protein A (FnBPA) is regulated by SaeR (144, 152). Interactions between AtlA and FnBPA facilitate biofilm formation (65). We found that the transcript levels for *fnbpA* were decreased in a Δ*saePQRS* strain upon fermentative growth, suggesting FnBPA may have a role in fermentative biofilm formation (Figure 3.2E). Consistent with this premise, a *fnbpA::Tn* strain was attenuated in fermentative biofilm formation (Figure 3.2F). It currently unclear what interactions between AtlA and FnBPA facilitate biofilm formation (65); however, the *fnbpA::Tn* strain was not deficient in

autolysis (data not shown), suggesting that the cell cleaving activity of AtlA operates independently of FnBPA.

Wall-teichoic acids are cell-wall glycopolymers that negatively influence AtlA activity (7, 133). *S. aureus* cultured fermentatively has decreased expression of WTA (104). One consequence of this is that heat-killed fermenting WT cells undergo AtlA-dependent cleavage at faster rate than respiring WT (104). We examined whether SaeRS influences WTA expression. To this end, the WT was cultured aerobically (positive control) and fermentatively while the Δ*saePQRS* strain was cultured fermentatively. Subsequently, the cells were heat-killed to inactivate native autolysins and provided as substrates in murein hydrolase assays. Murein hydrolase assays were conducted using proteins detached from the cell walls of a Δ*atlA* strain carrying either empty vector or a plasmid encoding for full-length AtlA (p*atlA*). Lysis was undetectable with CW-extracts from the Δ*atlA* strain carrying empty vector verifying that bacteriolytic activity under the conditions examined was entirely dependent upon AtlA, similar to findings reported earlier (data not shown) (104). Heat-killed Δ*saePQRS* cells were lysed at the same rate as fermentatively cultured WT cells by CW-extracts from the Δ*atlA* strain carrying p*atlA*, while WT cells cultured aerobically were resistant to lysis (Figure 3.S3). These data suggested that SaeRS does not influence WTA expression during fermentative growth. From Figures 3.2, 3.S1, 3.S2, and 3.S3 we concluded that the influence of SaeRS upon fermentative biofilm formation is exerted, at least in part, via altered expression of AtlA and FnBPA.

**Increased SaeR~P is required for fermentative biofilm formation and the SaeS kinase activity inhibitor zinc attenuates fermentative biofilm formation.** A high pool of phosphorylated SaeR (SaeR~P) is required for activation of the low affinity Class 1 target *fnbpA* (91). By inference, fermentative growth results in an increased pool of SaeR~P, which then promotes biofilm formation.

The LAC strain of *S. aureus* carries the *saeS*$^{L18}$ allele and does not form SaeRS-dependent biofilms aerobically (see Figure 3.1B). The *saeS*$^{P18}$ allele in strain Newman confers constitutive SaeS kinase activity, and thereby effects an increase in the pool of SaeR~P (1, 91, 144). We reasoned that strain Newman would display SaeS$^{P18}$ dependent biofilm formation in the presence of oxygen. Aerobic biofilm formation was indeed attenuated when the *saeS*$^{P18}$ allele in Newman was replaced with the *saeS*$^{L18}$ allele. Biofilm formation was also attenuated in a Newman Δ*saePQRS* strain (Figure 3.3A). Moreover, expressing the *saeS*$^{P18}$ allele under the transcriptional control of a constitutive promoter in the LAC WT strain resulted in increased aerobic biofilm formation (Figure 3.3B).

Zn inhibits the auto-kinase activity of SaeS (23). If a high pool of SaeR~P is associated with fermentative biofilm formation then Zn would be expected to inhibit SaeRS-dependent biofilm formation (23). Consistent with this premise, zinc supplementation resulted in decreased biofilm formation in the WT cultured fermentatively, but not in the Δ*saeS::Tn* strain (Figure 3.3C).

**SaeRS dependent biofilm formation is responsive to the cellular respiratory status and a menaquinone auxotroph forms Sae-dependent biofilms.** The primary influence of oxygen upon physiology is exerted in its capacity as a TEA for respiration. We examined whether SaeRS-dependent biofilm formation occurs in response to the altered respiratory status of the cell. In addition to oxygen, *S. aureus* can utilize nitrate as a TEA. Supplementing anaerobic biofilms with nitrate resulted in diminished biofilm formation by both the WT and the Δ*saePQRS* strains. However, as expected, ratiometric analyses revealed that this occurred to a lower degree in the Δ*saePQRS* strain (Figure 3.4A).

We reasoned that SaeRS-dependent biofilms would be formed aerobically if respiratory processes were inhibited by either chemical or genetic means. Consistent with our premise, supplementing aerobic cultures with the respiratory poison sodium azide increased biofilm formation in the WT, however, ratiometric analyses revealed that biofilm induction was attenuated in the Δ*saePQRS* strain (Figure 3.4B). Moreover, a menaquinone auxotroph (*menF::Tn*), which is incapable of respiring, displayed increased biofilm formation during aerobic growth. This phenotype was attenuated upon the introduction of the *saeS::Tn* or *saeR::Tn* mutations (Figure 3.4C).

**SaeRS and SrrAB influence fermentative biofilm formation independent of one another.** SrrAB-dependent biofilm formation is silenced in the *menF::Tn* strain, a strain incapable of respiring (104). Aerobic biofilm formation in the *menF::Tn saeS::Tn* strain was similar to that formed by the WT strain. These

data led us to reason that SrrAB and SaeRS are the dominant regulatory systems influencing fermentative biofilm formation and that they influence biofilm formation independent of each other. Consistent with our premise, biofilm formation was induced ~20 fold in the WT following fermentative growth, relative to aerobic growth; however, biofilm formation was largely uninduced in a strain lacking both SaeRS and SrrAB (Figure 3.S4). Further, the fermentative biofilm formation phenotype displayed by the Δ*srrAB saeS:Tn* double mutant strain was more severe than that of the Δ*srrAB* and *saeS:Tn* strains (Figure 3.5A). Ratiometric analyses of the data presented in Figure 3.5A indicated that introducing the Δ*srrAB* mutation into either the WT or *saeS::Tn* strains resulted in a similar fold-change decrease in biofilm formation (Figure 3.5B). Moreover, the presence of *srrAB* upon a multi-copy plasmid (p*srrAB*) was unable to suppress the fermentative biofilm formation defect of the Δ*saePQRS* strain (Figure 3.5C).

**SaeRS and SrrAB influence biofilm formation in a murine model of orthopedic implant-associated infection.** We next examined whether the SrrAB and SaeRS regulatory systems were required for biofilm formation *in vivo*, using an established mouse model of orthopedic implant-associated biofilm infection (5, 149). At seven days post-infection, a Δ*srrAB* strain displayed decreased bacterial burdens in the tissue surrounding the site of infection but not in the infected joint, the femur or the implant (Figure 3.S5). The Δ*saePQRS* strain was not attenuated in growth at day seven in any of the tissues examined (Figure 3.S5). At fourteen days post-infection, both the Δ*srrAB* and Δ*saePQRS* strains

displayed decreased bacterial burdens in the infected femur (Figure 3.6), whereas titers with Δ*srrAB* were also reduced in the joint (Figure 3.6). These findings suggest that SrrAB and SaeRS influence later stages of biofilm development *in vivo*, which might be regulated by limitations in oxygen availability as the infection progresses.

**Discussion.**

Biofilm formation is a crucial facet of staphylococcal infections. In a recent study, we found that growth conditions of diminished respiration elicit increased biofilm formation in *S. aureus* in a process dependent upon the AtlA murein hydrolase. The goal of the current study was to expand our understanding of the molecular and regulatory mechanism(s) driving fermentative biofilm formation. Herein we report that in addition to SrrAB, the SaeRS TCRS also modulates fermentative biofilm formation. A strain lacking SaeRS, was attenuated in biofilm formation, had decreased transcript levels for *atlA* during fermentative growth, and displayed phenotypes consistent with decreased AtlA-dependent autolysis. Our analyses support a model wherein SaeRS exerts its effect upon biofilm formation via AtlA (Figure 3.7).

Fibronectin binding protein A (FnBPA) interacts with AtlA to facilitate aerobic biofilm formation (65). Transcription of *fnbpA* is modulated by SaeR (91). The Δ*saePQRS* strain had decreased *fnbpA* transcript levels during fermentative growth, which led us to reason that FnBPA may also facilitate fermentative biofilm formation. Consistent with this idea, a strain a lacking FnBPA was attenuated in fermentative biofilm formation. Interactions between AtlA and FnBPA facilitate biofilm formation (65). However, it is currently unclear how exactly FnBPA interacts with AtlA to facilitate biofilm formation. We found that a *fnbpA::Tn* strain was not attenuated for autolysis suggesting FnBPA exerts its influence independent of the ability of AtlA to lyse cells.

Increased levels of phosphorylated SaeR result in increased transcription of *fnbpA* (91). Taken together with the data presented herein, one inference is that fermentative biofilm formation is a result of increased SaeRS activity and increased levels of phosphorylated SaeR (SaeR~P). In support of this hypothesis, strains carrying the *saeS*$^{P18}$ allele, which increases the cellular titer of SaeR~P, formed SaeRS-dependent biofilms during aerobic growth. Moreover, supplementing growth media with zinc, an inhibitor of SaeS kinase activity (23), attenuated SaeRS-dependent fermentative biofilm formation in the LAC WT strain.

Oxygen is a cell-permeable molecule that can exert its influence on physiology by either directly interacting with cellular factors or in its capacity as a TEA for respiration. Anaerobic SaeRS-dependent biofilm formation was suppressed upon supplementing growth media with nitrate, which serves as an electron acceptor. This lent support to a model wherein SaeRS is responsive to the cellular respiratory status (Figure 3.7). Further, emphasizing this model, SaeRS-dependent biofilm formation could be triggered by chemical or genetic inhibition of respiration. It is currently unclear which cellular molecule(s) are involved in transferring the stimulus to SaeS. SaeRS output is altered by a variety of extracellular stimuli and these alterations lead to both increased, as well as decreased kinase activity (1, 23, 45). The findings reported herein suggest that Sae activity may also be responsive to an intracellular signal and this results in increased kinase activity (Figure 3.7). The mechanistic details underlying the integration of internal and external signals, as well as repressing

and activating signals, by SaeS, are currently unclear. However, recent studies have postulated an intriguing theory wherein intramembrane HKs, such as SaeS, could achieve signal integration using a tripwire-like model (87, 98). In this model, the conformations adopted by the N-terminal domain govern the kinase activity of HK. The alterations in N-terminal domain conformation upon interactions with a stimulus would then dictate whether the system output is increased or decreased.

Clinical isolates of *S. aureus* that are incapable of respiration, termed as SCV, display increased resistance towards antibiotics and cause persistent infections (105, 122). SCV strains are typically heme or menaquinone auxotrophs (54, 122). We have previously found that a heme auxotroph forms SrrAB-dependent biofilms and this phenotype requires the presence of menaquinone (104). Consequently, a menaquinone auxotroph forms biofilms in a manner independent of SrrAB (104). In the current study, we found that a menaquinone auxotroph forms SaeRS-dependent biofilms. Thus, in conjunction with our prior studies, the results presented herein lend considerable insight into the regulatory mechanisms that may predominate within SCV strains.

One characteristic of the growth cycle of biofilms is the periodic detachment and shedding of bacterial cells (70). The detached cells effect the dispersal of infection (70). Consequently, biofilm-associated cells are considered as the etiologic agents of recurrent staphylococcal infections (70, 117). The regulatory and molecular mechanisms that drive biofilm formation or dispersal *in vivo* are largely unknown (70, 117). Our finding that both SrrAB and SaeRS are

required for biofilm formation in a mouse model of infection shed light on the regulatory factors that may operate *in vivo*. Since both SrrAB and SaeRS modulate the expression of factors involved in cell lysis it is tempting to speculate that these factors are also important for *in vivo* biofilm formation. However, further experimentation is necessary to draw this conclusion.

In summary, we report that SaeRS plays a role in anaerobic biofilm formation. Sae is responsive to the cellular respiratory status and decreased respiration elicits increased activity of SaeRS resulting in increased transcription of *atlA* and *fnbpA* and thereby effects biofilm formation. Further, both the SrrAB and SaeRS systems govern host colonization in an animal model of infection.

**Material and Methods:**

**Materials**. Restriction enzymes, quick DNA ligase kit, deoxynucleoside triphosphates, and Phusion DNA polymerase were purchased from New England Biolabs. The plasmid mini-prep kit, gel extraction kit and RNA protect were purchased from Qiagen. DNase I was purchased from Ambion. Lysostaphin was purchased from Ambi products. Oligonucleotides were purchased from Integrated DNA Technologies and sequences are listed in Table S1. Trizol and High-Capacity cDNA Reverse Transcription Kits were purchased from Life Technologies. Tryptic Soy broth (TSB) was purchased from MP biomedical. Unless otherwise specified all chemicals were purchased from Sigma-Aldrich and were of the highest purity available.

**Bacterial growth conditions.** Unless otherwise stated, the *S. aureus* strains used in this study (Table 1) were constructed in the community-associated *S. aureus* USA300 LAC strain that was cured of the native plasmid pUSA03 that confers erythromycin resistance (10). Overnight cultures of *S. aureus* were grown at 37 °C in 10 mL culture tubes containing 1-mL of TSB or 30-mL culture tubes containing 5 mL TSB. Difco BiTek agar was added (15 g $L^{-1}$) for solid medium. When selecting for or against plasmids, antibiotics where added to the following concentrations: 150 μg $mL^{-1}$ ampicillin; 30 μg $mL^{-1}$ chloramphenicol (Cm); 10 μg $mL^{-1}$ erythromycin (Erm).

*Growth model to assess biofilm formation.* Aerobic, overnight cultures, were diluted into fresh TSB and incubated statically at 37 °C. For aerobic growth, the cultures were grown in 96-well microtiter plates containing 200 μL in each well or six-well plates containing 6 mL in each well and were covered with an Aera seal (Excel scientific), which allowed for uniform gas exchange. For anaerobic growth, cultures were inoculated aerobically followed immediately by passage through an airlock (3 vacuum/gas exchange cycles) into a COY anaerobic chamber equipped with a catalyst to maintain oxygen concentrations below one ppm. Anaerobic growth in the presence of a TEA was achieved by supplementing the media with sodium nitrate (prepared fresh daily).

**Static model of biofilm formation.** Biofilm formation was examined as described earlier, with minor changes (99) (104). Overnight cultures were diluted into fresh TSB to a final optical density of 0.05 ($A_{590}$). 200-μL aliquots of diluted

cultures were added to the wells of a 96-well microtitre plate (Corning 3268) and the plate was subsequently incubated statically at 37 °C for 22 hours. Prior to harvesting the biofilm, the optical density ($A_{590}$) of the cultures was determined. The plate was subsequently washed twice with water, biofilms were heat fixed at 60 °C, and the plates were allowed to cool to room temperature. The biofilms were stained with 0.1% crystal violet, washed thrice with water, destained with 33% acetic acid and the absorbance of the resulting solution was recorded at 570 nm, standardized to an acetic acid blank, and subsequently to the optical density of the culture upon harvest. Finally, the data were normalized with respect to the WT or as described in the figure legends to obtain relative biofilm formation.

**Recombinant DNA and genetic techniques.** *E. coli* DH5α was used as a cloning host for plasmid construction. All clones were passaged through RN4220 (82) and subsequently transduced into the appropriate strains using bacteriophage 80α (111). All *S. aureus* mutant strains and plasmids were verified using PCR, sequencing of PCR products or plasmids (Genewiz, South Plainfield, NJ), or genetic/chemical complementation of phenotypes.

**Construction of mutant strains and plasmids.** The pCM28_*saePQRS* plasmid, containing *saePQRS* under the transcriptional control of their native promoter, was constructed using yeast recombinational cloning as previously

described (71, 100, 103). The *saePQRS* alleles and the upstream promoter region were amplified from the LAC chromosome.

**Quantitative real-time PCR assays.** Biofilms were cultured in the presence or absence of oxygen for twenty-two hours. At point of harvest the spent medium was discarded and the remaining culture was immediately resuspended in RNAProtect reagent (Qiagen) and treated according to manufacturer instructions. The treated culture was subjected to centrifugation, the supernatant was discarded, and the cell pellet was resuspended in RNase free 50 mM Tris, pH 8. Cell-free extracts were generated as earlier (99, 102). RNA was extracted using Trizol, as per manufacturer instructions. Downstream treatments of the purified RNA and construction of cDNA libraries was as described earlier (102). Primers for PCR were designed manually or using the Primer Express 3.0 software from Applied Biosystems. Quantitative real time PCR reactions (Table S1) were conducted as described earlier (102).

**Quantification of high-molecular weight extracellular DNA.** eDNA was analyzed as described earlier with some changes (73, 104). Overnight cultures were diluted into TSB to a final optical density of 0.05 ($A_{600}$) in a final volume of 6 mL per well of a six-well plate. The cultures were incubated statically at 37 °C for 22 hours. At point of harvest, the spent media supernatant was aspirated out of each well. One mL of 1X PBS (recipe as recommended by Cold-spring harbor protocols) was immediately added to the wells and a cell scraper was used to

transfer the contents to an eppendorf tube. The biomass was pelleted by centrifugation and the supernatant was removed by aspiration. The pellets were thoroughly resuspended in 1X PBS and vortexed for 5 minutes using a Vortex Genie 2 (Scientific Industries) at the highest speed possible using a vertical micro-tube adapter. Aliquots were removed for determination of the viable cell count (colony forming units) and samples were pelleted by centrifugation. Control experiments verified that the viable cell counts were not affected by the vortexing procedure (data not shown). Equal volumes of the supernatants were assessed for the presence of high molecular weight DNA (>10 kilobases) using agarose gel electrophoresis. To assess the eDNA in a semi-quantitative manner, the gels were photographed and the bands were subjected to density analysis using Image J software. For each sample, the spot densities were normalized to the viable cell count (colony forming units) and subsequently as mentioned in the figure legends.

**Cytoplasmic protein release assays.** Strains were cultured as described under eDNA analyses (104). The samples were vortexed briefly, biomass was transferred into a microcentrifuge tube, and cell pellets and spent media supernatants were partitioned by centrifugation. The spent media supernatant was retained for further analyses. The cell pellets were resuspended in lysis buffer (50 mM Tris, 150 mM NaCl, 4 µg lysostaphin, 8 µg DNAse, pH 7.5) and incubated at 37 °C until confluent lysis was observed. Cell lysates were clarified using centrifugation to obtain cell-free extracts. Catalase (Kat) activity was

assayed, in both the cell-free extracts as well as spent medium supernatants as described elsewhere (4, 99). The ratio of extracellular to intracellular Kat activity was utilized to determine protein release. In control experiments, Kat activity was undetectable in a *katA::Tn* strain (data not shown).

**Whole cell autolysis assays.** Overnight cultures were diluted into TSB to a final optical density of 0.05 ($A_{600}$) and cultured for four hours (104). Whole cell autolysis assays were conducted as described elsewhere with some changes (12, 104). Briefly, the cultures were harvested by centrifugation, cell pellets were washed twice, and resuspended in autolysis buffer (0.2 M sodium acetate, 150 mM NaCl, 0.01% Triton X-100, pH 5). The cell suspensions were then incubated at 37 °C with shaking and optical densities were recorded periodically.

**Murein hydrolase assays.** Biofilms were cultured for four hours and cells were harvested as mentioned under eDNA analyses (104). Thereafter, CW-extracts were prepared and murein hydrolase activity determined as described elsewhere with minor changes (95). Briefly, cell pellets were washed and CW-extracts were prepared by resuspension in 3 M lithium chloride and incubation for 25 minutes (95). Protein concentrations of the extracts were determined and between 0.1-0.5 µg of an individual extract was combined with heat-killed cell substrates (0.35 optical density ($A_{600}$)) in assay buffer (50mM Hepes, 150 mM NaCl, 0.01% Triton X-100, pH 7.5). Samples were incubated with shaking at 37 °C and optical densities were recorded periodically.

**Mouse model of *S. aureus* orthopedic implant biofilm infection.** A mouse model of *S. aureus* orthopedic implant infection was utilized as previously described (57-59, 131, 132). Male C57BL/6 mice (8-12 weeks old) were purchased from Charles River Laboratories (Frederick, MD). The mice were anesthetized with a ketamine/xylazine cocktail (Hospira, Lake Forest, IL, and Akorn, Decatur, IL; 100 and 5 mg/kg, respectively) and the surgical site was shaved and disinfected with povidone-iodine. A medial parapatellar arthrotomy with lateral displacement of the quadriceps-patella was performed to access the distal femur. Subsequently, a burr hole was created in the femoral intercondylar notch extending into the intramedullary canal using a 26-gauge needle, whereupon a precut 0.8-cm length, orthopedic-grade Kirschner (K) wire (0.6 mm diameter, Nitinol [nickel-titanium]; Custom Wire Technologies, Port Washington, WI) was inserted into the intramedullary canal, leaving approximately 1 mm protruding into the joint space. A total of $10^3$ CFU of the WT, Δ*srrAB*, or Δ*saePQRS* strains were inoculated at the implant tip. Analgesia (Buprenex, 0.1 mg/kg s.c.; Reckitt Benckiser, Hull, U.K.) was administered immediately following infection and again 24 hours later for pain relief. After this interval, all mice exhibited normal ambulation and no discernible pain behaviors. The studies were conducted in strict accordance with the recommendations in the Guide for the Care and Use of Laboratory Animals of the National Institutes of Health. The animal use protocol was approved by the Institutional Animal Care and Use Committee of the University of Nebraska Medical Center.

## Figure 3.1

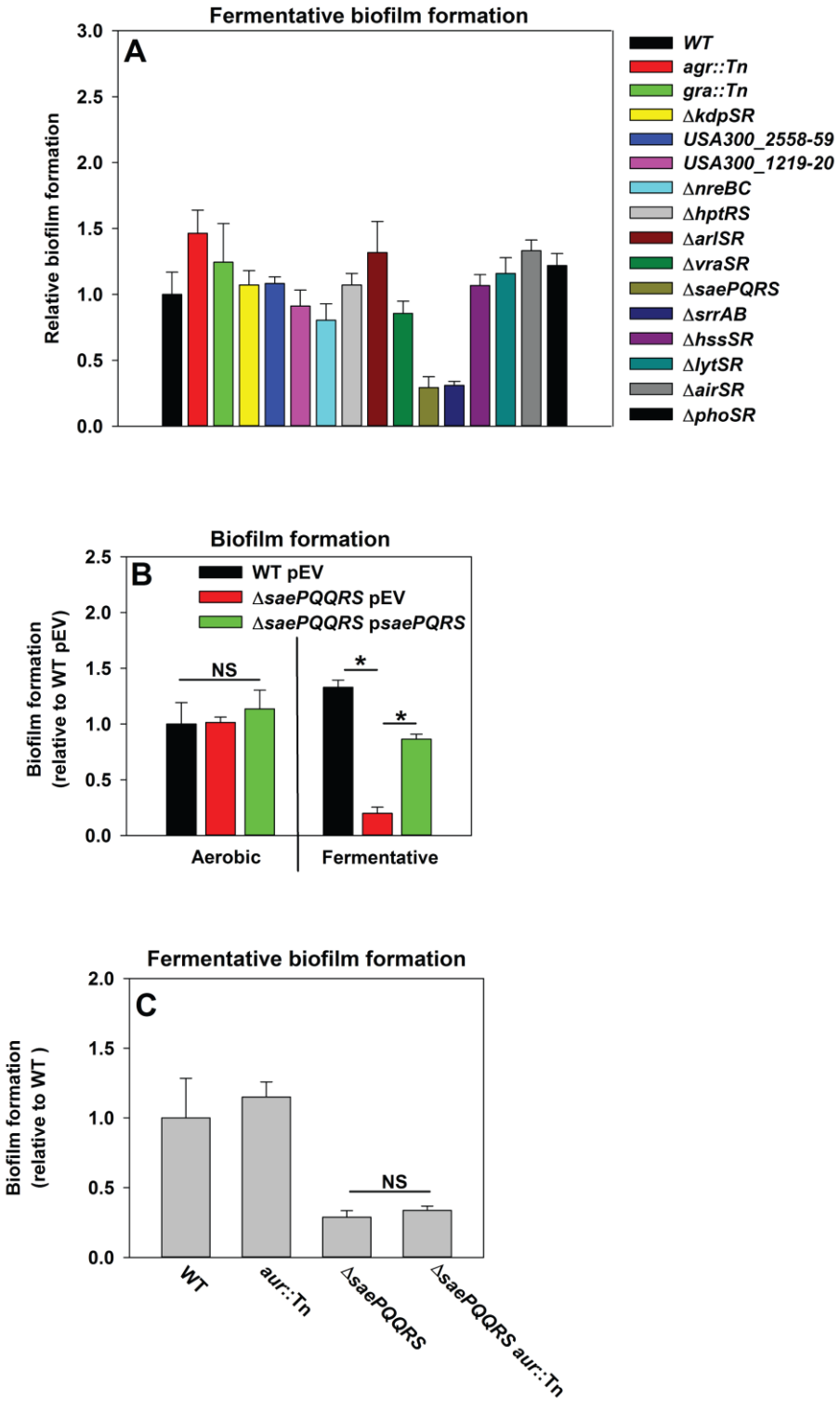
Fermentative biofilm formation
A
Relative biofilm formation
3.0
2.5
2.0
1.5
1.0
0.5
0.0
WT
agr::Tn
gra::Tn
ΔkdpSR
USA300_2558-59
USA300_1219-20
ΔnreBC
ΔhptRS
ΔarlSR
ΔvraSR
ΔsaePQRS
ΔsrrAB
ΔhssSR
ΔlytSR
ΔairSR
ΔphoSR
Biofilm formation
B
WT pEV
ΔsaePQQRS pEV
ΔsaePQQRS psaePQRS
Biofilm formation (relative to WT pEV)
NS
*
*
Aerobic
Fermentative
Fermentative biofilm formation
C
Biofilm formation (relative to WT )
NS
WT
aur::Tn
ΔsaePQQRS
ΔsaePQQRS aur::Tn

**Figure 3.1. Fermentative biofilm formation is dependent upon the SaeRS two-component system.** Panels A; A strain lacking SaeRS is attenuated in fermentative biofilm formation. Biofilm formation of the LAC (JMB1100; hereafter wild-type (WT), *agr::Tn* (JMB 1333), *gra::Tn* (JMB 1330), Δ*kdpSR* (JMB 1223), Δ*USA300_2558-59* (JMB 1232), Δ*USA300_1219-20* (JMB 1219), Δ*nreBC* (JMB 1145), Δ*hptRS* (JMB 1100), Δ*arlSR* (JMB 1383), Δ*vraSR* (JMB 1377), Δ*saePQRS* (JMB 1335), Δ*srrAB* (JMB 467), Δ*hssSR* (JMB 1359), Δ*lytSR* (JMB 1357), Δ*airSR* (JMB 1241), Δ*phoSR* (JMB 1359) strains following fermentative (anaerobic) growth is displayed. Panel B; The fermentative biofilm formation defect of the Δ*saePQRS* strain can be genetically complemented. Biofilm formation is displayed following aerobic or fermentative growth in the WT carrying pCM28 (pEV) or the Δ*saePQRS* strain carrying either pCM28 (pEV) or pCM28_*saePQRS* (p*saePQRS*). Panel C; The biofilm formation defect of a Δ*saePQRS* strain is not an outcome of increased Aur expression. Biofilm formation of the WT, Δ*saePQRS*, *aur::Tn* (JMB 6620) and the Δ*saePQRS aur::Tn* (JMB 6618) strains is displayed following fermentative growth. The data represent the average values of eight wells and error bars represent standard deviations. Error bars are displayed for all data, but on occasion may be too small to see. Statistical significance was calculated using a two-tail Student's t-test and p-values >0.05 were considered to be not significant (NS) while * indicates p-value of <0.05.

**Figure 3.2**

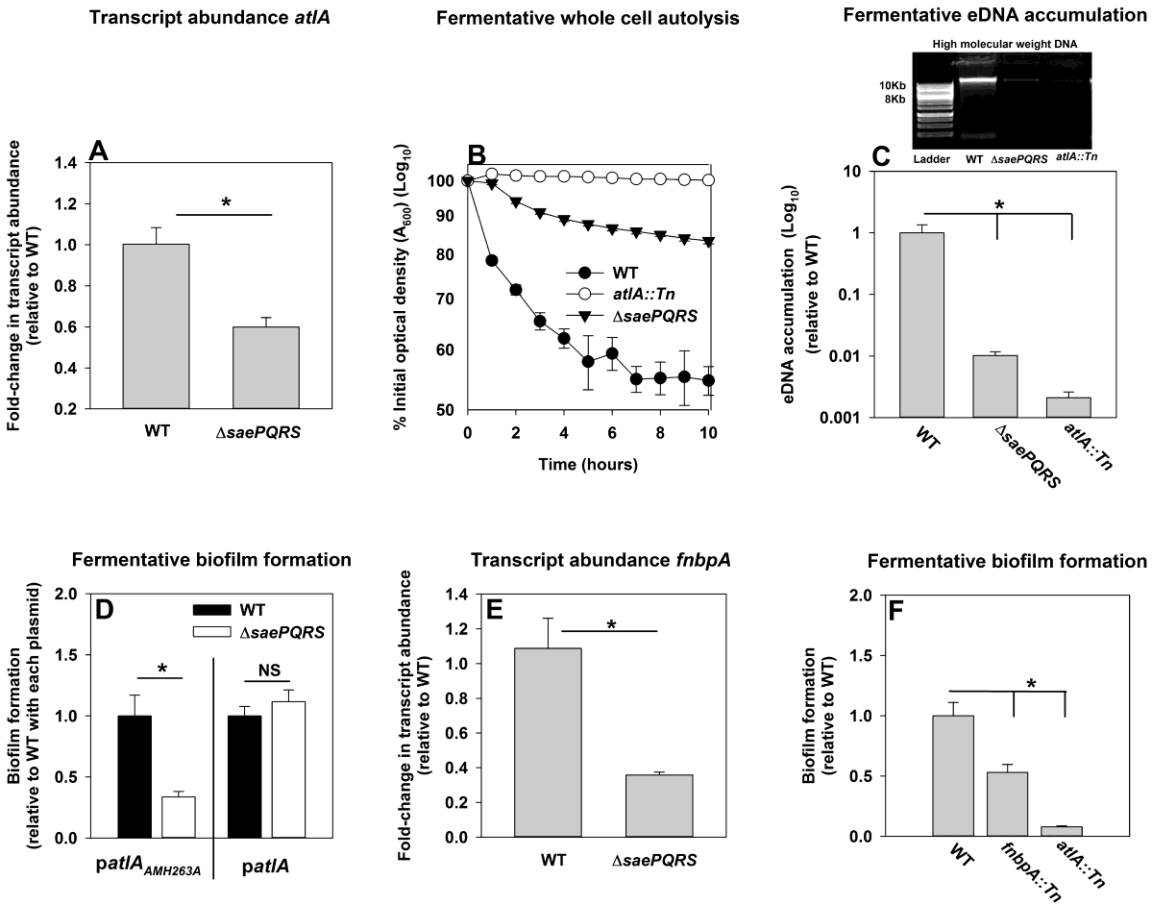


**Figure 3.2. SaeRS influences fermentative biofilm formation via the AtlA murein hydrolase and Fibronectin binding protein A.** Panel A; Transcript levels corresponding to *atlA* is decreased in a Δ*saePQRS* strain. Biofilms of the WT (JMB 1100) and Δ*saePQRS* (JMB 1335) strains were cultured fermentatively, mRNA was extracted, and the abundance of the *atlA* transcript was quantified. Data were normalized to 16S rRNA levels, and thereafter to levels observed in the WT. Panel B; Autolysis of fermenting *S. aureus* is decreased in a strain lacking SaeRS. The WT, Δ*saePQRS* and *atlA::Tn* (JMB 6625) strains were cultured fermentatively and autolysis was examined in whole-

cells. Panel C; High molecular weight DNA (eDNA) accumulation is decreased in the biofilm matrix of a Δ*saePQRS* strain. Biofilms of the WT, Δ*saePQRS*, and *atlA::Tn* were cultured fermentatively, eDNA was extracted, and analyzed using agarose gel electrophoeresis (inset photograph). The data were normalized to the viable cell count, and thereafter to eDNA accumulation in fermenting WT. Panel D; *atlA* in multicopy suppresses the biofilm formation defect of the Δ*saePQRS* strain. Fermentative biofilm formation is displayed for the WT and Δ*saePQRS* strains carrying either p*atlA*$_{AM\ H263A}$ or p*atlA*. Panel E; Transcripts corresponding to *fnbpA* are decreased in a Δ*saePQRS* strain. *fnbpA* transcripts levels were quantified from the same cDNA libraries as in Panel A. The data were normalized to 16S rRNA levels, and thereafter to levels observed in the WT. Panel F; A strain lacking fibronectin binding protein A is deficient in the formation of fermentative biofilms. Biofilm formation is displayed for the WT, *fnbpA::Tn* (JMB 8403) and the *atlA::Tn* (JMB 6625) strains following fermentative growth. Data presented represent the average value of eight wells (Panels D and F) or biological triplicates (Panels A, C and E). Data in Panel B represent the average value of technical duplicates from one set of autolysis assays. The autolysis assays were conducted on at least three separate occasions and similar results were obtained. Error bars in all panels represent standard deviations. Error bars are displayed for all data, but might be too small to see on occasion. Statistical significance was calculated using a two-tail Student's t-test and p-values >0.05 were considered to be not significant (NS) while * indicates p-value of <0.05.

## Figure 3.3

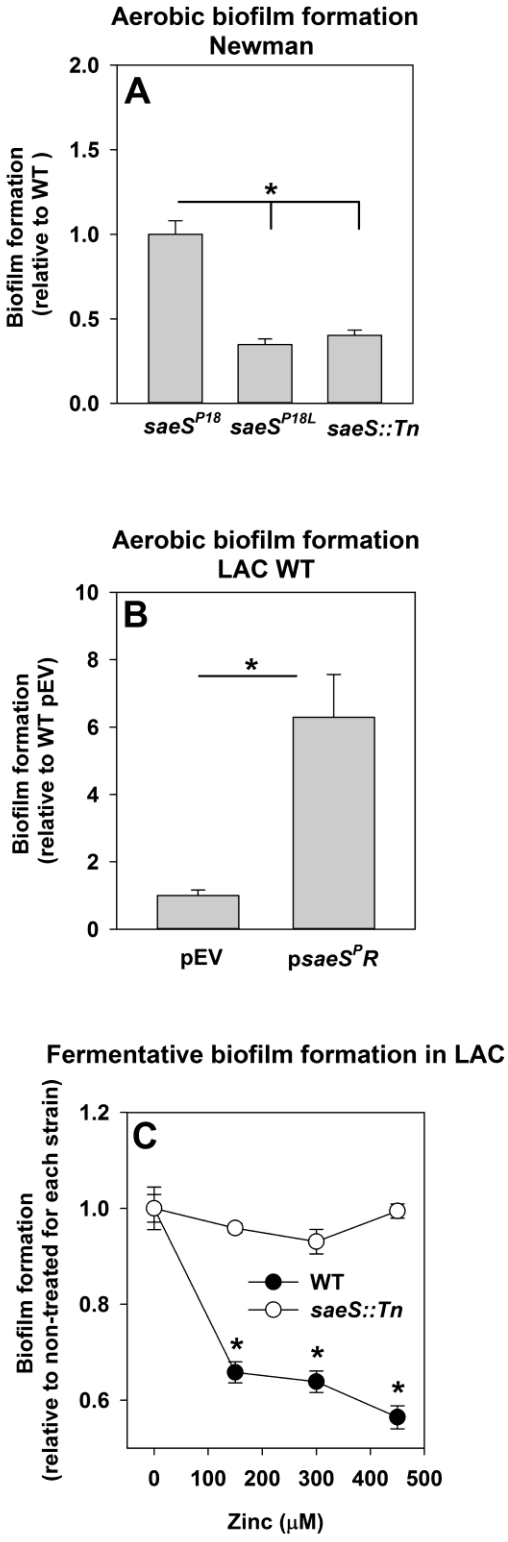
Aerobic biofilm formation
Newman
A
Biofilm formation
(relative to WT )
2.0
1.5
1.0
0.5
0.0
*
saeS^P18
saeS^P18L
saeS::Tn
Aerobic biofilm formation
LAC WT
B
Biofilm formation
(relative to WT pEV)
10
8
6
4
2
0
*
pEV
psaeS^PR
Fermentative biofilm formation in LAC
C
Biofilm formation
(relative to non-treated for each strain)
1.2
1.0
0.8
0.6
WT
saeS::Tn
*
*
*
0
100
200
300
400
500
Zinc (μM)

**Figure 3.3. Increased SaeR~P is required for fermentative biofilm formation and the SaeS kinase activity inhibitor zinc attenuates fermentative biofilm formation.** Panel A; The Newman strain of *S. aureus* forms SaeS$^{P18}$-dependent biofilms during aerobic growth. Aerobic biofilm formation for the Newman strain containing the natural *saeS*$^{P18}$ allele (JMB 1422), the *saeS*$^{L18}$ allele (JMB 8263), or the *saeS::Tn* (JMB 7077) mutation is displayed. Panel B; Constitutive expression of the *saeS*$^{P18}$ allele induces aerobic biofilm formation in the LAC WT strain. Biofilm formation of the LAC WT strain (JMB 1100) carrying pOS (pEV) or pOS_*saeS*$^{P18}$*R* following aerobic growth. Panel C; Supplementing media with zinc, an inhibitor of SaeS kinase activity, results in a concentration dependent decrease in fermentative biofilm formation. Biofilm formation of the LAC WT and the LAC *saeS::Tn* (JMB 7076) strain is displayed following fermentative growth in media supplemented with various concentrations of zinc. The data represent the average values of eight wells and error bars represent standard deviations. Error bars are displayed for all data, but on occasion may be too small to see. Statistical significance was calculated using a two-tail Student's t-test and * indicates p-value of <0.05.

## Figure 3.4

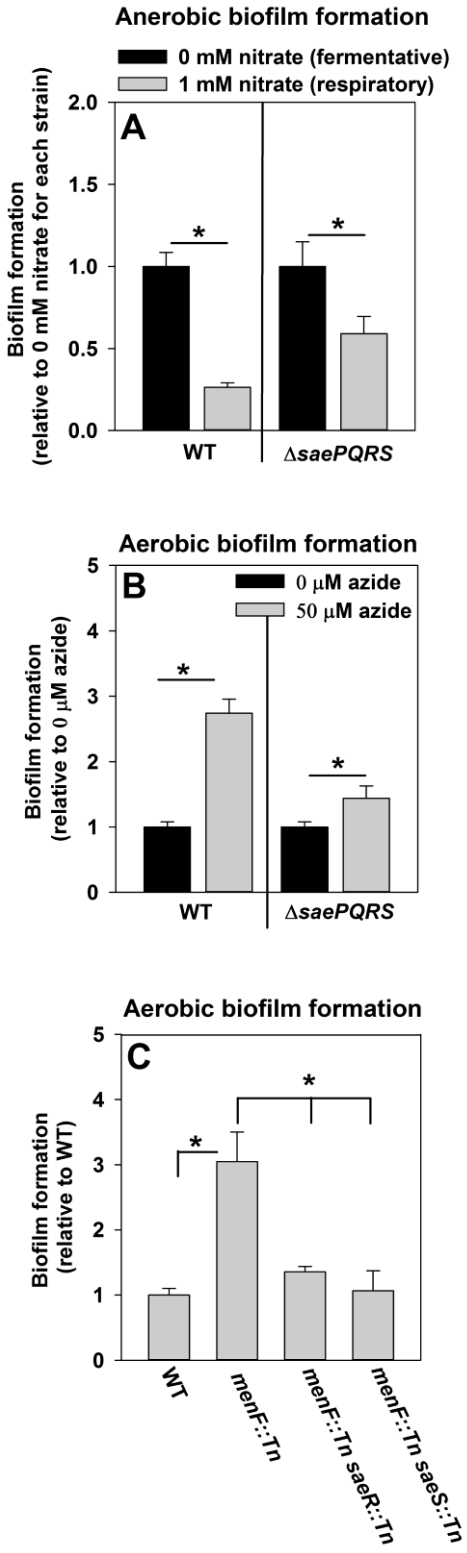
Anerobic biofilm formation
0 mM nitrate (fermentative)
1 mM nitrate (respiratory)
Biofilm formation
(relative to 0 mM nitrate for each strain)
2.0
1.5
1.0
0.5
0.0
A
*
*
WT
ΔsaePQRS
Aerobic biofilm formation
B
0 μM azide
50 μM azide
Biofilm formation
(relative to 0 μM azide)
5
4
3
2
1
0
*
*
WT
ΔsaePQRS
Aerobic biofilm formation
C
Biofilm formation
(relative to WT)
5
4
3
2
1
0
*
*
WT
menF::Tn
menF::Tn saeR::Tn
menF::Tn saeS::Tn

**Figure 3.4. SaeRS dependent biofilm formation is responsive to the cellular respiratory status and a menaquinone auxotroph forms Sae-dependent biofilms.** Panel A; Biofilm formation of a Δ*saePQRS* strain is largely unaltered upon supplementing anaerobic biofilms with the alternate electron acceptor nitrate. Biofilm formation of the WT (JMB 1100) and the Δ*saePQRS* (JMB 1335) strains following anaerobic growth in the presence or absence of 1 mM nitrate is displayed. Panel B; Biofilm formation in a Δ*saePQRS* strain is largely unaltered upon chemical inhibition of respiration. Biofilm formation of the WT and Δ*saePQRS* strains following aerobic growth in the presence or absence of 50 μM azide is displayed. Panel C; A menaquinone auxotroph forms SaeRS-dependent biofilms aerobically. Aerobic biofilm formation of the WT, *menF::Tn* (JMB 6219), *menF::Tn saeR::Tn* (JMB 7109), *menF::Tn saeS::Tn* (JMB 7081) strains is displayed. The data represent the average values of eight wells and error bars represent standard deviations. Error bars are displayed for all data, but on occasion may be too small to see. Statistical significance was calculated using a two-tail Student's t-test and * indicates p-value of <0.05.

## Figure 3.5

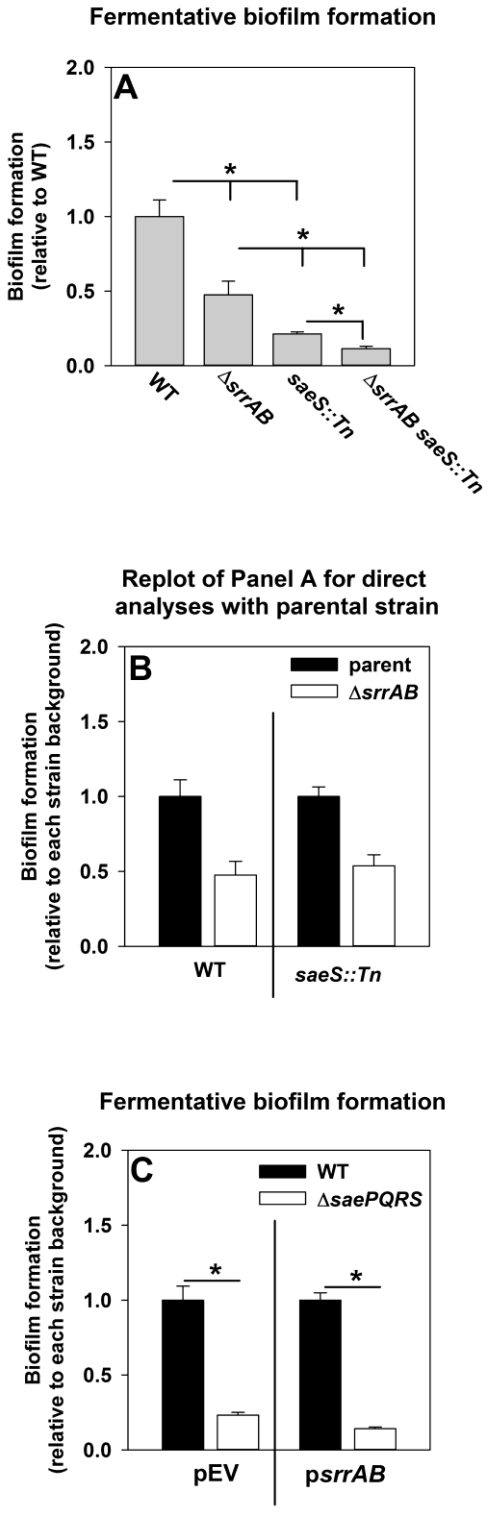
Fermentative biofilm formation
A
Biofilm formation (relative to WT)
2.0
1.5
1.0
0.5
0.0
*
*
*
WT
ΔsrrAB
saeS::Tn
ΔsrrAB saeS::Tn
Replot of Panel A for direct analyses with parental strain
B
Biofilm formation (relative to each strain background)
parent
ΔsrrAB
WT
saeS::Tn
Fermentative biofilm formation
C
Biofilm formation (relative to each strain background)
WT
ΔsaePQRS
pEV
psrrAB

**Figure 3.5. SaeRS and SrrAB influence fermentative biofilm formation independent of one another.** Panel A and B; The biofilm formation phenotypes of the Δ*saeS::Tn* and Δ*srrAB* mutations are additive. Biofilm formation of the WT (JMB 1100), Δ*srrAB* (JMB 1467), *saeS::Tn* (JMB 7076), and Δ*srrAB saeS::Tn* strains following fermentative growth is displayed. Data were normalized with respect to the WT (Panel A) or with respect to the parental strain into which the Δ*srrAB* mutation was introduced (i.e., WT or *saeS::Tn*) (Panel B). Panel C; The presence of *srrAB* in multi-copy does not rescue its biofilm formation defect of the Δ*saePQRS* strain. Biofilm formation of the WT and Δ*saePQRS* (JMB 1335) strains carrying either pCM28 (pEV) or pCM28_*srrAB* (p*srrAB*) is displayed following fermentative growth. The data represent the average values of eight wells and error bars represent standard deviations. Error bars are displayed for all data, but on occasion may be too small to see. Statistical significance was calculated using a two-tail Student's t-test and * indicates p-value of <0.05.

**Figure 3.6**

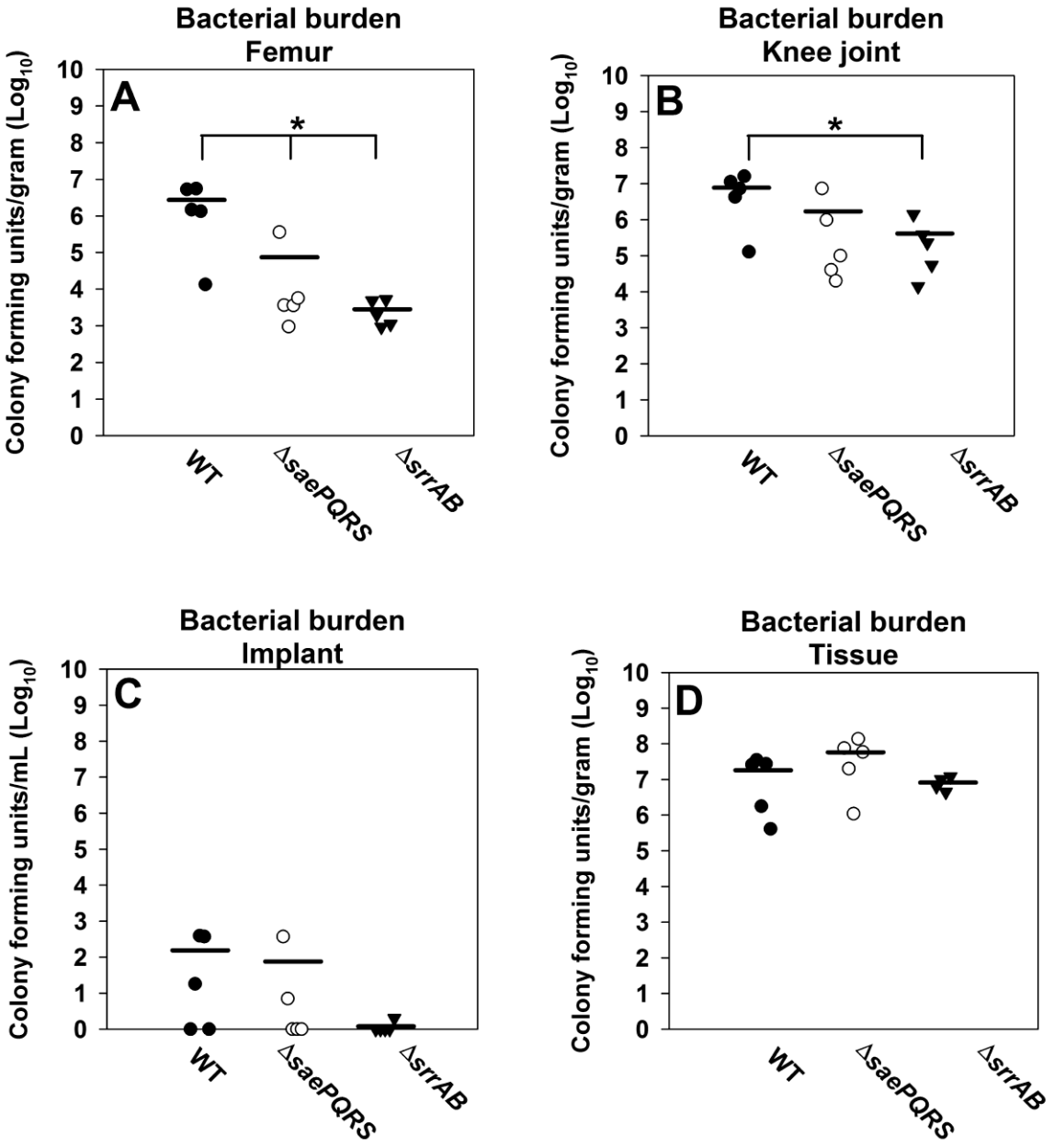


**Figure 3.6. SaeRS and SrrAB influence biofilm persistence in a murine model of orthopedic implant biofilm infection.** Panels A-D; Male C57BL/6 mice were infected with the WT (JMB 1100), Δ*saePQRS* (JMB 1335) and the Δ*srrAB* (JMB 1467) strains (n=5/group). Animals were sacrificed at 14 days

following infection, whereupon the implant was sonicated and host tissues surrounding the infected orthopedic implant site were homogenized to quantitate bacterial burdens. Results are expressed as CFU per milliliter for the implant and CFU per gram of tissue (for the soft tissue surrounding the knee, knee joint containing ligament and tendon structures, and femur) to normalize for differences in sampling size. Significant differences in bacterial burdens between mice are denoted by asterisks (*, $p < 0.05$). Statistics were conducted using a one-way analysis of variance (ANOVA), followed by Bonferroni's multiple-comparison test.

**Figure 3.7**

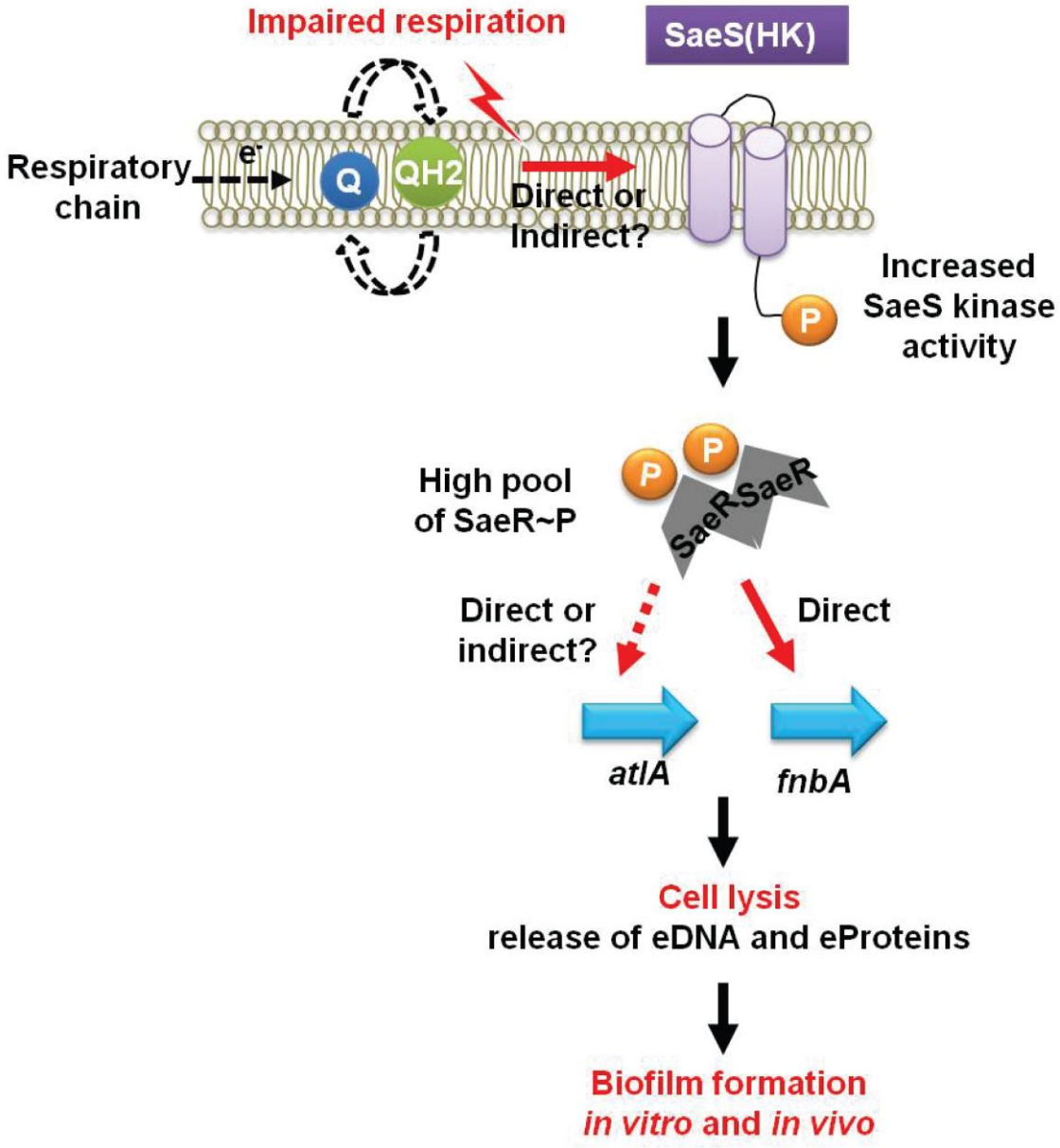


**Figure 3.7. A working model for the influence of respiration upon SaeRS-dependent autolysis and biofilm formation in *S. aureus*.** A decreased capacity to respire stimulates the SaeS HK, in an as yet unknown manner, and subsequently results in increased phosphorylation of SaeR. Increased levels of SaeR~P effects greater expression of the AtlA murein hydrolase facilitating

autolysis and the release of DNA and proteins. Increased titers of SaeR~P also results in increased expression of FnBPA. Increased FnBPA and the accumulation of polymeric cellular molecules released during autolysis increases biofilm formation.

**Table 3.1. Strains and plasmids used in this study.**

| **Strains used in this study** | | | |
|---|---|---|---|
| ***S. aureus* Strains** | **Genotype/Description** | **Genetic Background** | **Source/ Reference** |
| JMB1100 | Wild-type; USA300_LAC (erm sensitive); MRSA; CC8; $SaeS^{L18}$ | LAC | (10) |
| RN4220 | Restriction minus; MSSA; CC8 | NCTC8325 | (82) |
| JMB 1467 | Δ*srrAB* (SAUSA300_1441-42) | LAC | (119) |
| JMB 2047 | Δ*srrAB::tet* | LAC | (101) |
| JMB 2078 | *katA::Tn* (ermB) (SAUSA300_1232) | LAC | V. Torres |
| JMB 1422 | parent, Newman, MSSA, CC8; $SaeS^{P18}$ | Newman | Eric Skaar and (37) |
| JMB 8263 | $SaeS^{P18L}$ chromosomal allelic replacement | Newman | (89). |
| JMB 7076 | *saeS::Tn(ermB)* | LAC | This work, BEI resources (39) |
| JMB 7077 | *saeS::Tn(ermB)* | Newman | This work, BEI resources (39) |
| JMB 6625 | *atlA::Tn(ermB)* | LAC | This work, BEI resources (39) |
| JMB 6623 | Δ*saePQRS::spec atlA::Tn(ermB)* | LAC | This work |
| JMB 6620 | *aur::Tn(ermB)* | LAC | This work, BEI resources |

| | | | |
|---|---|---|---|
| | | | (39) |
| JMB 6618 | Δ*saePQRS::spec aur::Tn(ermB)* | LAC | This work |
| JMB 6029 | *menF::Tn(ermB)* | LAC | This work, BEI resources (39) |
| JMB 6219 | *menF::Tn(tet)* | LAC | (104) |
| JMB 7081 | *saeS::Tn(ermB) menF::Tn(tet)* | LAC | This work |
| JMB 7100 | *saeR::Tn(ermB)* | LAC | This work, BEI resources (39) |
| JMB 7109 | *saeR::Tn(ermB) menF::Tn(tet)* | LAC | This work |
| JMB 6460 | Δ*srrAB::tet* Δ*saePQRS::spec* | LAC | This work |
| JMB 8403 | *fnbA::Tn(ermB)* | LAC | This work, BEI resources (39) |
| JMB 1148 | Δ*hptRS* | LAC | (119) |
| JMB 1357 | Δ*lytSR* | LAC | (119) |
| JMB 1330 | *graS::erm* | LAC | (10) |
| JMB 1335 | Δ*saePQRS::spec* | LAC | (113) |
| JMB 1219 | ΔSAUSA300_1219-1220 | LAC | (119) |
| JMB 1383 | Δ*arlSR* | LAC | (119) |
| JMB 1358 | Δ*phoSR* | LAC | (119) |
| JMB 1241 | Δ*airSR* | LAC | (119) |
| JMB 1377 | Δ*vraSR* | LAC | (119) |
| JMB 1333 | Δ*agr::tetM* | LAC | (76) |
| JMB 1223 | Δ*kdpSR* | LAC | (119) |
| JMB 1359 | Δ*hssSR* | LAC | (119) |
| JMB 1145 | Δ*nre*SR | LAC | (119) |

| | | | |
|---|---|---|---|
| JMB 1232 | ΔSAUSA300_2558-2559 | LAC | (119) |

**Other Strains**

| | |
|---|---|
| *Escherichia coli* PX5 | Protein Express |
| *Sacchromyces cerevisiae FY2* | William Belden |

**Plasmids used in this study**

| **Plasmid name** | **Insert Locus/function** | **Source/Reference** |
|---|---|---|
| pCM28 | Insertless cloning vector | A. Horswill |
| pCM28_*saePQRS* | *saePQRS* complementing vector | This work |
| pCM28_*srrAB* | *srrAB* complementing vector | (101) |
| pOS-1 | Insertless cloning vector | |
| pOS_*saeQRS*$^{P18}$ | Vector carrying constitutively active SaeS allele, cloned from Newman | Victor Torres |
| pTnTet | Construction of *menF::Tn* (Tet) | (11) |
| pJB141 | *atlA* complementing vector | (12) |
| pJB135 | $atlA_{GL}$ complementing vector | (12) |
| pJB122 | $atlA_{AMH263A}$ complementing vector | (12) |
| pJB128 | Insertless cloning vector | (12) |
| pJB111 | $atlA_{AM}$ complementing vector | (12) |

# CHAPTER 4

## Resumption of respiration results in the detachment and dispersal of pre-formed fermentative *Staphylococcus aureus* biofilms

**Abstract:**

Biofilms are communities of bacterial cells that are attached to a surface and encased within an extracellular matrix. Oxygen is utilized by *S. aureus* as a TEA. Infected human tissues are hypoxic or anoxic. Decreased oxygen concentrations have been found to elicit a programmed cell lysis phenomenon in *S. aureus* that culminates in the establishment of biofilms. PCL is governed, in part, by the SrrAB TCRS in response to alterations in the respiratory status of the cell. PCL is effected via increased expression of the AtlA murein-hydrolase, resulting in autolysis, the release of cellular polymers such as DNA and culminating in increased biofilm formation. Biofilm formation imparts protection from innate immunity as well as therapeutic agents. Herein we report that pre-formed biofilms established by fermenting *S. aureus* could be prompted to detach and disperse upon exposure to a TEA (oxygen or nitrate). Exposure to oxygen (reaeration) results in increased growth but decreased transcription of *atlA* and decreased release of eDNA, suggesting a reversal of PCL. Reaeration is also accompanied by increased transcription of *sspA* which encodes for a protease capable of cleaving AtlA. Biofilm dispersal was blocked in a strain that is incapable of respiration, suggesting changes in cellular respiratory status are required to trigger dispersal. SrrAB is responsive to changes in the respiratory status of the

cell. The transcription of *atlA* and *sspA* upon reaeration was modulated in a divergent manner by SrrAB. Genetic data are presented that suggest that SrrAB achieves divergent regulation of *atlA* by using the small RNA, *rsaE*, as an intermediary.

**Introduction:**

*S. aureus* is a commensal organism that colonizes between 20-50% of the human population (38, 51, 108, 114, 164). In response to certain stimuli, *S. aureus* has the capability to colonize nearly every tissue of the body and cause aggressive infections (78). Classically, *S. aureus* infections were nosocomial in origin, however, these infections increasingly transpire in community settings (78, 148). Treatment of *S. aureus* infections has become increasingly complex due an increase in antibiotic resistance. Clinical isolates have been identified that are resistant to nearly all known antibiotics, including the last-line antibiotics linezolid and daptomycin (20, 129, 130).

Persistent *S. aureus* infections, such as osteomyelitis, are associated with the ability of this bacterium to establish biofilms (28, 137). Biofilms are complex communities of bacteria attached to a surface, or to each other, and embedded in a polymeric matrix (6, 27, 28). The matrix is composed of organic materials, synthesized by the bacteria, and provides protection from the human innate immunity and therpeutic agents (6, 27, 28). When living in biofilms bacteria make lifestyle choices together, in a manner reminiscent of multi-cellular organisms (6,

27, 28). Reflective of their clinical significance, biofilms are considered to be the etiologic agents of recurrent staphylococcal infections (70, 117).

*S. aureus* biofilms are composed of one or more polymeric molecules (DNA, proteins, or polysaccharides) that provide structural integrity and may also facilitate intercellular adhesion (9, 29, 126, 136). The extracellular polymer(s) utilized to facilitate biofilm formation can vary between staphylococcal isolates with some favoring DNA and/or proteins and others polysaccharides (9, 29, 126, 136). The complexity of biofilm formation results in this process being highly regulated and deterministic. Biofilm formation in *S. aureus* is responsive to diverse signals including nutrient limitation and quorum sensing (9, 70, 92, 117).

One characteristic of the growth cycle of biofilms is the periodic detachment and shedding of bacterial cells (70). The detached cells effect the dispersal of infection (70). Changes in the levels of quorum sensing molecules is one stimulus that initiates dispersal in *S. aureus* (9). Dispersal is achieved by the production of proteins that degrade the core polymeric molecules that constitute the biofilm, thereby effecting cell detachment (9). Production of a particular matrix degrading protein will presumably be governed by the composition of the matrix polymers.

*S. aureus* is a facultative anaerobe. Oxygen is the primary TEA supporting its respiratory growth (19, 54). However, upon limitation of oxygen, *S. aureus* can utilize fermentative pathways to generate energy (19, 54). Oxygen concentrations vary between healthy and infected or necrotic tissues, as well as in wounds, where they are estimated to be below 1% (hypoxic) or anoxic

(complete lack of oxygen) (3, 18, 151). Oxygen concentrations progressively decrease, in colonized sites, as infection proceeds.

Oxygen impacts *S. aureus* biofilm formation in its capacity as a TEA for cellular respiration (104). Decreased oxygen concentrations or its absence (fermentative growth) inhibit respiration, which serves as a signal that elicits PCL culminating in increased biofilm formation. Consistent with this logic chemical or physiological conditions that diminish the ability of cells to respire prompt an increased biofilm formation response. AtlA, a peptidoglycan hydrolase, is the dominant factor facilitating cell-lysis. AltA-dependent cell lysis results in the release of high molecular weight DNA and cytosolic proteins into the extracellular milieu. The exracellular DNA (eDNA) and proteins are incorporated into the biofilm matrix and serve as integral structural elements (104).

The ability of *S. aureus* to sense various environmental stimuli, and rapidly calibrate its cellular physiology in response, is a cornerstone of its success as a pathogen. TCRS are modular regulatory systems that facilitate the integration of multiple stimuli into signaling circuits, allowing for a rapid response to environmental alterations (145, 146). TCRS consist of a histidine kinase (HK) and a response regulator (RR). The system input occurs at the level of the HK which is the protein that interacts with the stimuli. The stimuli can be either intracellular or extracellular, and the HK itself can be either membrane associated or cytosolic. HKs can have one or more of the following functionalities: they can undergo autophosphorylation, transfer phosphoryl groups to the RR or remove phosphoryl groups from the RR. Interaction with a

signal molecule alters the functionality of the HK thereby effecting changes in the levels of the phosphoryl group upon the RR. The levels of phosphoryl groups upon the RR at any given point determine whether system output is increased or decreased. In the case of DNA binding RR's, changes in the phoshporyl levels alter the affinity of the protein for DNA leading to changes in gene transcription and a tailored physiological response (145, 146). PCL and biofilm formation under low oxygen tension are governed, in part, by the SrrAB TCRS, wherein SrrA is a DNA binding RR and SrrB is the HK (104).

The goal of the current study was to examine whether the cellular respiratory status could serve as a stimulus that prompts pre-formed biofilms of *S. aureus* to detach and disperse. We report that exposing fermenting *S. aureus* to a TEA prompts biofilms to disperse. Exposure of fermenting cells to oxygen (reaeration) elicited a programmed response: decreased transcription of *atlA*, but increased transcription of the gene encoding for the AtlA degrading protease SspA (*sspA*). The transcriptional changes in *atlA* and *sspA* transcription upon reaeration were modulated by SrrAB. A previous study found SrrAB positively modulates *atlA* transcription fermentatively. Herein we report data suggesting that the small RNA *rsaE* is employed as an intermediary by SrrAB, thereby allowing the divergent regulation of *atlA*.

**Results:**

**Biofilms formed by fermenting *S. aureus* detach and disperse when provided with a terminal electron acceptor and the cells resume growth.** Oxygen is a TEA utilized by *S. aureus* for respiration to generate energy for biomass production (19, 54). When *S. aureus* is deprived of oxygen and compelled to rely upon fermentative growth for energy generation it establishes biofilms (104). We examined whether this process could be reversed upon providing fermenting cells with a TEA. To this end the community-associated MRSA strain LAC (hereafter wild-type; WT) was cultured fermentatively and subsequently one set was exposed to oxygen (reaeration) and thereafter colony forming units and biofilm formation was assessed in both sets. Reaeration of cultures resulted in increased growth, but decreased biofilm formation in the WT strain (Figure 4.1A and 4.1B). *S. aureus* can also utilize nitrate as an electron acceptor. Biofilm formation decreased when fermentatively cultured biofilms of the WT strain were exposed to nitrate (Figure 4.1C).

**Reaeration results in decreased transcription of *atlA* and reduced accumulation of eDNA**. AtlA, a peptidoglycan hydrolase, is the dominant factor required for the formation of fermentative biofilms (104). Simple enegertics would suggest that biofilm dispersal would require for inhibition or reversal of processes involved in biofilm formation. Thus, we reasoned that reaeration would result in decreased transcription of *atlA*. Consistent with our premise, *atlA* transcription was decreased by ~2 fold when fermenting WT cultures were reaerated (Figure

4.2A). As a positive control in our experiment we also assessed the transcript levels corresponding to *kat*, a gene encoding for catalase (Kat). Kat (*kat*) is required to scavenge reactive oxygen species and its expression would be expected to increase upon reaeration. Indeed, *kat* transcript levels increased by ~4 fold (Figure 4.2A).

One outcome of *S. aureus* autolysis is the release of high molecular weight genomic DNA into the extracellular milieu (eDNA) (41, 126). Decreased AtlA-activity would be expected to lead to decreased release of eDNA. Consistent with this reasoning, reaerated WT displayed decreased accumulation of high molecular weight DNA in its biofilm matrixes, relative to fermenting WT (Figure 4.2B).

**Reaeration results in increased transcription of the gene encoding for the AtlA degrading serine protease, SspA**. Biofilm dispersal would require the production of proteins capable of degrading the biofilm matrix polymers. Extracellular proteins are an integral component of fermenting biofilms (104). Studies have found that the extracellular serine protease, SspA, is involved in biofilm formation (9, 22, 139). AtlA is a bifunctional enzyme that is proteolytically cleaved into a N-acetylmuramyl-L-alanine amidase and endo-β-N-acetylglucosaminidase (116). A recent study found that purified SspA is capable of cleaving AtlA-derived peptidoglycan hydrolases (22). Further, supplementing WT biofilms with purified SspA results in decreased biofilm formation (22). Thus, we reasoned that *S. aureus* would increase the transcription of *sspA* upon

reaeration. Consistent with this premise, the transcript levels corresponding to SspA increased by ~3 fold upon aeration (Figure 4.3).

**Changes in cellular respiratory status elicit biofilm dispersal.** Diminished respiration elicits biofilm formation in *S. aureus* (104). We examined wehether alterations in the cellular respiratory status also determine whether cells should undergo biofilm dispersal. Biofilm dispersal would be predicted to be blocked in a strain that is incapable of respiring since this strain would experience no changes in the cellular respiratory status upon reaeration. A heme auxotroph has non-functional terminal oxidases and is unable to respire upon oxygen (54). Consistent with our premise, biofilm dispersal, upon reaeration or supplementation with nitrate, was attenuated in a *hemB::Tn* strain (Figure 4.4A and 4.4B).

**SrrAB divergently modulates *atlA* and *sspA* transcript levels upon reaeration.** SrrAB is responsive to changes in the cellular respiratory status (77, 104). We examined whether SrrAB influences the transcription of genes involved in biofilm dispersal. The WT and Δ*srrAB* strains were cultured fermentatively or reaerated and the transcript levels corresponding to *atlA* and *sspA* were determined. Transcript levels of *atlA* decreased in the WT strain upon reaeration while they increased in a Δ*srrAB* strain (Figure 4.5A). Transcript levels of *sspA* increased upon reaeration in both strains (Figure 4.5B). However, ratiometric analyses revealed that the induction in transcript levels was attenuated in the

Δ*srrAB* strain. From these data we conclude that SrrAB negatively influences *atlA* transcription upon reaeration, but positively influences *sspA* transcription.

**SrrAB negatively influences *sspA* transcription during fermentative growth, and the fermentative biofilm formation defect of a Δ*srrAB* strain can be rescued upon co-culture with a serine protease inhibitor.** A strain lacking SrrAB is deficient in the formation of fermentative biofilms. SrrAB influences *atlA* transcription during fermentative growth (104). We examined whether SrrAB also influences *sspA* transcription during fermentative growth. A *srrAB* strain displayed ~2.5 fold increase in *sspA* transcript levels (Figure 4.6A). Increased levels of SspA would be detrimental to biofilm formation. We examined whether the spent-media supernatant from a Δ*srrAB* strain contained anti-biofilm activity. Biofilms of the WT and Δ*srrAB* strains were cultured fermentatively and sterile cell-free spent-media supernatant was isolated. Subsequently the WT strain was cultured in the presence or absence of the isolated sterile spent-media supernatant and fermentative biofilm formation was examined. Supplementation with spent-media supernatant from the Δ*srrAB* strain, but not from the WT strain, diminished biofilm formation, confirming the presence of an anti-biofilm molecule in the supernatant from the Δ*srrAB* strain (Figure 4.6B).

SspA is a serine protease. If the Δ*srrAB* strain produces a greater amount of SspA, then chemical inhibition of serine protease activity would be expected to suppress the biofilm formation defect of this strain. In contrast, inhibition of cysteine protease or metalloprotease activity, which are alternate proteases

produced by *S. aureus*, should not rescue biofilm formation. Consistent with our premise, the biofilm formation defect of the Δ*srrAB* strain was partially suppressed upon co-culture with the serine protease inhibitor phenylmethylsulfonyl flouride. No rescue was observed upon co-culturing the Δ*srrAB* strain in the presence of the cysteine protease inhibitor, E-64, or the metalloprotease inhibitor, 1,10 phenanthroline (Figure 4.6C, 4.6D and 4.6E).

**Biofilm dispersal occurs at a faster rate in a Δ*srrAB* strain, consistent with increased production of SspA in this strain.** The Δ*srrAB* strain produces a decreased amount of transcript relative to *atlA* upon fermentative growth, but an increased amount of *sspA*. Thus upon reaeration, we reasoned that the biofilm formed by this strain would disperse at a faster rate. Indeed, reaeration resulted in faster dispersal of the biofilm formed by fermenting Δ*srrAB,* than the WT (Figure 4.7).

**RsaE modulates *S. aureus* biofilm formation in a AtlA-dependent manner and *rsaE* transcript is decreased upon reaeration in a SrrAB-dependent manner.** SrrAB modulates the transcription of *atlA* in a divergent manner: positively during fermentative growth, but negatively during reaeration. One way in which SrrAB could achieve this would be by using an alternate regulatory system as an intermediary. SrrAB regulates expression of the small RNA RsaE (36). RsaE in turn positively regulates the transcript levels for *atlA* (46). We examined whether RsaE influences biofilm formation in *S. aureus* and whether

this occurs in a AtlA-dependent manner. Biofilm formation was examined in the WT and *atlA::Tn* strains carrying a plasmid expressing *rsaE* in sense and under the transcriptional control of an inducible promoter. AtlA expression during fermentative growth is substantially increased. Thus, biofilm formation was assessed aerobically, to avoid the effect of unregulated cell lysis upon over-expression of AtlA. Biofilm formation increased in the WT strain in synchrony with increasing concentration of inducer in the medium, but not in the *atlA::Tn* strain (Figure 4.8A).

We reasoned that upon reaeration transcript levels for *rsaE* would decrease and that this would occur in a SrrAB-dependent manner. Consistent with this prediction, transcript levels for *rsaE* decreased by ~3 fold upon reaeration and this decrease was mediated entirely by SrrAB (Figure 4.8B).

**Discussion:**

Biofilm dispersal results in the dissemination of infections and consequently biofilm-associated cells serve as the etiologic agents of recurrent staphylococcal infections (70, 117). Diminished respiration elicits biofilm formation by *S. aureus* (104). The goal of the current study was to examine whether alterations in the cellular respiratory status serve as a signal that prompts pre-formed biofilms to disperse. We report that exposure of fermenting *S. aureus* to a TEA (oxygen (reaeration) or to nitrate) resulted in biofilm dispersal. Moreover, biofilm dispersal, upon reaeration, was blocked in a heme auxotroph, a strain incapable of respiring.

Fermentative growth results in increased expression of AtlA resulting in cell lysis and the release of cellular polymers such as DNA. AtlA expression would be expected to be decreased upon initiation of dispersal. Consistent with this premise, *atlA* transcript was decreased upon reaeration. Moreover, DNA accumulation in the extracellular mileu of reaerated cells was also substantially decreased, relative to fermenting cells. An alternate approach to decrease AtlA activity upon reaeration would be to proteolytically cleave the protein and thereby render it inactive. SspA is a serine protease that cleaves AtlA-derived peptidoglycan hydrolases (22). The transcript levels for *sspA* increased upon reaeration, suggesting that SspA is used to modulate the amounts of active autolysin.

The changes in transcript levels for *sspA* and *atlA* suggested that a regulatory mechanism was being triggered when cells were being reaerated. The SrrAB regulatory system is responsive to changes in the cellular respiratory status (77, 104). Thus, SrrAB could be modulating the changes in transcript levels. Indeed, a strain lacking SrrAB was unable to effect changes in *atlA* and *sspA* transcript levels upon reaeration.

We have previously reported that SrrAB positively influences AtlA expression during fermentative growth (104). Thus, we examined the possibility that SrrAB may also modulate SspA levels during fermentative growth. Indeed, SrrAB negatively influenced *sspA* transcription during fermentative growth. Moreover, supplementation of growth media with the serine protease inhibitor PMSF suppressed the fermentative biofilm formation defect of the Δ*srrAB* strain,

confirming that this strain produces an increased amount of serine protease(s). The biofilms formed by the Δ*srrAB* strain also dispersed at a faster rate, upon reaeration, consistent with increased levels of SspA.

How does SrrAB achieve divergent regulation of two cellular targets? One way to explain this would be if SrrAB modulates their expression directly under one growth phase, but indirectly via an alternate regulatory system in the second growth phase. In support of this model, the promoter regions for both *sspA* and *atlA* contain the recently described SrrA binding site (101). One regulatory system that could be utilized as an intermediary by SrrAB, was the small RNA *rsaE*. SrrAB modulates the expression of *rsaE*, while *rsaE* is known to modulate the expression of *sspA* and *atlA* (36, 46). We found that the overexpression of *rsaE* elicited biofilm formation in an AtlA-dependent manner. Moreover, the expression of *rsaE* was decreased upon reaeration and this was completely SrrAB-dependent.

SrrAB increases fermentative biofilm formation upon the cellular enrichment of reduced menaquione (104). However, upon reaeration, in the context of a dispersing biofilm, the levels of reduced menaquinone would be expected to be low. Mechanistically, how does one explain the divergent roles of SrrAB? Considering that SrrAB is a TCRS, the following assumptions could readily reconcile these findings: a) the cellular accumulation of SrrA~P is altered upon reaeration and b) SrrA~P displays variable affinity for target promoter regions, as observed with alternate RR's. Under this scenario, low levels of SrrA~P would bind high-affinity DNA sequences, while high levels of SrrA~P

would bind to low-affinity DNA sequences. Thus the SrrAB regulon would be composed of 2 classes of genes. A preliminary assessment of promoter regions known to be SrrA targets provides some support to this idea. The consensus sequence for SrrA was reported to be $AAATAN_{3-6}TTAT$. It is interesting to note that genes known to be repressed by SrrA have a spacer region of 3 base-pairs, while the spacer regions tend to be longer in positively influenced genes (data not displayed). Further, in our hands, during fermentative growth, SrrAB typically acts as a repressor (~7 alternate targets). However, these ideas need further experimentation.

HBOT is a treatment in which patients are placed inside a chamber with pressure higher than sea level (138, 141). In the chamber patients inhale 100% oxygen, intermittently (138, 141). It is intriguing to note that HBOT is a medically approved therapy used in managing necrotizing soft tissue infections and chronic osteomyelitis, infections which are closely associated with the ability of *S. aureus* to form biofilms (48, 117, 138). Current evidence suggests that HBOT allows the body to resolve infections due its beneficial effects upon human innnate immunity (72, 165). Polymorphonuclear leukocytes (PMNs) and macrophages form the first line of defense against bacterial infections (109). These cells assault bacteria with reactive-oxygen species (ROS) produced by the enzymes NADPH oxidase and myeloperoxidase, to help resolve infections (109). Increased oxygen diffusion into tissues, due to HBOT therapy, is presumed to boost the function of the PMN's and macrophages (72, 165). However, in light of our findings, we propose that HBOT therapy is likely beneficial due to a two-fold effect. In addition

to boosting innate immunity, increased oxygen diffusion into the tissues elicits biofilm dispersal in *S. aureus*. Biofilm dispersal allows increased contact between the innate immune system and the bacteria, thereby allowing infections to be cleared. However, this remains to be tested experimentally.

In summary, we report that pre-formed biofilms of *S. aureus* can be prompted to disperse upon the resumption of respiration. The dispersal process is achieved via divergent regulation of *atlA* and *sspA* resulting in decreased accumulation of polymeric molecules that faciltate matrix formation. Dispersal is a regulated process that is modulated via the SrrAB TCRS and the *rsaE* small RNA in response to the respiratory status of the cell.

**Material and Methods:**

**Materials**. Restriction enzymes, quick DNA ligase kit, deoxynucleoside triphosphates, and Phusion DNA polymerase were purchased from New England Biolabs. The plasmid mini-prep kit, gel extraction kit and RNA protect were purchased from Qiagen. DNase I was purchased from Ambion. Lysostaphin was purchased from Ambi products. Oligonucleotides were purchased from Integrated DNA Technologies and sequences are listed in Table S1. Trizol and High-Capacity cDNA Reverse Transcription Kits were purchased from Life Technologies. Tryptic Soy broth (TSB) was purchased from MP biomedical. Unless otherwise specified all chemicals were purchased from Sigma-Aldrich and were of the highest purity available.

**Bacterial growth conditions.** Unless otherwise stated, the *S. aureus* strains used in this study (Table 1) were constructed in the community-associated *S. aureus* USA300 LAC strain that was cured of the native plasmid pUSA03 that confers erythromycin resistance (10). Overnight cultures of *S. aureus* were grown at 37 °C in 10 mL culture tubes containing 1 mL of TSB or 30 mL culture tubes containing 5 mL TSB. Difco BiTek agar was added (15 g $L^{-1}$) for solid medium. When selecting for or against plasmids, antibiotics where added as previously (104).

*Growth model to assess biofilm formation.* The experimental setup was as described earlier (104). Aerobic, overnight cultures, were diluted into fresh TSB and incubated statically at 37 °C. For aerobic growth, the cultures were grown in 96-well microtiter plates containing 200 µL in each well or six-well plates containing 6 mL in each well and were covered with an Aera seal (Excel scientific), which allowed for uniform gas exchange. For anaerobic growth, cultures were inoculated aerobically followed immediately by passage through an airlock (3 vacuum/gas exchange cycles) into a COY anaerobic chamber equipped with a catalyst to maintain oxygen concentrations below one ppm. Anaerobic growth in the presence of a TEA was achieved by supplementing the media with sodium nitrate (prepared fresh daily).

**Recombinant DNA and genetic techniques.** *E. coli* DH5α was used as a cloning host for plasmid construction. All clones were passaged through RN4220 (82) and subsequently transduced into the appropriate strains using bacteriophage 80α (111). All *S. aureus* mutant strains and plasmids were verified using PCR, sequencing of PCR products or plasmids (Genewiz, South Plainfield, NJ), or genetic/chemical complementation of phenotypes.

**Static model of biofilm formation.** Biofilm formation was examined as described earlier, with minor changes (99). Overnight cultures were diluted into fresh TSB to a final optical density of 0.05 ($A_{590}$). 200 µL aliquots of diluted cultures were added to the wells of a 96-well microtitre plate (Corning 3268) and the plate was subsequently incubated statically at 37 °C for 22 hours. Where mentioned, biofilms were re-exposed to oxygen (reaeration) or supplemented with nitrate for 8 hours. Prior to harvesting the biofilm, the optical density ($A_{590}$) of the cultures was determined. The plate was subsequently washed twice with water, biofilms were heat fixed at 60 °C, and the plates were allowed to cool to room temperature. The biofilms were stained with 0.1% crystal violet, washed thrice with water, destained with 33% acetic acid and the absorbance of the resulting solution was recorded at 570 nm, standardized to an acetic acid blank, and subsequently to the optical density of the culture upon harvest. Finally, the data were normalized with respect to the WT or as described in the figure legends to obtain relative biofilm formation.

**Quantitative real-time PCR assays.** Cell growth was described earlier (102). Briefly, overnight cultures were diluted 100-fold into fresh TSB (~0.1 A600) and grown in capped microcentrifuge tubes until anaerobiosis was achieved (~1 A600). Anaerobic conditions were verified by addition of 0.001% resazurin to control tubes and the medium color was monitored over time. Cultures were grown for another 30 minutes to equilibrate completely to fermentative growth. Oxygen was reintroduced to one set of cultures by placing the cultures into glass tubes in an aerobic environment with a liquid to headspace ratio of 1:15. Cells were grown for an additional 25 minutes before 0.5 ml aliquots of cells were harvested. At point of harvest the spent medium was discarded and the remaining culture was immediately resuspended in RNAProtect reagent (Qiagen) and treated according to manufacturer instructions. The treated culture was subjected to centrifugation, the supernatant was discarded, and the cell pellet was resuspended in RNase free 50 mM Tris, pH 8. Cell-free extracts were generated using bead beating. RNA was extracted using Trizol, as per manufacturer instructions. Downstream treatments of the purified RNA and construction of cDNA libraries was as described earlier (102). Primers for PCR were designed manually or using the Primer Express 3.0 software from Applied Biosystems. Quantitative real time PCR reactions (Table S1) were conducted as described earlier (102).

**Quantification of high-molecular weight extracellular DNA.** eDNA was analyzed as described earlier with some changes (73). Overnight cultures were diluted into TSB to a final optical density of 0.05 ($A_{600}$) in a final volume of 6 mL per well of a six-well plate. The cultures were incubated statically at 37 °C for 22 hours or reaerated for 8 hours. At point of harvest, the spent media supernatant was aspirated out of each well. One mL of 1X phosphate buffered saline (PBS) was immediately added to the wells and a cell scraper was used to transfer the contents to an eppendorf tube. The biomass was pelleted by centrifugation and the supernatant was removed by aspiration. The pellets were thoroughly resuspended in 1X PBS and vortexed for 5 minutes using a Vortex Genie 2 (Scientific Industries) at the highest speed possible using a vertical micro-tube adapter. Aliquots were removed for determination of the viable cell count (colony forming units) and samples were pelleted by centrifugation. Control experiments verified that the viable cell counts were not affected by the vortexing procedure (data not shown). Equal volumes of the supernatants were assessed for the presence of high molecular weight DNA (>10 kilobases) using agarose gel electrophoresis. To assess the eDNA in a semi-quantitative manner, the gels were photographed and the bands were subjected to density analysis using Image J software. For each sample, the spot densities were normalized to the viable cell count (colony forming units) and subsequently as mentioned in the figure legends.

**Figure 4.1**

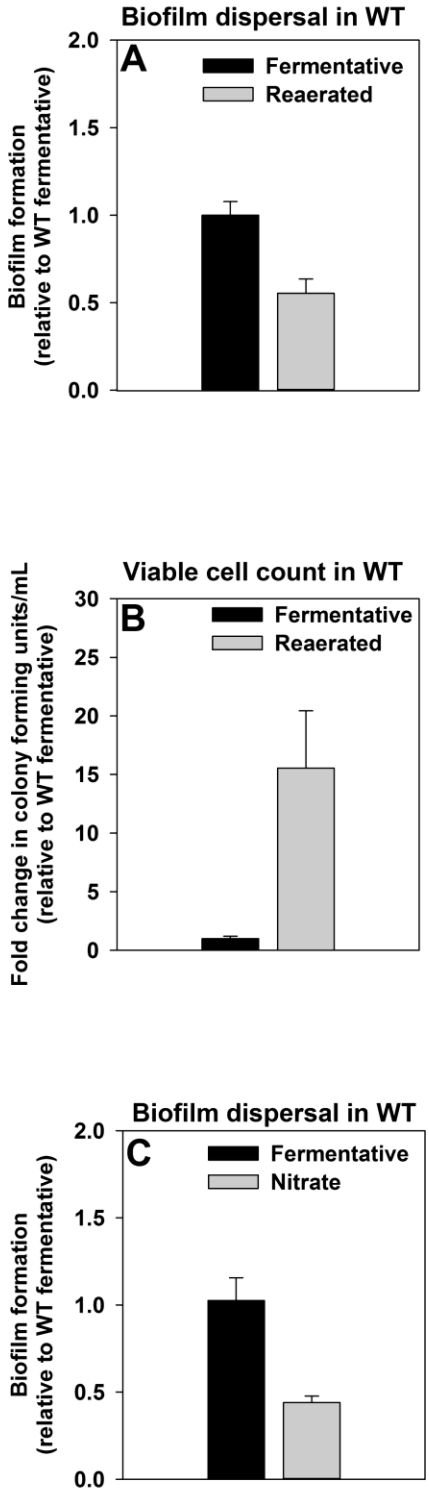
Biofilm dispersal in WT
A
Fermentative
Reaerated
Biofilm formation
(relative to WT fermentative)
2.0
1.5
1.0
0.5
0.0
Viable cell count in WT
B
Fermentative
Reaerated
Fold change in colony forming units/mL
(relative to WT fermentative)
30
25
20
15
10
5
0
Biofilm dispersal in WT
C
Fermentative
Nitrate
Biofilm formation
(relative to WT fermentative)
2.0
1.5
1.0
0.5
0.0

**Figure 4.1. Biofilms formed by fermenting *S. aureus* disperse when provided with a terminal electron acceptor and the cells resume growth.** Panels A; Biofilms formed by fermenting *S. aureus* disperse upon exposure of cells to oxygen (reaeration). Biofilm formation of the LAC (JMB1100; hereafter wild-type (WT) isolate following fermentative growth or upon reaeration (fermentative growth followed by aerobic growth) is displayed. Panel B; Reaearation results in increased viable cell count, suggesting increased growth of cells. Biofilms of the WT were cultured fermentatively or upon reaeration, biomass was homogenized and viable cell counts were obtained. Panel C; Biofilms formed by fermenting *S. aureus* disperse upon exposure of cells to nitrate. Biofilm formation of the WT following fermentative growth or upon exposure of fermenting cells to nitrate is displayed. The data represent the average values of six wells (Panels A and C) or triplicates (Panel B) and error bars represent standard deviations. Error bars are displayed for all data, but on occasion may be too small to see.

**Figure 4.2**

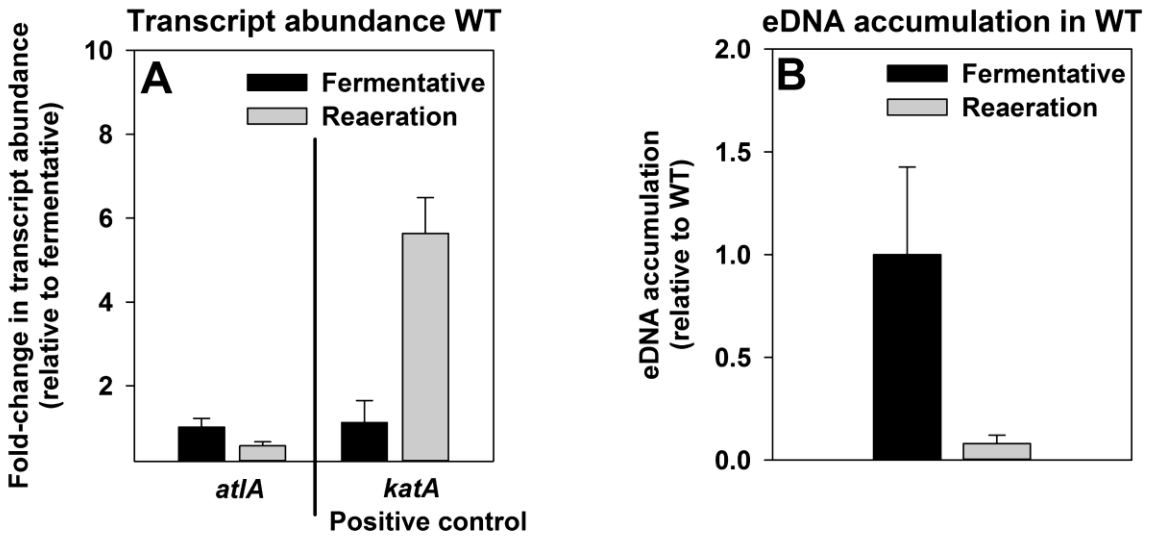


**Figure 4.2. Reaeration results in decreased transcription of *atlA* and reduced accumulation of eDNA.** Panel A; The *atlA* transcript is decreased upon reaeration. Biofilms of the WT (JMB 1100) were cultured fermentatively or reaerated, mRNA was extracted, and the abundance of the *atlA* and *katA* (positive control) transcript was quantified. The data were normalized to 16S rRNA levels, and thereafter, to levels observed fermentatively. Panel B; High molecular weight DNA (eDNA) accumulation is decreased in the biofilm matrix of reaerated cells. Biofilms of the WT were cultured fermentatively or reaerated, eDNA was extracted, and analyzed using agarose gel electrophoeresis. The data were normalized to the viable cell count, and thereafter, to eDNA accumulation in fermenting WT. The data represent the average values of triplicates and error bars represent standard deviations. Error bars are displayed for all data, but on occasion may be too small to see.

**Figure 4.3**

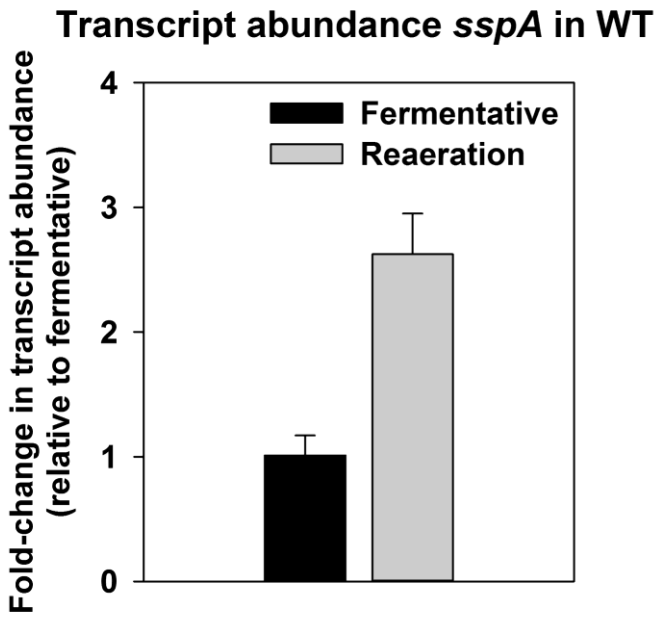


**Figure 4.3. Reaeration results in increased transcription of the gene encoding for the AtlA degrading serine protease, SspA.** Biofilms of the WT (JMB 1100) were cultured fermentatively or reaerated, mRNA was extracted, and the abundance of the *sspA* transcript was quantified. The data were normalized to 16S rRNA levels, and thereafter, to levels observed fermentatively. The data represent the average values of triplicates and error bars represent standard deviations.

**Figure 4.4**

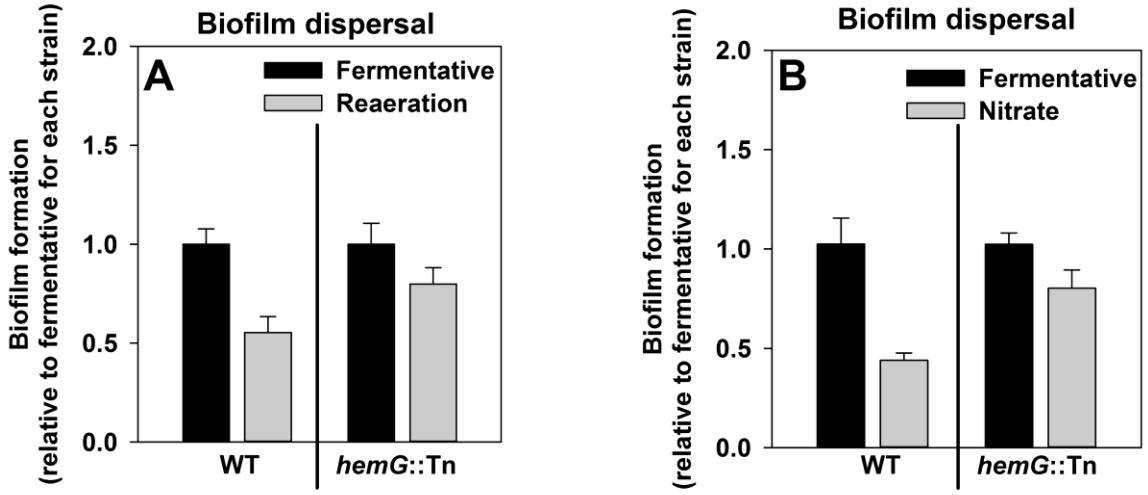


**Figure 4.4. Changes in cellular respiratory status elicit biofilm dispersal.** Panel A and B; Biofilms formed by a heme auxotroph, that is incapable of respiration, do not disperse upon exposure of cells to a TEA. Biofilm formation of the WT (JMB 1100) and *hemG::Tn* (JMB 4444) strains following fermentative growth and upon reaeration (fermentative growth followed by aerobic growth) (Panel A) or fermentative growth and following exposure to nitrate (Panel B) are displayed. The data represent the average values of six (Panel A) or seven (Panel B) wells and error bars represent standard deviations. Error bars are displayed for all data, but on occasion may be too small to see.

**Figure 4.5**

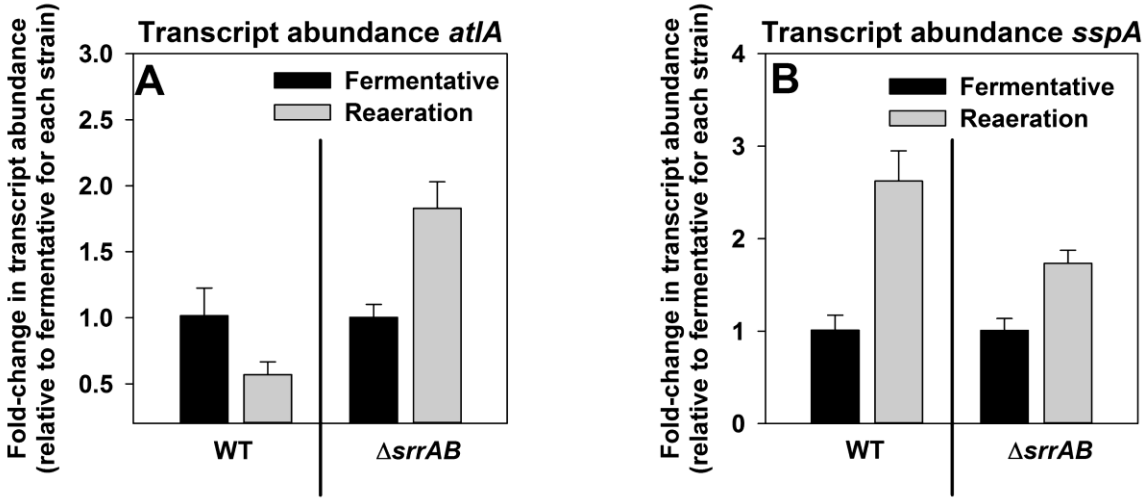


**Figure 4.5. SrrAB divergently modulates *atlA* and *sspA* transcript levels upon reaeration.** Panel A and B; SrrAB negatively influences *atlA* transcript levels, but positively influences *sspA* transcript levels, upon reaeration. Biofilms of the WT (JMB 1100) and Δ*srrAB* (JMB 1467) were cultured fermentatively or reaerated, mRNA was extracted, and the abundance of the *atlA* (Panel A) and *sspA* (Panel B) transcript was quantified. The data were normalized to 16S rRNA levels, and thereafter, to levels observed fermentatively for each strain. The data represent the average values of triplicates and error bars represent standard deviations.

**Figure 4.6**

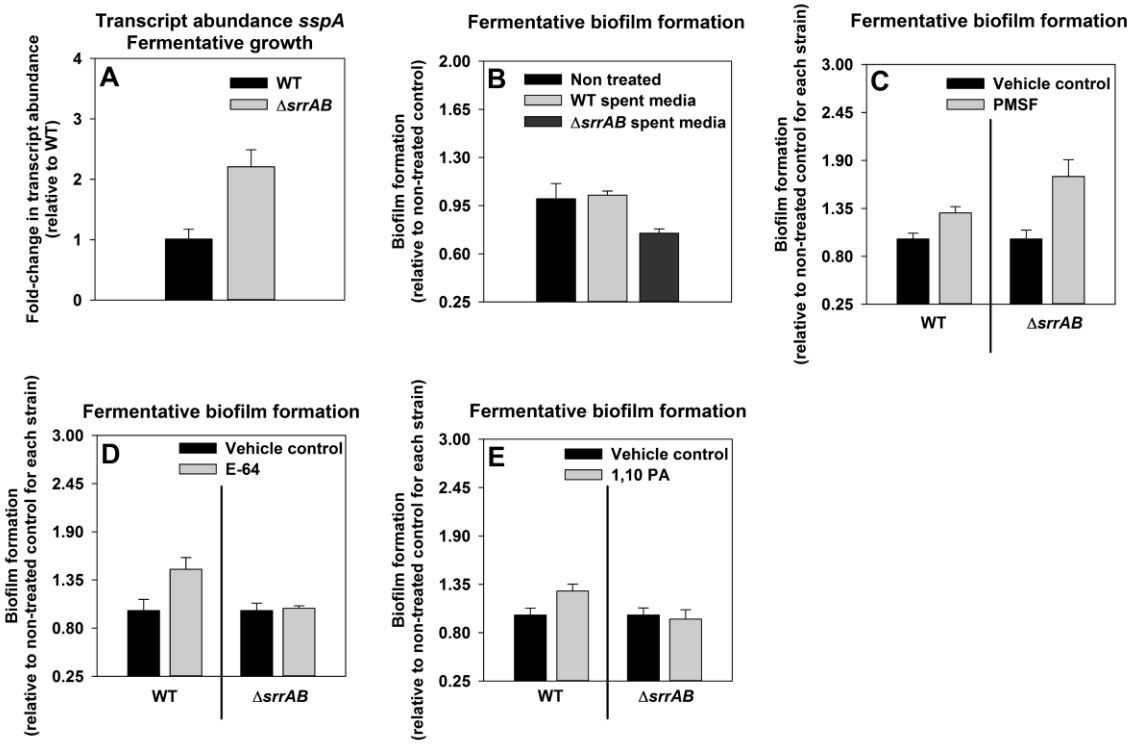


**Figure 4.6. SrrAB negatively influences *sspA* transcription during fermentative growth, and the fermentative biofilm formation defect of a Δ*srrAB* strain can be rescued upon co-culture with a serine protease inhibitor.** Panel A; SrrAB negatively influences *sspA* transcript levels during fermentative growth. Biofilms of the WT (JMB 1100) and Δ*srrAB* (JMB 1467) strains were cultured fermentatively, mRNA was extracted, and the abundance of *sspA* transcript was quantified. The data were normalized to 16S rRNA levels, and thereafter, to levels observed in the WT strain. Panel B; The spent-media supernatant from a Δ*srrAB* strain has anti-biofilm activity. Biofilms of the WT and Δ*srrAB* were cultured fermentatively and spent-media supernatant were isolated. Subsequently, fermentative biofilm formation was assessed for the WT strain

alone or co-cultured with the isolated supernatant from either the WT strain or the Δ*srrAB* strain. Panel C, D and E; Supplementing growth media with a serine protease inhibitor partially suppresses the fermentative biofilm formation defect of the Δ*srrAB* strain, but no rescue is observed with a cysteine or metallo-protease inhibitor. Fermentative biofilm formation is displayed for the WT and the Δ*srrAB* strains cultured in the presence of either the vehicle or 10 µM of the serine protease inhibitor phenylmethylsulfonyl flouride (PMSF) (Panel C), 10 µM of the cysteine protease inhibitor E-64 (Panel E) or 10 µM of the metalloprotease inhibitor, 1,10 phenanthroline (1,10 PA) (Panel F). The data represent the average values of eight wells (Panel A) or six wells (Panels B, C, D and E) and error bars represent standard deviations. Error bars are displayed for all data, but on occasion may be too small to see. For data in Panel B, the spent-media supernatant was isolated from triplicate cultures and combined prior to use in experiments.

**Figure 4.7**

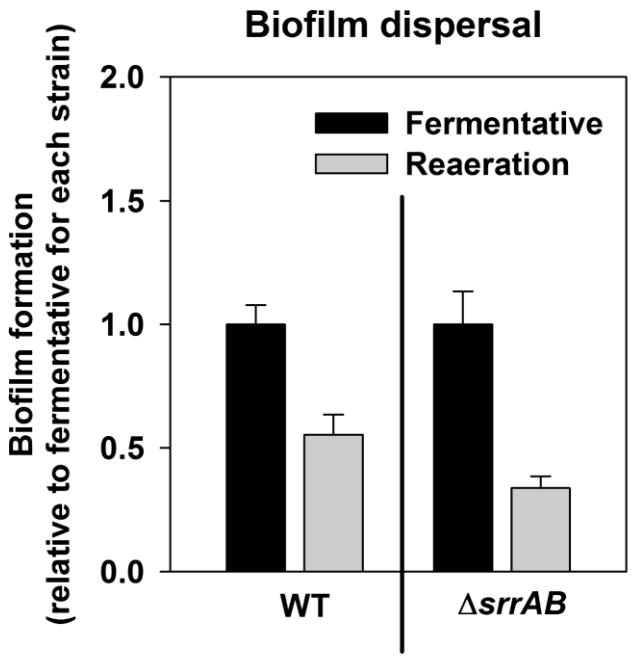


**Figure 4.7. Biofilm dispersal occurs at a faster rate in a Δ*srrAB* strain, consistent with increased production of SspA in this strain.** Biofilm formation is displayed for the WT (JMB1100) and the Δ*srrAB* (JMB 1467) strains following fermentative growth or upon reaeration (fermentative growth followed by aerobic growth). The data represent the average values of six wells and error bars represent standard deviations.

**Figure 4.8**

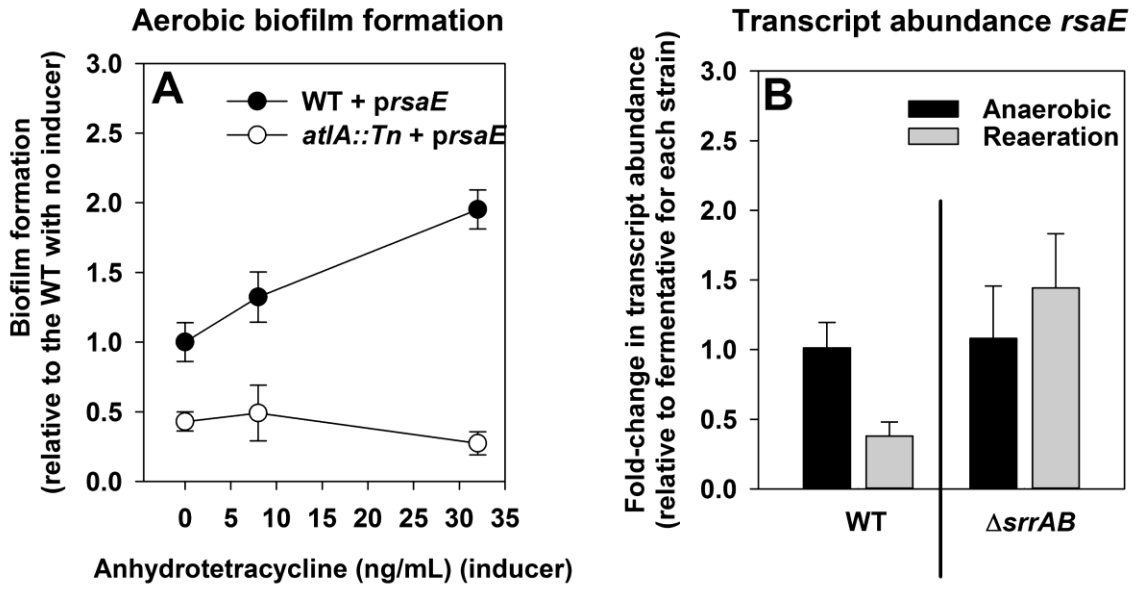


**Figure 4.8. RsaE modulates *S. aureus* biofilm formation in a AtlA-dependent manner and *rsaE* transcript is decreased upon reaeration in a SrrAB-dependent manner.** Panel A; RsaE modulates *S. aureus* biofilm formation in a AtlA-dependent manner. Biofilm formation is displayed for the WT (JMB1100) and the *atlA::Tn* (JMB 6625) strains carrying a plasmid encoding for *rsaE* expressed in sense (p*rsaE*), following aerobic growth in the absence or in the presence of varying amounts of anhydrotetracycline to induce transcription. Panel B; The transcript for *rsaE* is decreased upon reaeration in a SrrAB-dependent manner. Biofilms of the WT (JMB 1100) and Δ*srrAB* (JMB 1467) were cultured fermentatively or reaerated, mRNA was extracted, and the abundance of the *atlA* (Panel A) and *sspA* (Panel B) transcript was quantified. The data were normalized to 16S rRNA levels, and thereafter, to levels observed fermentatively for each strain. The data represent the average values of eight wells (Panel A) or

triplicates (Panels B) and error bars represent standard deviations. Error bars are displayed for all data, but on occasion may be too small to see.

**Table 4.1. Strains and plasmids used in this study.**

| **Strains used in this study** | | | |
|---|---|---|---|
| ***S. aureus* Strains** | **Genotype/Description** | **Genetic Background** | **Source/ Reference** |
| JMB1100 | Wild-type; USA300_LAC (erm sensitive); MRSA; CC8 | LAC | (10) |
| JMB 1467 | Δ*srrAB* (SAUSA300_1441-42) | LAC | (119) |
| JMB 2047 | Δ*srrAB::tet* | LAC | (101) |
| JMB 6625 | *atlA::Tn(ermB)* | LAC | This work, BEI resources (39) |
| JMB 6029 | *menF::Tn(ermB)* | LAC | This work, BEI resources (39) |
| JMB 6219 | *menF::Tn(tet)* | LAC | (104) |
| **Other Strains** | | | |
| *Escherichia coli* PX5 | | | Protein Express |
| *Sacchromyces cerevisiae FY2* | | | William Belden |
| **Plasmids used in this study** | | | |
| **Plasmid name** | **Insert Locus/function** | | **Source/Reference** |
| pML100 | Insertless cloning vector | | Paul Dunman |
| pML100_*rsaE* | *rsaE* expressed in sense | | This work |

# CHAPTER 5

# CONCLUDING REMARKS

The goal of this study was to expand our understanding of how oxygen, a critical variable in disease progression, affects the ability of *S. aureus* to form biofilms, the etiologic agents of recurrent infections. The work reported in chapter two finds that oxygen impacts *S. aureus* biofilm formation in its capacity as a TEA. Decreased respiration results in programmed cell lysis via increased expression of AtlA and decreased expression of WTA. These processes are governed by the SrrAB TCRS and evidence suggests this occurs in response to the accumulation of reduced menaquinone. The AtlA-dependent release of cytosolic components facilitates biofilm formation. However, it is unclear whether SrrB directly interacts with menaquinone, or whether SrrB activity is being stimulated as a downstream effect of reduced menaquinone accumulation. SrrB shares similarities with the histidine kinase ArcB from *E. coli*. ArcB has been proposed to interact with the cellular quinone pool via three cytosolic cysteine residues. SrrB also contains three conserved cysteine residues. However, replacement of two of the three cysteine residues resulted in a strain that phenocopied a WT strain (Mashruwala & Boyd, unpublished). While this experiment does not rule out a role for the cysteine residue in SrrB function, these questions will likely be answered upon biochemical experimentation by measuring the interactions between menaquinone and purified SrrB. It is also unclear whether SrrA affects transcription of *atlA* and the *tar* genes by directly

binding to the promoter region for these genes, and awaits further biochemical testing. SrrA is a member of the OmpR family of response regulatory proteins which are typically phosphorylated at a conserved aspartate residue. Phosphorylation induces dimerization, and thereby, increases the affinity of the protein for DNA. Mutating the aspartate residue to an alanine resulted in a strain that phenocopies a Δ*srrAB* strain for multiple phenotypes (Mashruwala *et. al*., forthcoming). One inference of this finding is that SrrA exerts its effect upon certain phenotypes as a transcriptional activator (Mashruwala *et. al*., forthcoming). However, mutation at the aspartate residue can often result in protein dysfunction. Therefore it was necessary to examine this by alternate means. One method was to use a phosphomimetic strain that may result in constitutive DNA binding by SrrA. Unfortunately, the replacement of the aspartate residue with a glutamate did not result in phosphomimetic SrrA (Mashruwala & Boyd, unpublished). It also remains to be determined what is the phosporylation status of the SrrA pool during respiratory or fermentative growth. The use of the Phos-tag system is likely to yield insights into this question. The studies reported in Chapter three lead to the supposition that the regulation of *atlA* is achieved via *rsaE*. However, this awaits further experimentation. Previous studies have reported that AtlA is capable of binding to DNA (52). In the context of biofilm formation, the role of AtlA in cell-lysis has been explored in multiple studies, however, it remains to be explored whether AtlA has additional moonlighting function(s).

The work reported in Chapter 3 finds that SaeRS plays a role in anaerobic biofilm formation. Sae is responsive to the cellular respiratory status and decreased respiration elicits increased activity of SaeRS resulting in increased transcription of *atlA* and *fnbpA* and thereby effects biofilm formation. However, it is currently unclear what cellular molecule(s) influence SaeS activity and this will require further experimentation. A number of interesting possibilities present themselves for exploration. Similar to SrrAB, it is possible that signal transmission to SaeS also requires the presence of menaquinone. However, genetic experiments to test this will be difficult to design or interpret due the inherent overlap with SrrAB function. Biochemical tests examining the effects of menaquinone upon SaeS kinase activity are likely to provide an answer. Alternatively, the decrease in proton motive force, or one of its consitutent components (ΔpH and Δpsi), experienced during anaerobic growth, could also trigger SaeS activity. It is also possible that genetic screens could be utilized to look for the signal. One possible screen design would be to construct a strain wherein the transcription of the gene encoding for green flourescent protein is placed under the control of a promoter region that requires high SaeR~P for activation. The resultant strain could be utilized to screen for signal molecules. Additional scenarios to consider are that SaeS activity is not being directly triggered by a stimulus and that increased activity is simply a downstream effect of non-related cellular processes. SaeP and SaeQ modulate the phosphatase activity of SaeS (67). One possiblity is that increased SaeS activity is achieved simply via downreguation of SaePQ activity or expression. $SaeS^{P18}$ imparts

constitutive SaeS kinase activity. Interestingly, the transcript for *saeS*$^{P18}$ displays increased stability *in vivo* (68). This leads to the hypothesis that the levels of SaeS during fermentative growth could be increased by simply stabilizing the *saeS* transcript and thereby elevating protein production. However, these ideas require further testing. It is also worth noting that while the promoter region for *atlA* contains a putative SaeR binding site, it also remains to be tested whether SaeR directly binds to this promoter region.

The work reported in Chapter 4 finds that pre-formed biofilms of *S. aureus* can be prompted to detach and disperse upon the resumption of respiration. The dispersal process is achieved via divergent regulation of *atlA* and *sspA* resulting in decreased accumulation of polymeric molecules that faciltate matrix formation. Dispersal is a regulated process that is modulated via the SrrAB TCRS and the *rsaE* small RNA in response to the respiratory status of the cell. In this context it is worth noting that RsaE-dependent downregulation is predicted to occur via interactions with the 5'UTR region of target mRNAs (46). However, a limited numbers of studies on *rsaE* function in *S. aureus* have been conducted and few cellular targets have been verified *in vitro*. Thus, it will be worth examining whether *atlA* and *sspA* are indeed direct targets for *rsa*E. The data reported in Chapter two and four also lead me to hypothesize that it may be possible to modulate SrrAB-dependent biofilm formation by amending the media with compounds that mimic menaquinone. This idea was examined by measuring biofilm formation in the presence of absence of oxygen and in media amended with varying concentrations of 1,4-benzoquinone, 1,4-napthoquinone,

menadione, plumbagin, ubiquinone, menaquinone or menaquinol. In addition to being quinone analogs the selected compounds also varied in their redox potential with the highest being 1,4-benzoquinone at +274 mV to the lowest being ubiquinone at -100 mV. However, supplementation of these compounds did not alter biofilm formation (Mashruwala & Boyd, unpublished).

In Chapter three it was reported that both the SrrAB and the SaeRS systems govern biofilm formation in the context of an animal model of infection. It would be interesting to examine whether HBOT could be used to treat implant-associated biofilm infections in animal models. However, any such studies would be challenging to conduct due to the fact that HBOT also boosts activity of the innate immune system. It is tempting to speculate that it would be possible to conduct such studies in mice that lack the ability to produce PMNs or macrophages. However, I am not an expert on mice studies and thus it is unclear from a non-expert perspective whether the severe debilitation of innate immunity in these models would render debatable the physiological relevance of the results. It is clear that the approach and experimental design are likely to be crucial in these experiments. Nitrate, the alternate electron acceptor for *S. aureus* is also capable of prompting biofilm dispersal. Organic-nitrate based drugs, such as glyceryl trinitrate and isosorbide mononitrate, are clinically prescribed for chronic angina (107). It is tempting to speculate that nitrate drugs could be utilized to disperse biofilms, *in vivo*, in the context of an animal model of infection. However, similar to oxygen, this approach also presents potential complications. The mechanism of action for nitrate based drugs is predicated upon the human

body rapidly converting the drugs to nitric oxide (107). Indeed the half-life of the nitrate form itself is extremely low in the human body (107). The nitric oxide itself serves as vasodilatory stimulus and results in decreased blood pressure (107). Nitrate drugs would be expected to behave in a similar manner in mice, which share physiologies similar to humans, thereby complicating experimental design and interpretation. In the context of human infections, unwarranted vasodilation would self-evidently interfere with therapeutic interventions in a clinical setting.

# APPENDIX

## SUPPLEMENTARY MATERIAL- CHAPTER 2

**Figure 2.S1**

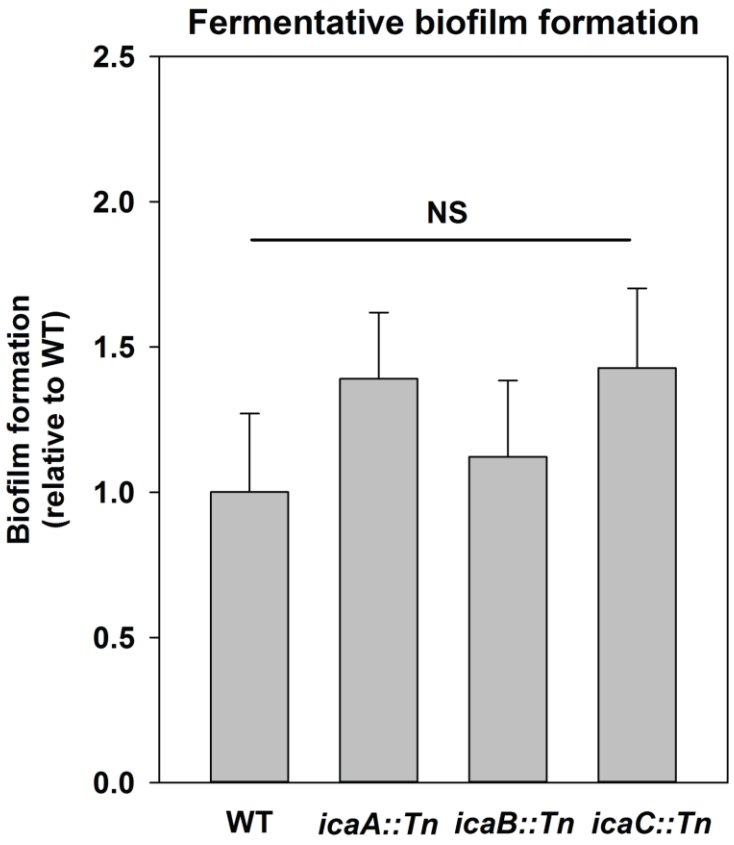


**Figure 2.S1. Polysaccharide intercellular adhesin (PIA) is dispensable for fermentative biofilm formation.** Biofilm formation of the WT (JMB 1100), *icaA::Tn* (JMB 5577), *icaB::Tn* (JMB 5579), and *icaC::Tn* (JMB 5578) strains following fermentative growth is displayed. Data represent the average value of eight wells and error bars represent standard deviation. Statistical significance

was calculated using a two-tail Student's t-test and p-values >.05 were considered to be not significant.

**Figure 2.S2**

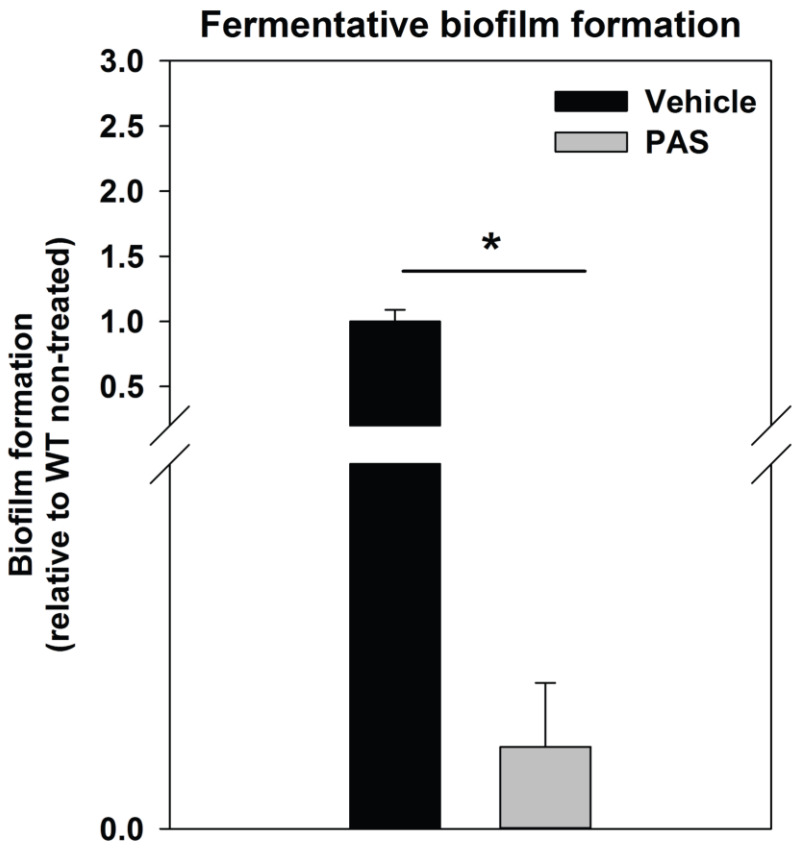


**Figure 2.S2. Supplementing growth media with the autolysis inhibitor polyanethole sulfonate (PAS) attenuates fermentative biofilm formation.** Biofilm formation of the WT (JMB 1100) cultured fermentatively in the presence of vehicle or 300 µg/mL PAS is displayed. Data represent the average value of eight wells and error bars represent standard deviation. Statistical significance was calculated using a two-tail Student's t-test and * indicates p-value of <.05.

**Figure 2.S3**

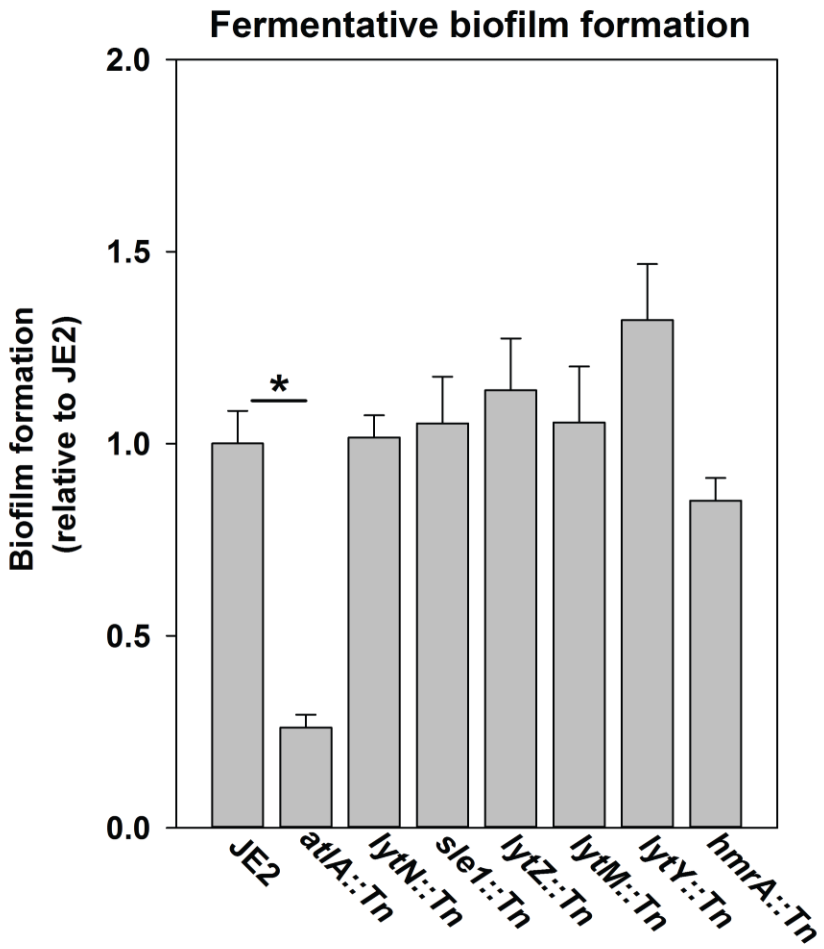


**Figure 2.S3. Fermentative biofilm formation is dependent on the AtlA murein hydrolase.** Biofilm formation of the WT (JMB 2977), *atlA::Tn* (JMB 6625), *lytN::Tn* (JMB 7265), *sle1::Tn* (JMB 7266), *lytZ::Tn* (JMB 7269), *lytM::Tn* (JMB 7271), *lytY::Tn* (JMB 7268), and *hmrA::Tn* (JMB 7270) strains cultured fermentatively is displayed. Data represent the average value of eight wells and error bars represent standard deviation. Statistical significance was calculated using a two-tail Student's t-test and * indicates p-value of <.05.

**Figure 2.S4**

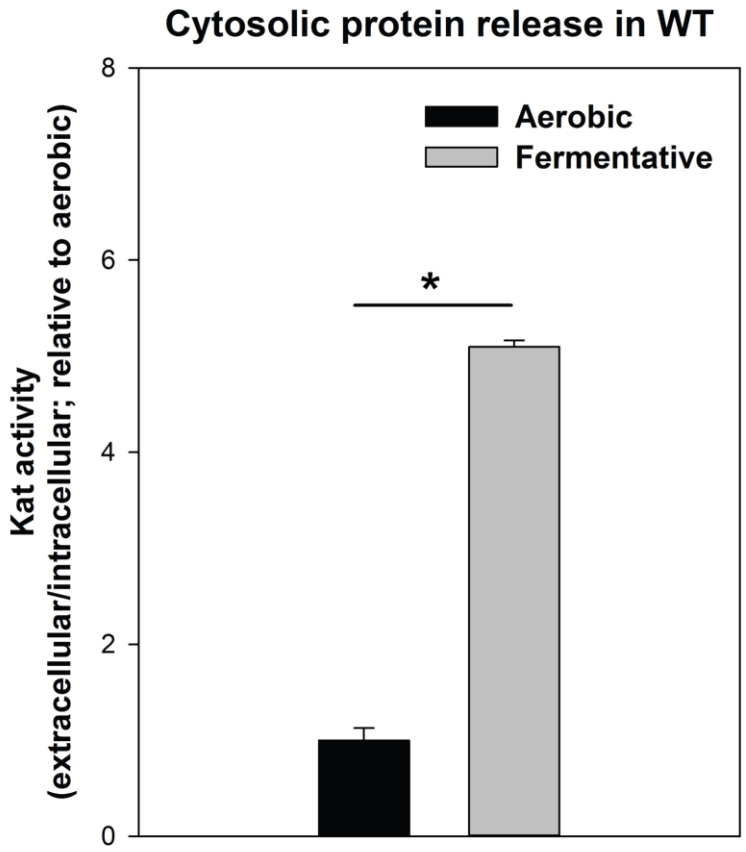


**Figure 2.S4. Cytosolic protein release is increased upon fermentative growth.** Biofilms of the WT (JMB 1100) were cultured aerobically or fermentatively and the activity of the cytosolic protein catalase (Kat) was measured in the spent media supernatant. Extracellular Kat activity was normalized to intracellular Kat activity and thereafter to levels under aerobic growth. Statistical significance was calculated using a two-tail Student's t-test and * indicates p-value of <.05.

**Figure 2.S5**

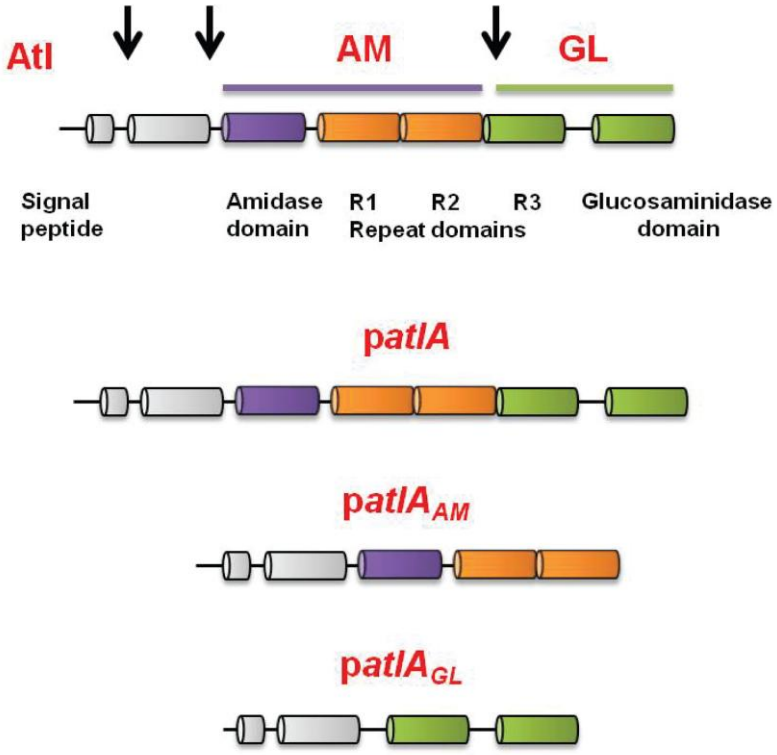


**Figure 2.S5. Representation of the full length AtlA precursor protein and of the plasmid encoded variants used in this study.** *S. aureus* AtlA is a bifunctional protein with an amidase and a glucosaminidase domain. The schematic is a modification of previous illustrations (12, 50). AtlA is post-translationally processed (indicated by arrows) between the propeptide and AM domain and between the repeat domains to free AM-R1-2 and R3-GM. The four allelic variants used in this study were constructed previously (12). The alleles are carried upon multi-copy plasmids that encode for full length AtlA (p*atlA*), the amidase and repeat domains (AM-R1-R2) (p*atlA*$_{AM}$), catalytically inactivated

amidase and repeat domains via a point mutation H263A ($AM_{H263A}$-R1-R2) (p*atlA*$_{AMH263A}$) (not displayed), or glucosaminidase (R3-GM).

**Figure 2.S6**

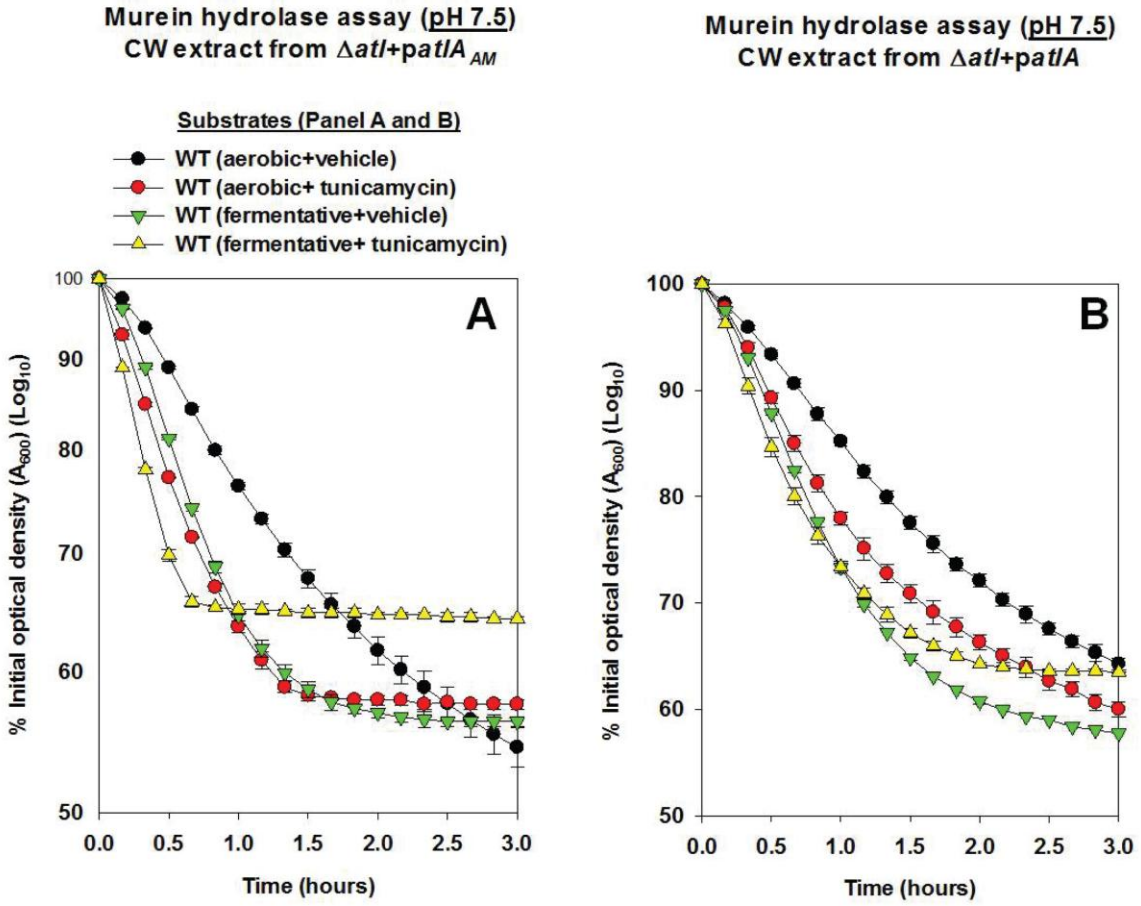


**Figure 2.S6. AtlA- and AM-dependent cleavage of heat-killed cells is modulated via altered expression of wall-teichoic acids.** Murein hydrolase assays were conducted using CW-extracts detached from a Δ*atlA* (KB 5000) strain carrying p*atlA*$_{AM}$ (Panel A) or p*atlA* (Panel B) and upon heat-killed cells of the WT (JMB 1100) cultured aerobically or fermentatively and in the presence or absence of 100 ng/mL of tunicamycin as substrates (pH 7.5). Data represent the average value of technical duplicates from one set of substrate preparation. The heat-killed substrates were prepared on least three separate occasions and similar results were obtained. Error bars represent standard deviations.

**Figure 2.S7**

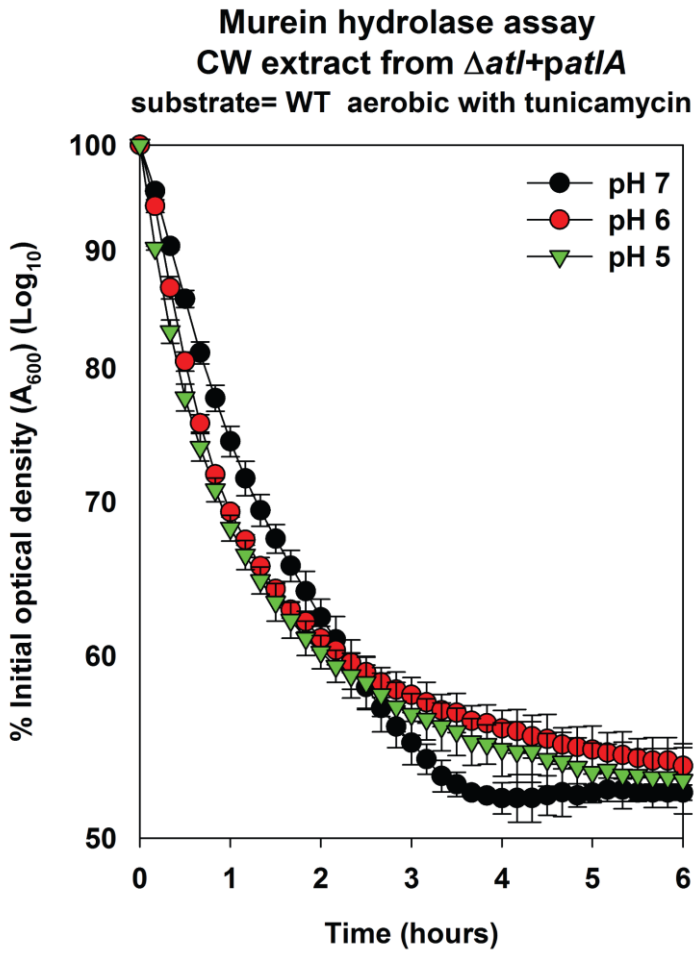


**Figure 2.S7. AtlA-dependent lysis rates of heat-killed tunicamycin treated cells are not altered upon alterations in the assay buffer pH.** Murein hydrolase assays were conducted at pH 7, pH 6, or pH 5 using CW-extracts detached from a Δ*atlA* (KB 5000) strain carrying p*atlA* upon heat-killed cells of the WT cultured aerobically in the presence of 100 ng/mL of tunicamycin as substrates. Data represent the average value of technical duplicates from one set of substrate preparation. The heat-killed substrates were prepared on at least

three separate occasions and similar results were obtained. Error bars represent standard deviations.

**Figure 2.S8**

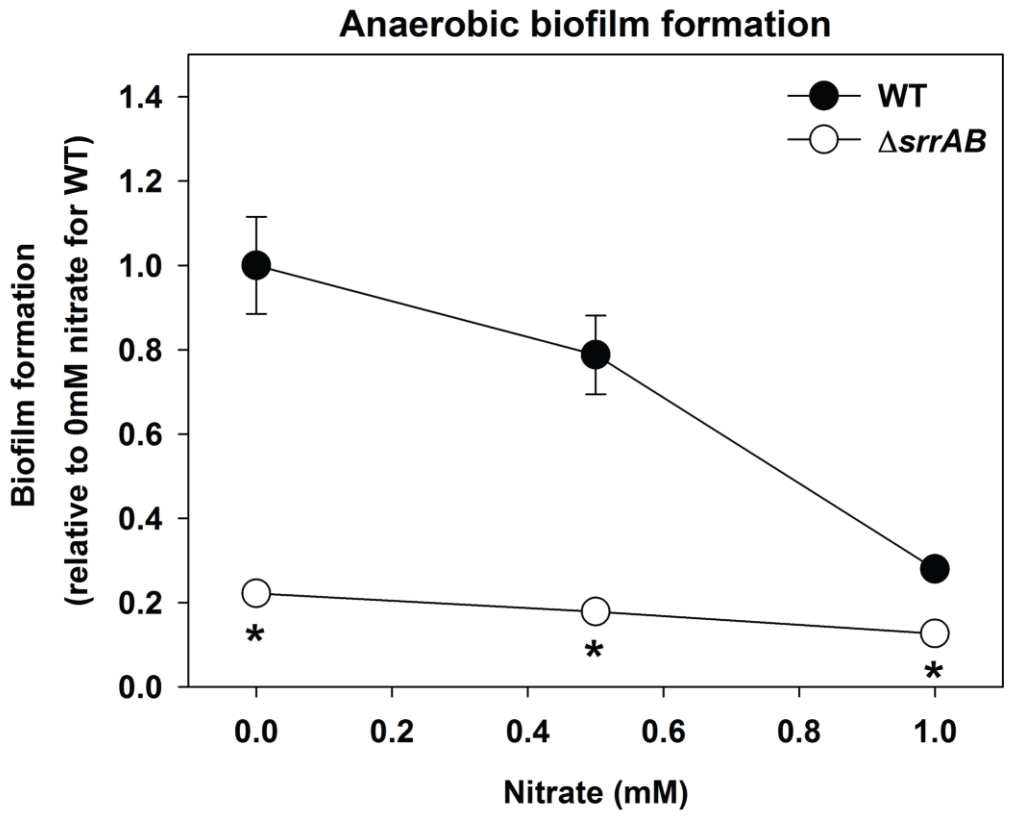


**Figure 2.S8. Biofilm formation of a Δ*srrAB* strain is largely unaltered upon supplementing anaerobic biofilms with the alternate terminal electron acceptor nitrate.** Biofilm formation following fermentative growth in the presence or absence of varying concentrations of sodium nitrate is displayed for the WT (JMB1100) and Δ*srrAB* (JMB1467) strains. Data represent the average value of eight and error bars represent standard deviation. Statistical significance was calculated using a two-tail Student's t-test and p-values >.05 were considered to be not significant while * indicates p-value of <.05.

**Supplementary table 2.1: Oligonucleotides used in this study**

| **RT- PCR primers** | |
|---|---|
| *tarO* For | AATTGCCGCTGCCTTAGTAGTT |
| *tarO* Rev | TGTACCCATTGGCAACGAAA |
| *tarA* For | GATGGGACAGGAGTAGTCAAAGCT |
| *tarA* Rev | ACCAGGTATACGATGCGCTAGAG |
| *tarH* For | GGCTTGTTGGCATCAATGG |
| *tarH* Rev | CCGCCAATGATATTGCTCAA |
| *tarB* For | ATGTGTCTGACAAGGCAATGGT |
| *tarB* Rev | CACTAAGTAAAAATCCGTCGCTTGA |
| *atlA* For | GGTGCAGTCGGTAACCCTAGAT |
| *altA* Rev | TGAACGTGCAAATGAAGCATAGT |

| **Cloning primers** | |
|---|---|
| pLL39_yeast F | GCCCAATCACTAGTGAATTCCCGAAGCTTAGTTACGCTAGG GATAACAG |
| yeast_srrPro R | ATATCTTGGATGTGTCATTAACTATATTACCCTGTTATCCC |
| yeast_srrPro F | GGGATAACAGGGTAATATAGTTAATGACACATCCAAGATAT |
| srrAB_pLL39 R | GGTAATAAAAAAGCTTGCATGCCTGCAGGTTTTATTCTGGTT TTGGTAG |

# SUPPLEMENTARY MATERIAL- CHAPTER 3

## Figure 3.S1

### SaeR binding sequence upstream of *atlA*

**AAAAAGTTAACCTCGCTTAATTAAA**

**Figure 3.S1. Putative SaeR binding site in the promoter regions of *atlA*.** Depiction of the direct repeat sequence (underlined) separated by a six base-pair spacer region that is characteristic of sequences known to be bound by SaeR (consensus sequence= $GTTAAN_6GTTAA$). This direct repeat is located ~240 base-pairs upstream of the translational start site. The binding site differed from the consensus sequence only by the dispensable base, guanine.

**Figure 3.S2**

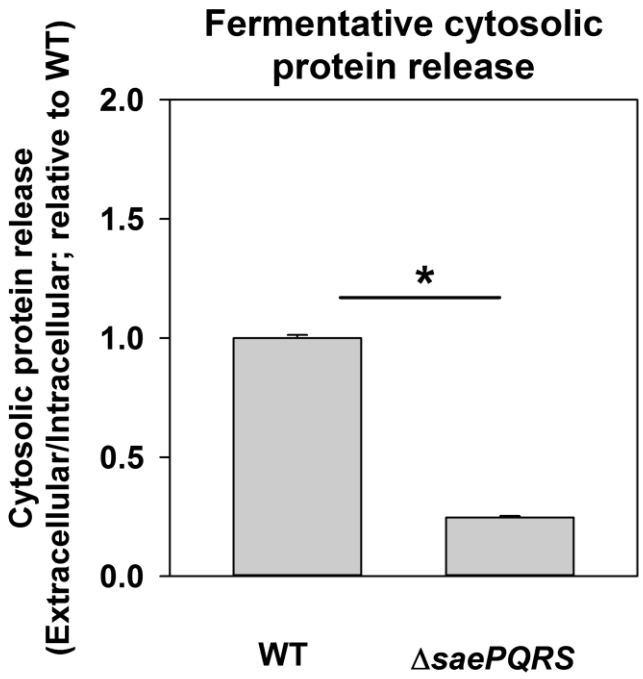


**Figure 3.S2. Cytosolic protein release is decreased in a Δ*saePQRS* strain during fermentative growth.** Biofilms of the WT (JMB 1100) and Δ*saePQRS* (JMB 1335) were cultured fermentatively and the activity of the cytosolic protein catalase (Kat) was measured in the spent media supernatant. Extracellular Kat activity was normalized to intracellular Kat activity and thereafter to levels in the WT. The data represent the average value of triplicates. Error bars represent standard deviations. Statistical significance was calculated using a two-tail Student's t-test and * indicates p-value of <0.05.

**Figure 3.S3**

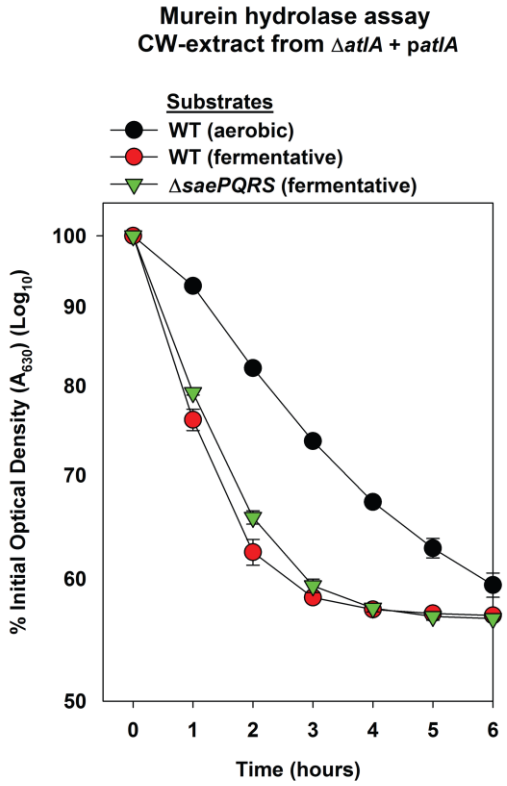


**Figure 3.S3. Heat-killed fermentatively cultured Δ*saePQRS* cells are cleaved at the same rate as the WT.** Murein-hydrolase activity was determined using cell-wall (CW) extracts detached from a Δ*atlA* strain (KB 5000) carrying a plasmid encoding for full-length AtlA (p*atlA*). The substrates were heat-killed cells of the WT cultured aerobically or fermentatively and the Δ*saePQRS* strain cultured fermentatively (pH of 7.5). The data represent the average value of technical duplicates from one set of substrate preparations. Preparation of heat-killed substrates was conducted on least two separate occasions and similar results were obtained. Error bars represent standard deviations. Error bars are displayed for all data, but might be too small to see on occasion.

**Figure 3.S4**

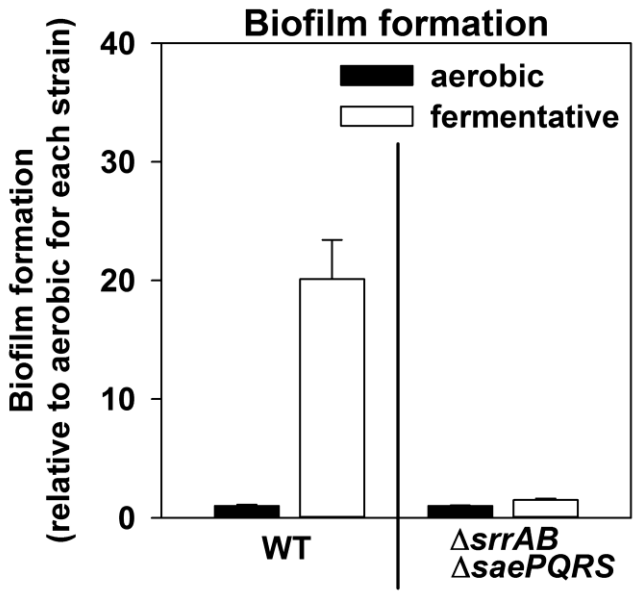


**Figure 3.S4. Fermentative biofilm formation induction is nearly absent in the Δ*srrAB* Δ*saeRS* strain.** Biofilm formation is displayed for the WT (JMB 1100) and the Δ*srrAB* Δ*saeRS* (JMB 6460) strains following aerobic and fermentative growth. To allow assessment of induction levels the data were normalized to the biofilm levels displayed by each strain under aerobic growth. The data represent the average of eight wells and error bars represent standard deviations. Error bars are displayed for all data, but might be too small to see on occasion.

**Figure 3.S5**

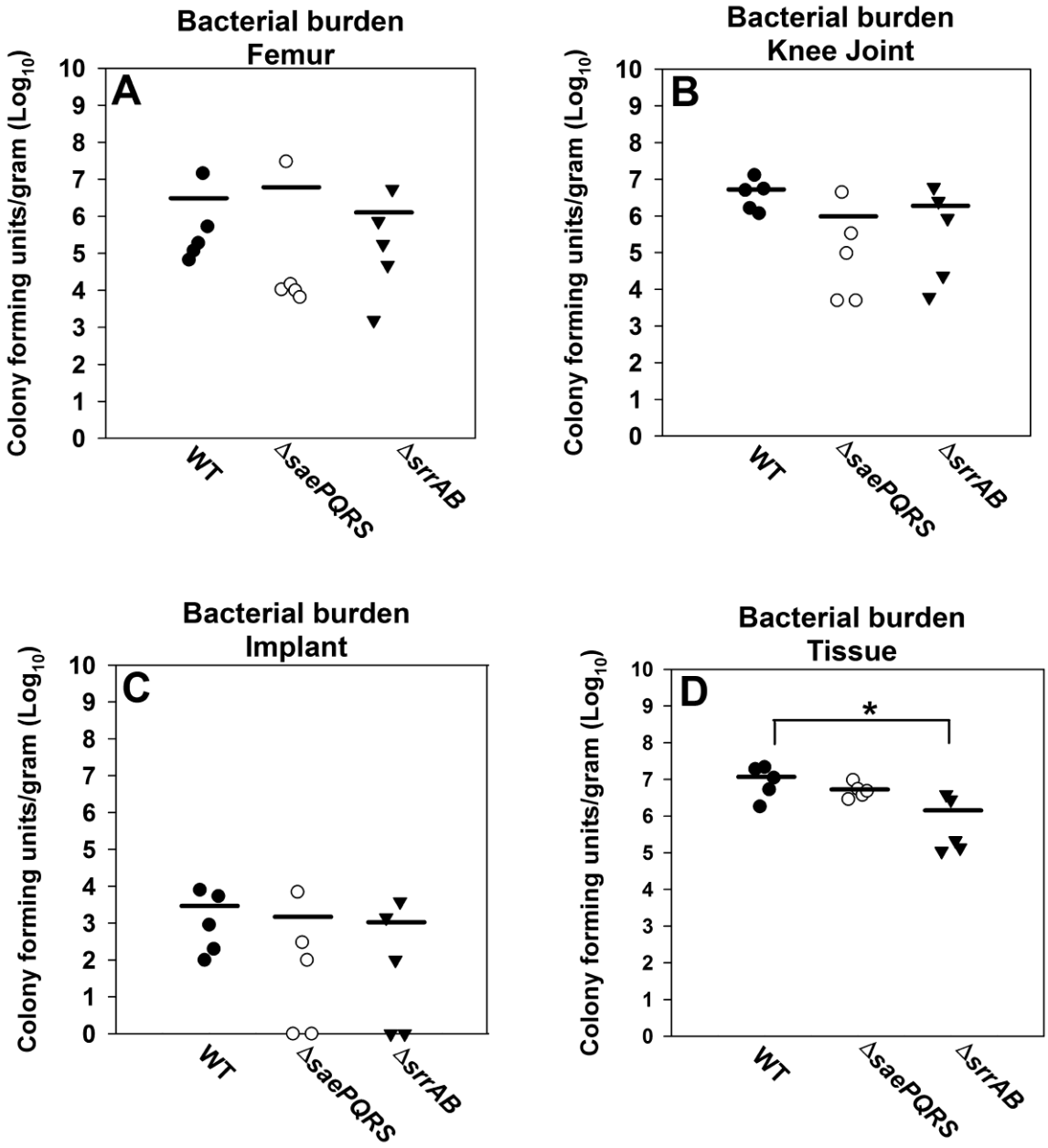


**Figure 3.S5. SaeRS and SrrAB influence biofilm persistence in a murine model of orthopedic implant biofilm infection.** Panels A-D; Male C57BL/6 mice were infected with the WT (JMB 1100), Δ*saePQRS* (JMB 1335) and the

Δ*srrAB* (JMB 1467) strains (n=5/group). Animals were sacrificed at 7 days following infection, whereupon the implant was sonicated and host tissues surrounding the infected orthopedic implant site were homogenized to quantitate bacterial burdens. Results are expressed as CFU per milliliter for the implant and CFU per gram of tissue (for the soft tissue surrounding the knee, knee joint containing ligament and tendon structures, and femur) to normalize for differences in sampling size. Significant differences in bacterial burdens between mice are denoted by asterisks (*, $p < 0.05$). Statistics were conducted using a one-way analysis of variance (ANOVA), followed by Bonferroni's multiple-comparison test.

## REFERENCES


1. Adhikari, R. P., and R. P. Novick. 2008. Regulatory organization of the staphylococcal *sae* locus. Microbiology 154:949-59.
2. Archer, N. K., M. J. Mazaitis, J. W. Costerton, J. G. Leid, M. E. Powers, and M. E. Shirtliff. 2011. *Staphylococcus aureus* biofilms: properties, regulation, and roles in human disease. Virulence 2:445-59.
3. Arnold, F., D. West, and S. Kumar. 1987. Wound healing: the effect of macrophage and tumour derived angiogenesis factors on skin graft vascularization. Br J Exp Pathol 68:569-74.
4. Beers, R. F., Jr., and I. W. Sizer. 1952. A spectrophotometric method for measuring the breakdown of hydrogen peroxide by catalase. J Biol Chem 195:133-40.
5. Bernthal, N. M., A. I. Stavrakis, F. Billi, J. S. Cho, T. J. Kremen, S. I. Simon, A. L. Cheung, G. A. Finerman, J. R. Lieberman, J. S. Adams, and L. S. Miller. 2010. A mouse model of post-arthroplasty *Staphylococcus aureus* joint infection to evaluate in vivo the efficacy of antimicrobial implant coatings. PLoS One 5:e12580.
6. Bispo, P. J., W. Haas, and M. S. Gilmore. 2015. Biofilms in infections of the eye. Pathogens 4:111-36.
7. Biswas, R., R. E. Martinez, N. Gohring, M. Schlag, M. Josten, G. Xia, F. Hegler, C. Gekeler, A. K. Gleske, F. Gotz, H. G. Sahl, A. Kappler, and A. Peschel. 2012. Proton-binding capacity of *Staphylococcus aureus* wall teichoic acid and its role in controlling autolysin activity. PLoS One 7:e41415.
8. Biswas, R., L. Voggu, U. K. Simon, P. Hentschel, G. Thumm, and F. Gotz. 2006. Activity of the major *staphylococcal* autolysin Atl. FEMS Microbiol Lett 259:260-8.
9. Boles, B. R., and A. R. Horswill. 2008. Agr-mediated dispersal of *Staphylococcus aureus* biofilms. PLoS Pathog 4:e1000052.
10. Boles, B. R., M. Thoendel, A. J. Roth, and A. R. Horswill. 2010. Identification of genes involved in polysaccharide-independent *Staphylococcus aureus* biofilm formation. PLoS One 5:e10146.
11. Bose, J. L., P. D. Fey, and K. W. Bayles. 2013. Genetic tools to enhance the study of gene function and regulation in *Staphylococcus aureus*. Appl Environ Microbiol 79:2218-24.
12. Bose, J. L., M. K. Lehman, P. D. Fey, and K. W. Bayles. 2012. Contribution of the *Staphylococcus aureus* Atl AM and GL murein hydrolase activities in cell division, autolysis, and biofilm formation. PLoS One 7:e42244.
13. Brady, R. A., J. G. Leid, J. H. Calhoun, J. W. Costerton, and M. E. Shirtliff. 2008. Osteomyelitis and the role of biofilms in chronic infection. FEMS Immunol Med Microbiol 52:13-22.
14. Burke, K. A., and J. Lascelles. 1975. Nitrate reductase system in *Staphylococcus aureus* wild type and mutants. J Bacteriol 123:308-16.

15. Calamita, H. G., W. D. Ehringer, A. L. Koch, and R. J. Doyle. 2001. Evidence that the cell wall of *Bacillus subtilis* is protonated during respiration. Proc Natl Acad Sci U S A 98:15260-15263.
16. Campbell, J., A. K. Singh, J. P. Santa Maria, Jr., Y. Kim, S. Brown, J. G. Swoboda, E. Mylonakis, B. J. Wilkinson, and S. Walker. 2011. Synthetic lethal compound combinations reveal a fundamental connection between wall teichoic acid and peptidoglycan biosyntheses in *Staphylococcus aureus*. ACS Chem Biol 6:106-16.
17. Campbell, J., A. K. Singh, J. G. Swoboda, M. S. Gilmore, B. J. Wilkinson, and S. Walker. 2012. An antibiotic that inhibits a late step in wall teichoic acid biosynthesis induces the cell wall stress stimulon in *Staphylococcus aureus*. Antimicrob Agents Chemother 56:1810-20.
18. Carreau, A., B. El Hafny-Rahbi, A. Matejuk, C. Grillon, and C. Kieda. 2011. Why is the partial oxygen pressure of human tissues a crucial parameter? Small molecules and hypoxia. J Cell Mol Med 15:1239-53.
19. Cassat, J. E., N. D. Hammer, J. P. Campbell, M. A. Benson, D. S. Perrien, L. N. Mrak, M. S. Smeltzer, V. J. Torres, and E. P. Skaar. 2013. A secreted bacterial protease tailors the *Staphylococcus aureus* virulence repertoire to modulate bone remodeling during osteomyelitis. Cell Host Microbe 13:759-72.
20. Chang, S., D. M. Sievert, J. C. Hageman, M. L. Boulton, F. C. Tenover, F. P. Downes, S. Shah, J. T. Rudrik, G. R. Pupp, W. J. Brown, D. Cardo, and S. K. Fridkin. 2003. Infection with vancomycin-resistant *Staphylococcus aureus* containing the *vanA* resistance gene. N Engl J Med 348:1342-7.
21. Chaudhari, S. S., V. C. Thomas, M. R. Sadykov, J. L. Bose, D. J. Ahn, M. C. Zimmerman, and K. W. Bayles. 2016. The LysR-type transcriptional regulator, CidR, regulates stationary phase cell death in *Staphylococcus aureus*. Mol Microbiol 101:942-53.
22. Chen, C., V. Krishnan, K. Macon, K. Manne, S. V. Narayana, and O. Schneewind. 2013. Secreted proteases control autolysin-mediated biofilm growth of *Staphylococcus aureus*. J Biol Chem 288:29440-52.
23. Cho, H., D. W. Jeong, Q. Liu, W. S. Yeo, T. Vogl, E. P. Skaar, W. J. Chazin, and T. Bae. 2015. Calprotectin Increases the Activity of the SaeRS Two Component System and Murine Mortality during *Staphylococcus aureus* Infections. PLoS Pathog 11:e1005026.
24. Cosgrove, K., G. Coutts, I. M. Jonsson, A. Tarkowski, J. F. Kokai-Kun, J. J. Mond, and S. J. Foster. 2007. Catalase (KatA) and alkyl hydroperoxide reductase (AhpC) have comensatory roles in peroxide stress resistance and are required for survival, persistence, and nasal colonization in *Staphylococcus aureus*. J Bacteriol 189:1025-1035.
25. Costerton, J. W. 1995. Overview of microbial biofilms. J Ind Microbiol 15:137-40.
26. Costerton, J. W., Z. Lewandowski, D. E. Caldwell, D. R. Korber, and H. M. Lappin-Scott. 1995. Microbial biofilms. Annu Rev Microbiol 49:711-45.
27. Costerton, J. W., L. Montanaro, and C. R. Arciola. 2005. Biofilm in implant infections: its production and regulation. Int J Artif Organs 28:1062-8.

28. Costerton, J. W., P. S. Stewart, and E. P. Greenberg. 1999. Bacterial biofilms: a common cause of persistent infections. Science 284:1318-22.
29. Cramton, S. E., C. Gerke, N. F. Schnell, W. W. Nichols, and F. Gotz. 1999. The intercellular adhesion (*ica*) locus is present in *Staphylococcus aureus* and is required for biofilm formation. Infect Immun 67:5427-33.
30. Cramton, S. E., M. Ulrich, F. Gotz, and G. Doring. 2001. Anaerobic conditions induce expression of polysaccharide intercellular adhesin in *Staphylococcus aureus* and *Staphylococcus epidermidis*. Infect Immun 69:4079-85.
31. Davies, D. 2003. Understanding biofilm resistance to antibacterial agents. Nat Rev Drug Discov 2:114-22.
32. Dietrich, L. E., C. Okegbe, A. Price-Whelan, H. Sakhtah, R. C. Hunter, and D. K. Newman. 2013. Bacterial community morphogenesis is intimately linked to the intracellular redox state. J Bacteriol 195:1371-80.
33. Dietrich, L. E., T. K. Teal, A. Price-Whelan, and D. K. Newman. 2008. Redox-active antibiotics control gene expression and community behavior in divergent bacteria. Science 321:1203-6.
34. Dinges, M. M., P. M. Orwin, and P. M. Schlievert. 2000. Exotoxins of *Staphylococcus aureus*. Clin Microbiol Rev 13:16-34, table of contents.
35. Dubrac, S., and T. Msadek. 2004. Identification of genes controlled by the essential YycG/YycF two-component system of *Staphylococcus aureus*. J Bacteriol 186:1175-81.
36. Durand, S., F. Braun, E. Lioliou, C. Romilly, A. C. Helfer, L. Kuhn, N. Quittot, P. Nicolas, P. Romby, and C. Condon. 2015. A nitric oxide regulated small RNA controls expression of genes involved in redox homeostasis in *Bacillus subtilis*. PLoS Genet 11:e1004957.
37. Duthie, E. S., and L. L. Lorenz. 1952. Staphylococcal coagulase; mode of action and antigenicity. J Gen Microbiol 6:95-107.
38. Enright, M. C., D. A. Robinson, G. Randle, E. J. Feil, H. Grundmann, and B. G. Spratt. 2002. The evolutionary history of methicillin-resistant *Staphylococcus aureus* (MRSA). Proc Natl Acad Sci U S A 99:7687-92.
39. Fey, P. D., J. L. Endres, V. K. Yajjala, T. J. Widhelm, R. J. Boissy, J. L. Bose, and K. W. Bayles. 2013. A genetic resource for rapid and comprehensive phenotype screening of nonessential *Staphylococcus aureus* genes. MBio 4:e00537-12.
40. Flemming, H. C., and J. Wingender. 2010. The biofilm matrix. Nat Rev Microbiol 8:623-33.
41. Foulston, L., A. K. Elsholz, A. S. DeFrancesco, and R. Losick. 2014. The extracellular matrix of *Staphylococcus aureus* biofilms comprises cytoplasmic proteins that associate with the cell surface in response to decreasing pH. MBio 5:e01667-14.
42. Fournier, B., and D. C. Hooper. 2000. A new two-component regulatory system involved in adhesion, autolysis, and extracellular proteolytic activity of *Staphylococcus aureus*. J Bacteriol 182:3955-64.
43. Frankel, M. B., A. P. Hendrickx, D. M. Missiakas, and O. Schneewind. 2011. LytN, a murein hydrolase in the cross-wall compartment of

*Staphylococcus aureus*, is involved in proper bacterial growth and envelope assembly. J Biol Chem 286:32593-605.

44. Gaupp, R., S. Schlag, M. Liebeke, M. Lalk, and F. Gotz. 2010. Advantage of upregulation of succinate dehydrogenase in *Staphylococcus aureus* biofilms. J Bacteriol 192:2385-94.
45. Geiger, T., C. Goerke, M. Mainiero, D. Kraus, and C. Wolz. 2008. The virulence regulator Sae of *Staphylococcus aureus*: promoter activities and response to phagocytosis-related signals. J Bacteriol 190:3419-28.
46. Geissmann, T., C. Chevalier, M. J. Cros, S. Boisset, P. Fechter, C. Noirot, J. Schrenzel, P. Francois, F. Vandenesch, C. Gaspin, and P. Romby. 2009. A search for small noncoding RNAs in *Staphylococcus aureus* reveals a conserved sequence motif for regulation. Nucleic Acids Res 37:7239-57.
47. Geng, H., P. Zuber, and M. M. Nakano. 2007. Regulation of respiratory genes by ResD-ResE signal transduction system in *Bacillus subtilis*. Methods Enzymol 422:448-64.
48. Gesell L.B., e. 2008. Hyperbaric Oxygen Therapy Indications. Undersea Hyperbaric Medical Society.
49. Goerke, C., U. Fluckiger, A. Steinhuber, V. Bisanzio, M. Ulrich, M. Bischoff, J. M. Patti, and C. Wolz. 2005. Role of *Staphylococcus aureus* global regulators *sae* and *sigmaB* in virulence gene expression during device-related infection. Infect Immun 73:3415-21.
50. Gotz, F., C. Heilmann, and T. Stehle. 2014. Functional and structural analysis of the major amidase (Atl) in *Staphylococcus*. Int J Med Microbiol 304:156-63.
51. Graham, P. L., 3rd, S. X. Lin, and E. L. Larson. 2006. A U.S. population-based survey of *Staphylococcus aureus* colonization. Ann Intern Med 144:318-25.
52. Grilo, I. R., A. M. Ludovice, A. Tomasz, H. de Lencastre, and R. G. Sobral. 2014. The glucosaminidase domain of Atl - the major *Staphylococcus aureus* autolysin has DNA-binding activity. Microbiologyopen 3:247-56.
53. Hamdan-Partida, A., T. Sainz-Espunes, and J. Bustos-Martinez. 2010. Characterization and persistence of *Staphylococcus aureus* strains isolated from the anterior nares and throats of healthy carriers in a Mexican community. J Clin Microbiol 48:1701-5.
54. Hammer, N. D., M. L. Reniere, J. E. Cassat, Y. Zhang, A. O. Hirsch, M. Indriati Hood, and E. P. Skaar. 2013. Two heme-dependent terminal oxidases power *Staphylococcus aureus* organ-specific colonization of the vertebrate host. MBio 4 (4):e00241-13
55. Hancock, I. C., G. Wiseman, and J. Baddiley. 1976. Biosynthesis of the unit that links teichoic acid to the bacterial wall: inhibition by tunicamycin. FEBS Lett 69:75-80.
56. Hassett, D. J., J. F. Ma, J. G. Elkins, T. R. McDermott, U. A. Ochsner, S. E. West, C. T. Huang, J. Fredericks, S. Burnett, P. S. Stewart, G. McFeters, L. Passador, and B. H. Iglewski. 1999. Quorum sensing in *Pseudomonas aeruginosa* controls expression of catalase and superoxide

dismutase genes and mediates biofilm susceptibility to hydrogen peroxide. Mol Microbiol 34:1082-93.

57. Heim, C. E., D. Vidlak, and T. Kielian. 2015. Interleukin-10 production by myeloid-derived suppressor cells contributes to bacterial persistence during *Staphylococcus aureus* orthopedic biofilm infection. J Leukoc Biol.
58. Heim, C. E., D. Vidlak, T. D. Scherr, C. W. Hartman, K. L. Garvin, and T. Kielian. 2015. IL-12 promotes myeloid-derived suppressor cell recruitment and bacterial persistence during *Staphylococcus aureus* orthopedic implant infection. J Immunol 194:3861-72.
59. Heim, C. E., D. Vidlak, T. D. Scherr, J. A. Kozel, M. Holzapfel, D. E. Muirhead, and T. Kielian. 2014. Myeloid-derived suppressor cells contribute to *Staphylococcus aureus* orthopedic biofilm infection. J Immunol 192:3778-92.
60. Henares, B., S. Kommineni, O. Chumsakul, N. Ogasawara, S. Ishikawa, and M. M. Nakano. 2014. The ResD response regulator, through functional interaction with NsrR and *fur*, plays three distinct roles in *Bacillus subtilis* transcriptional control. J Bacteriol 196:493-503.
61. Herbert, S., A. K. Ziebandt, K. Ohlsen, T. Schafer, M. Hecker, D. Albrecht, R. Novick, and F. Gotz. 2010. Repair of global regulators in *Staphylococcus aureus* 8325 and comparative analysis with other clinical isolates. Infect Immun 78:2877-89.
62. Horsburgh, M. J., J. L. Aish, I. J. White, L. Shaw, J. K. Lithgow, and S. J. Foster. 2002. sigmaB modulates virulence determinant expression and stress resistance: characterization of a functional *rsbU* strain derived from *Staphylococcus aureus* 8325-4. J Bacteriol 184:5457-67.
63. Horsburgh, M. J., E. Ingham, and S. J. Foster. 2001. In *Staphylococcus aureus*, Fur is an interactive regulator with PerR, contributes to virulence, and Is necessary for oxidative stress resistance through positive regulation of catalase and iron homeostasis. J Bacteriol 183:468-75.
64. Houston, P., S. E. Rowe, C. Pozzi, E. M. Waters, and J. P. O'Gara. 2011. Essential role for the major autolysin in the fibronectin-binding protein-mediated *Staphylococcus aureus* biofilm phenotype. Infect Immun 79:1153-65.
65. Houston, P., S. E. Rowe, C. Pozzi, E. M. Waters, and J. P. O'Gara. 2011. Essential role for the major autolysin in the fibronectin-binding protein-mediated *Staphylococcus aureus* biofilm phenotype. Infect Immun 79:1153-65.
66. Ishikawa, S., Y. Hara, R. Ohnishi, and J. Sekiguchi. 1998. Regulation of a new cell wall hydrolase gene, *cwlF*, which affects cell separation in *Bacillus subtilis*. J Bacteriol 180:2549-55.
67. Jeong, D. W., H. Cho, M. B. Jones, K. Shatzkes, F. Sun, Q. Ji, Q. Liu, S. N. Peterson, C. He, and T. Bae. 2012. The auxiliary protein complex SaePQ activates the phosphatase activity of sensor kinase SaeS in the SaeRS two-component system of *Staphylococcus aureus*. Mol Microbiol 86:331-48.

68. Jeong, D. W., H. Cho, H. Lee, C. Li, J. Garza, M. Fried, and T. Bae. 2011. Identification of the P3 promoter and distinct roles of the two promoters of the SaeRS two-component system in *Staphylococcus aureus*. J Bacteriol 193:4672-84.
69. Jolliffe, L. K., R. J. Doyle, and U. N. Streips. 1981. The Energized Membrane and Cellular Autolysis in *Bacillus subtilis*. Cell 25:753-763.
70. Joo, H. S., and M. Otto. 2012. Molecular basis of *in vivo* biofilm formation by bacterial pathogens. Chem Biol 19:1503-13.
71. Joska, T. M., A. Mashruwala, J. M. Boyd, and W. J. Belden. 2014. A universal cloning method based on yeast homologous recombination that is simple, efficient, and versatile. J Microbiol Methods 100:46-51.
72. Kalns, J., J. Lane, A. Delgado, J. Scruggs, E. Ayala, E. Gutierrez, D. Warren, D. Niemeyer, E. George Wolf, and R. A. Bowden. 2002. Hyperbaric oxygen exposure temporarily reduces Mac-1 mediated functions of human neutrophils. Immunol Lett 83:125-31.
73. Kaplan, J. B., E. A. Izano, P. Gopal, M. T. Karwacki, S. Kim, J. L. Bose, K. W. Bayles, and A. R. Horswill. 2012. Low levels of beta-lactam antibiotics induce extracellular DNA release and biofilm formation in *Staphylococcus aureus*. MBio 3:e00198-12.
74. Kemper, M. A., M. M. Urrutia, T. J. Beveridge, A. L. Koch, and R. J. Doyle. 1993. Proton motive force may regulate cell wall-associated enzymes of *Bacillus subtilis*. J Bacteriol 175:5690-6.
75. Kerr, J. F., A. H. Wyllie, and A. R. Currie. 1972. Apoptosis: a basic biological phenomenon with wide-ranging implications in tissue kinetics. Br J Cancer 26:239-57.
76. Kiedrowski, M. R., J. S. Kavanaugh, C. L. Malone, J. M. Mootz, J. M. Voyich, M. S. Smeltzer, K. W. Bayles, and A. R. Horswill. 2011. Nuclease modulates biofilm formation in community-associated methicillin-resistant *Staphylococcus aureus*. PLoS One 6:e26714.
77. Kinkel, T. L., C. M. Roux, P. M. Dunman, and F. C. Fang. 2013. The *Staphylococcus aureus* SrrAB Two-Component System Promotes Resistance to Nitrosative Stress and Hypoxia. MBio 4 (6):e00696-13.
78. Klevens, R. M., M. A. Morrison, J. Nadle, S. Petit, K. Gershman, S. Ray, L. H. Harrison, R. Lynfield, G. Dumyati, J. M. Townes, A. S. Craig, E. R. Zell, G. E. Fosheim, L. K. McDougal, R. B. Carey, and S. K. Fridkin. 2007. Invasive methicillin-resistant *Staphylococcus aureus* infections in the United States. Jama-Journal of the American Medical Association 298:1763-1771.
79. Koch, A. L. 1986. The pH in the neighborhood of membranes generating a protonmotive force. J Theor Biol 120:73-84.
80. Kohler, C., C. von Eiff, M. Liebeke, P. J. McNamara, M. Lalk, R. A. Proctor, M. Hecker, and S. Engelmann. 2008. A defect in menadione biosynthesis induces global changes in gene expression in *Staphylococcus aureus*. J Bacteriol 190:6351-64.
81. Kolodkin-Gal, I., A. K. Elsholz, C. Muth, P. R. Girguis, R. Kolter, and R. Losick. 2013. Respiration control of multicellularity in *Bacillus subtilis* by a

complex of the cytochrome chain with a membrane-embedded histidine kinase. Genes Dev 27:887-99.

82. Kreiswirth, B. N., S. Lofdahl, M. J. Betley, M. O'Reilly, P. M. Schlievert, M. S. Bergdoll, and R. P. Novick. 1983. The toxic shock syndrome exotoxin structural gene is not detectably transmitted by a prophage. Nature 305:709-12.
83. Kristian, S. A., T. A. Birkenstock, U. Sauder, D. Mack, F. Gotz, and R. Landmann. 2008. Biofilm formation induces C3a release and protects *Staphylococcus epidermidis* from IgG and complement deposition and from neutrophil-dependent killing. J Infect Dis 197:1028-35.
84. Kroemer, G., L. Galluzzi, P. Vandenabeele, J. Abrams, E. S. Alnemri, E. H. Baehrecke, M. V. Blagosklonny, W. S. El-Deiry, P. Golstein, D. R. Green, M. Hengartner, R. A. Knight, S. Kumar, S. A. Lipton, W. Malorni, G. Nunez, M. E. Peter, J. Tschopp, J. Yuan, M. Piacentini, B. Zhivotovsky, and G. Melino. 2009. Classification of cell death: recommendations of the Nomenclature Committee on Cell Death 2009. Cell Death Differ 16:3-11.
85. Kuroda, M., T. Ohta, I. Uchiyama, T. Baba, H. Yuzawa, I. Kobayashi, L. Cui, A. Oguchi, K. Aoki, Y. Nagai, J. Lian, T. Ito, M. Kanamori, H. Matsumaru, A. Maruyama, H. Murakami, A. Hosoyama, Y. Mizutani-Ui, N. K. Takahashi, T. Sawano, R. Inoue, C. Kaito, K. Sekimizu, H. Hirakawa, S. Kuhara, S. Goto, J. Yabuzaki, M. Kanehisa, A. Yamashita, K. Oshima, K. Furuya, C. Yoshino, T. Shiba, M. Hattori, N. Ogasawara, H. Hayashi, and K. Hiramatsu. 2001. Whole genome sequencing of meticillin-resistant *Staphylococcus aureus*. Lancet 357:1225-40.
86. Kuwana, T., M. R. Mackey, G. Perkins, M. H. Ellisman, M. Latterich, R. Schneiter, D. R. Green, and D. D. Newmeyer. 2002. Bid, Bax, and lipids cooperate to form supramolecular openings in the outer mitochondrial membrane. Cell 111:331-42.
87. Liu, Q., H. Cho, W. S. Yeo, and T. Bae. 2015. The extracytoplasmic linker peptide of the sensor protein SaeS tunes the kinase activity required for staphylococcal virulence in response to host signals. PLoS Pathog 11:e1004799.
88. Luong, T. T., and C. Y. Lee. 2007. Improved single-copy integration vectors for *Staphylococcus aureus*. J Microbiol Methods 70:186-90.
89. Luong, T. T., K. Sau, C. Roux, S. Sau, P. M. Dunman, and C. Y. Lee. 2010. *Staphylococcus aureus* ClpC divergently regulates capsule via *sae* and *codY* in strain newman but activates capsule via *codY* in strain UAMS-1 and in strain Newman with repaired *saeS*. J Bacteriol 193:686-94.
90. Lyell, A. 1989. Ogston,Alexander, Micrococci, and Lister,Joseph. Journal of the American Academy of Dermatology 20:302-310.
91. Mainiero, M., C. Goerke, T. Geiger, C. Gonser, S. Herbert, and C. Wolz. 2009. Differential target gene activation by the *Staphylococcus aureus* two-component system SaeRS. J Bacteriol 192:613-23.

92. Majerczyk, C. D., M. R. Sadykov, T. T. Luong, C. Lee, G. A. Somerville, and A. L. Sonenshein. 2008. *Staphylococcus aureus* CodY negatively regulates virulence gene expression. J Bacteriol 190:2257-65.
93. Makgotlho, P. E., G. Marincola, D. Schafer, Q. Liu, T. Bae, T. Geiger, E. Wasserman, C. Wolz, W. Ziebuhr, and B. Sinha. 2013. SDS interferes with SaeS signaling of *Staphylococcus aureus* independently of SaePQ. PLoS One 8:e71644.
94. Malpica, R., B. Franco, C. Rodriguez, O. Kwon, and D. Georgellis. 2004. Identification of a quinone-sensitive redox switch in the ArcB sensor kinase. Proc Natl Acad Sci U S A 101:13318-23.
95. Mani, N., P. Tobin, and R. K. Jayaswal. 1993. Isolation and characterization of autolysis-defective mutants of *Staphylococcus aureus* created by Tn917-lacZ mutagenesis. J Bacteriol 175:1493-9.
96. Mann, P. A., A. Muller, K. A. Wolff, T. Fischmann, H. Wang, P. Reed, Y. Hou, W. Li, C. E. Muller, J. Xiao, N. Murgolo, X. Sher, T. Mayhood, P. R. Sheth, A. Mirza, M. Labroli, L. Xiao, M. McCoy, C. J. Gill, M. G. Pinho, T. Schneider, and T. Roemer. 2016. Chemical Genetic Analysis and Functional Characterization of *Staphylococcal* Wall Teichoic Acid 2-Epimerases Reveals Unconventional Antibiotic Drug Targets. PLoS Pathog 12:e1005585.
97. Masalha, M., I. Borovok, R. Schreiber, Y. Aharonowitz, and G. Cohen. 2001. Analysis of transcription of the *Staphylococcus aureus* aerobic class Ib and anaerobic class III ribonucleotide reductase genes in response to oxygen. J Bacteriol 183:7260-72.
98. Mascher, T. 2014. Bacterial (intramembrane-sensing) histidine kinases: signal transfer rather than stimulus perception. Trends Microbiol 22:559-65.
99. Mashruwala, A. A., S. Bhatt, S. Poudel, E. S. Boyd, and J. M. Boyd. 2016. The DUF59 containing protein SufT is involved in the maturation of iron-sulfur (FeS) proteins during conditions of high FeS cofactor demand in *Staphylococcus aureus*. PLoS Genet 12:e1006233.
100. Mashruwala, A. A., and J. M. Boyd. 2015. *De Novo* assembly of plasmids using yeast recombinational cloning. Methods Mol Biol 1373:33-41.
101. Mashruwala, A. A., and J. M. Boyd. 2017. The *Staphylococcus aureus* SrrAB regulatory system modulates hydrogen peroxide resistance factors, which imparts protection to aconitase during aerobic growth. PLoS One 12:e0170283.
102. Mashruwala, A. A., Y. Y. Pang, Z. Rosario-Cruz, H. K. Chahal, M. A. Benson, L. A. Mike, E. P. Skaar, V. J. Torres, W. M. Nauseef, and J. M. Boyd. 2015. Nfu facilitates the maturation of iron-sulfur proteins and participates in virulence in *Staphylococcus aureus*. Mol Microbiol 95:383-409.
103. Mashruwala, A. A., C. A. Roberts, S. Bhatt, K. L. May, R. K. Carroll, L. N. Shaw, and J. M. Boyd. 2016. Staphylococcus aureus SufT: an essential iron-sulphur cluster assembly factor in cells experiencing a high-demand for lipoic acid. Mol Microbiol. 102(6):1099-1119

104. Mashruwala, A. A., A. Van De Guchte, and J. M. Boyd. 2017. Impaired respiration elicits SrrAB-dependent programmed cell lysis and biofilm formation in *Staphylococcus aureus*. ELife, In Press
105. Melter, O., and B. Radojevic. 2010. Small colony variants of *Staphylococcus aureus*--review. Folia Microbiol (Praha) 55:548-58.
106. Memmi, G., D. R. Nair, and A. Cheung. 2011. Role of ArlRS in autolysis in methicillin-sensitive and methicillin-resistant *Staphylococcus aureus* strains. J Bacteriol 194:759-67.
107. Miller, M. R., and I. L. Megson. 2007. Recent developments in nitric oxide donor drugs. Br J Pharmacol 151:305-21.
108. Naimi, T. S., K. H. LeDell, K. Como-Sabetti, S. M. Borchardt, D. J. Boxrud, J. Etienne, S. K. Johnson, F. Vandenesch, S. Fridkin, C. O'Boyle, R. N. Danila, and R. Lynfield. 2003. Comparison of community- and health care-associated methicillin-resistant *Staphylococcus aureus* infection. JAMA 290:2976-84.
109. Nauseef, W. M. 2008. Biological roles for the NOX family NADPH oxidases. J Biol Chem 283:16961-5.
110. Navarre, W. W., H. Ton-That, K. F. Faull, and O. Schneewind. 1999. Multiple enzymatic activities of the murein hydrolase from staphylococcal phage phi11. Identification of a D-alanyl-glycine endopeptidase activity. J Biol Chem 274:15847-56.
111. Novick, R. P. 1991. Genetic systems in *staphylococci*. Methods Enzymol 204:587-636.
112. Novick, R. P., and D. Jiang. 2003. The staphylococcal SaeRS system coordinates environmental signals with Agr quorum sensing. Microbiology 149:2709-17.
113. Nygaard, T. K., K. B. Pallister, P. Ruzevich, S. Griffith, C. Vuong, and J. M. Voyich. 2010. SaeR binds a consensus sequence within virulence gene promoters to advance USA300 pathogenesis. J Infect Dis 201:241-54.
114. Ohara-Nemoto, Y., H. Haraga, S. Kimura, and T. K. Nemoto. 2008. Occurrence of staphylococci in the oral cavities of healthy adults and nasal oral trafficking of the bacteria. J Med Microbiol 57:95-9.
115. Ohnishi, R., S. Ishikawa, and J. Sekiguchi. 1999. Peptidoglycan hydrolase LytF plays a role in cell separation with CwlF during vegetative growth of *Bacillus subtilis*. J Bacteriol 181:3178-84.
116. Oshida, T., M. Sugai, H. Komatsuzawa, Y. M. Hong, H. Suginaka, and A. Tomasz. 1995. A *Staphylococcus aureus* autolysin that has an N-acetylmuramoyl-L-alanine amidase domain and an endo-beta-N-acetylglucosaminidase domain: cloning, sequence analysis, and characterization. Proc Natl Acad Sci U S A 92:285-9.
117. Otto, M. 2008. *Staphylococcal* biofilms. Curr Top Microbiol Immunol 322:207-28.
118. Pang, X., S. H. Moussa, N. M. Targy, J. L. Bose, N. M. George, C. Gries, H. Lopez, L. Zhang, K. W. Bayles, R. Young, and X. Luo. Active Bax and Bak are functional holins. Genes Dev 25:2278-90.

119. Pang, Y. Y., J. Schwartz, S. Bloomberg, J. M. Boyd, A. R. Horswill, and W. M. Nauseef. 2013. Methionine sulfoxide reductases protect against oxidative stress in *Staphylococcus aureus* encountering exogenous oxidants and human neutrophils. J Innate Immun 6:353-64.
120. Pasztor, L., A. K. Ziebandt, M. Nega, M. Schlag, S. Haase, M. Franz-Wachtel, J. Madlung, A. Nordheim, D. E. Heinrichs, and F. Gotz. 2010. Staphylococcal major autolysin (Atl) is involved in excretion of cytoplasmic proteins. J Biol Chem 285:36794-803.
121. Pragman, A. A., J. M. Yarwood, T. J. Tripp, and P. M. Schlievert. 2004. Characterization of virulence factor regulation by SrrAB, a two-component system in *Staphylococcus aureus*. J Bacteriol 186:2430-8.
122. Proctor, R. A., C. von Eiff, B. C. Kahl, K. Becker, P. McNamara, M. Herrmann, and G. Peters. 2006. Small colony variants: a pathogenic form of bacteria that facilitates persistent and recurrent infections. Nat Rev Microbiol 4:295-305.
123. Ranjit, D. K., J. L. Endres, and K. W. Bayles. 2011. *Staphylococcus aureus* CidA and LrgA proteins exhibit holin-like properties. J Bacteriol 193:2468-76.
124. Regassa, L. B., R. P. Novick, and M. J. Betley. 1992. Glucose and nonmaintained pH decrease expression of the accessory gene regulator (agr) in *Staphylococcus aureus*. Infect Immun 60:3381-8.
125. Rice, K. C., and K. W. Bayles. 2008. Molecular control of bacterial death and lysis. Microbiol Mol Biol Rev 72:85-109, table of contents.
126. Rice, K. C., E. E. Mann, J. L. Endres, E. C. Weiss, J. E. Cassat, M. S. Smeltzer, and K. W. Bayles. 2007. The *cidA* murein hydrolase regulator contributes to DNA release and biofilm development in *Staphylococcus aureus*. Proc Natl Acad Sci U S A 104:8113-8.
127. Sadykov, M. R., T. Hartmann, T. A. Mattes, M. Hiatt, N. J. Jann, Y. Zhu, N. Ledala, R. Landmann, M. Herrmann, H. Rohde, M. Bischoff, and G. A. Somerville. 2011. CcpA coordinates central metabolism and biofilm formation in *Staphylococcus epidermidis*. Microbiology 157:3458-68.
128. Said-Salim, B., B. Mathema, and B. N. Kreiswirth. 2003. Community-acquired methicillin-resistant Staphylococcus aureus: an emerging pathogen. Infect Control Hosp Epidemiol 24:451-5.
129. Sanchez Garcia, M., M. A. De la Torre, G. Morales, B. Pelaez, M. J. Tolon, S. Domingo, F. J. Candel, R. Andrade, A. Arribi, N. Garcia, F. Martinez Sagasti, J. Fereres, and J. Picazo. 2010. Clinical outbreak of linezolid-resistant *Staphylococcus aureus* in an intensive care unit. JAMA 303:2260-4.
130. Sass, P., A. Berscheid, A. Jansen, M. Oedenkoven, C. Szekat, A. Strittmatter, G. Gottschalk, and G. Bierbaum. 2012. Genome sequence of *Staphylococcus aureus* VC40, a vancomycin- and daptomycin-resistant strain, to study the genetics of development of resistance to currently applied last-resort antibiotics. J Bacteriol 194:2107-8.
131. Scherr, T. D., M. L. Hanke, O. Huang, D. B. James, A. R. Horswill, K. W. Bayles, P. D. Fey, V. J. Torres, and T. Kielian. 2015. *Staphylococcus*

*aureus* Biofilms Induce Macrophage Dysfunction Through Leukocidin AB and Alpha-Toxin. MBio 6.

132. Scherr, T. D., K. E. Lindgren, C. R. Schaeffer, M. L. Hanke, C. W. Hartman, and T. Kielian. 2014. Mouse model of post-arthroplasty *Staphylococcus epidermidis* joint infection. Methods Mol Biol 1106:173-81.
133. Schlag, M., R. Biswas, B. Krismer, T. Kohler, S. Zoll, W. Yu, H. Schwarz, A. Peschel, and F. Gotz. 2010. Role of staphylococcal wall teichoic acid in targeting the major autolysin Atl. Mol Microbiol 75:864-73.
134. Schlag, S., S. Fuchs, C. Nerz, R. Gaupp, S. Engelmann, M. Liebeke, M. Lalk, M. Hecker, and F. Gotz. 2008. Characterization of the oxygen-responsive NreABC regulon of *Staphylococcus aureus*. J Bacteriol 190:7847-58.
135. Schurig-Briccio, L. A., T. Yano, H. Rubin, and R. B. Gennis. 2014. Characterization of the type 2 NADH:menaquinone oxidoreductases from *Staphylococcus aureus* and the bactericidal action of phenothiazines. Biochim Biophys Acta 1837:954-63.
136. Schwartz, K., A. K. Syed, R. E. Stephenson, A. H. Rickard, and B. R. Boles. 2012. Functional amyloids composed of phenol soluble modulins stabilize *Staphylococcus aureus* biofilms. PLoS Pathog 8:e1002744.
137. Sedghizadeh, P. P., S. K. Kumar, A. Gorur, C. Schaudinn, C. F. Shuler, and J. W. Costerton. 2009. Microbial biofilms in osteomyelitis of the jaw and osteonecrosis of the jaw secondary to bisphosphonate therapy. J Am Dent Assoc 140:1259-65.
138. Shah, J. Hyperbaric oxygen therapy. J Am Col Certif Wound Spec 2:9-13.
139. Shaw, L., E. Golonka, J. Potempa, and S. J. Foster. 2004. The role and regulation of the extracellular proteases of *Staphylococcus aureus*. Microbiology 150:217-28.
140. Shimizu, S., Y. Eguchi, W. Kamiike, Y. Itoh, J. Hasegawa, K. Yamabe, Y. Otsuki, H. Matsuda, and Y. Tsujimoto. 1996. Induction of apoptosis as well as necrosis by hypoxia and predominant prevention of apoptosis by Bcl-2 and Bcl-X(L). Cancer Research 56:2161-2166.
141. Soh, C. R., R. Pietrobon, J. J. Freiberger, S. T. Chew, D. Rajgor, M. Gandhi, J. Shah, and R. E. Moon. 2012. Hyperbaric oxygen therapy in necrotising soft tissue infections: a study of patients in the United States Nationwide Inpatient Sample. Intensive Care Med 38:1143-51.
142. Somerville, G. A., and R. A. Proctor. 2009. At the crossroads of bacterial metabolism and virulence factor synthesis in staphylococci. Microbiology and Molecular Biology Reviews 73:233-248.
143. Somerville, G. A., B. Said-Salim, J. M. Wickman, S. J. Raffel, B. N. Kreiswirth, and J. M. Musser. 2003. Correlation of acetate catabolism and growth yield in *Staphylococcus aureus*: implications for host-pathogen interactions. Infect Immun 71:4724-32.
144. Steinhuber, A., C. Goerke, M. G. Bayer, G. Doring, and C. Wolz. 2003. Molecular architecture of the regulatory Locus *sae* of *Staphylococcus aureus* and its impact on expression of virulence factors. J Bacteriol 185:6278-86.

145. Stephenson, K., and J. A. Hoch. 2002. Two-component and phosphorelay signal-transduction systems as therapeutic targets. Curr Opin Pharmacol 2:507-12.
146. Stock, A. M., V. L. Robinson, and P. N. Goudreau. 2000. Two-component signal transduction. Annu Rev Biochem 69:183-215.
147. Sun, F., C. Li, D. Jeong, C. Sohn, C. He, and T. Bae. 2010. In the *Staphylococcus aureus* two-component system Sae, the response regulator SaeR binds to a direct repeat sequence and DNA binding requires phosphorylation by the sensor kinase SaeS. J Bacteriol 192:2111-27.
148. Tenover, F. C., L. K. McDougal, R. V. Goering, G. Killgore, S. J. Projan, J. B. Patel, and P. M. Dunman. 2006. Characterization of a strain of community-associated methicillin-resistant *Staphylococcus aureus* widely disseminated in the United States. J Clin Microbiol 44:108-118.
149. Thurlow, L. R., M. L. Hanke, T. Fritz, A. Angle, A. Aldrich, S. H. Williams, I. L. Engebretsen, K. W. Bayles, A. R. Horswill, and T. Kielian. 2011. *Staphylococcus aureus* biofilms prevent macrophage phagocytosis and attenuate inflammation in vivo. J Immunol 186:6585-96.
150. Tong, S. Y., J. S. Davis, E. Eichenberger, T. L. Holland, and V. G. Fowler, Jr. 2015. *Staphylococcus aureus* infections: epidemiology, pathophysiology, clinical manifestations, and management. Clin Microbiol Rev 28:603-61.
151. Vogelberg, K. H., and M. Konig. 1993. Hypoxia of diabetic feet with abnormal arterial blood flow. Clin Investig 71:466-70.
152. Voyich, J. M., C. Vuong, M. DeWald, T. K. Nygaard, S. Kocianova, S. Griffith, J. Jones, C. Iverson, D. E. Sturdevant, K. R. Braughton, A. R. Whitney, M. Otto, and F. R. DeLeo. 2009. The SaeR/S gene regulatory system is essential for innate immune evasion by *Staphylococcus aureus*. J Infect Dis 199:1698-706.
153. Wadstrom, T., and K. Hisatsune. 1970. Bacteriolytic enzymes from *Staphylococcus aureus*. Specificity of action of endo-beta-N-acetylglucosaminidase. Biochem J 120:735-44.
154. Wakeman, C. A., N. D. Hammer, D. L. Stauff, A. S. Attia, L. L. Anzaldi, S. I. Dikalov, M. W. Calcutt, and E. P. Skaar. 2012. Menaquinone biosynthesis potentiates haem toxicity in *Staphylococcus aureus*. Mol Microbiol 86:1376-92.
155. Wecke, J., M. Lahav, I. Ginsburg, E. Kwa, and P. Giesbrecht. 1986. Inhibition of wall autolysis of *staphylococci* by sodium polyanethole sulfonate "liquoid". Arch Microbiol 144:110-5.
156. Weinmann, M., V. Jendrossek, R. Handrick, D. Guner, B. Goecke, and C. Belka. 2004. Molecular ordering of hypoxia-induced apoptosis: critical involvement of the mitochondrial death pathway in a FADD/caspase-8 independent manner. Oncogene 23:3757-69.
157. Weinrick, B., P. M. Dunman, F. McAleese, E. Murphy, S. J. Projan, Y. Fang, and R. P. Novick. 2004. Effect of mild acid on gene expression in *Staphylococcus aureus*. J Bacteriol 186:8407-23.

158. Wilde, A. D., D. J. Snyder, N. E. Putnam, M. D. Valentino, N. D. Hammer, Z. R. Lonergan, S. A. Hinger, E. E. Aysanoa, C. Blanchard, P. M. Dunman, G. A. Wasserman, J. Chen, B. Shopsin, M. S. Gilmore, E. P. Skaar, and J. E. Cassat. 2015. Bacterial hypoxic responses revealed as critical determinants of the host-pathogen outcome by TnSeq analysis of *Staphylococcus aureus* invasive infection. PLoS Pathog 11:e1005341.
159. Williamson, D. A., A. Lim, M. G. Thomas, M. G. Baker, S. A. Roberts, J. D. Fraser, and S. R. Ritchie. 2013. Incidence, trends and demographics of *Staphylococcus aureus* infections in Auckland, New Zealand, 2001-2011. BMC Infect Dis 13:569.
160. Yabu, K., and S. Kaneda. 1995. Salt-induced cell lysis of *Staphylococcus aureus*. Curr Microbiol 30:299-303.
161. Yamaguchi, H., K. Furuhata, T. Fukushima, H. Yamamoto, and J. Sekiguchi. 2004. Characterization of a new *Bacillus subtilis* peptidoglycan hydrolase gene, *yvcE* (named *cwlO*), and the enzymatic properties of its encoded protein. J Biosci Bioeng 98:174-81.
162. Yarwood, J. M., J. K. McCormick, and P. M. Schlievert. 2001. Identification of a novel two-component regulatory system that acts in global regulation of virulence factors of *Staphylococcus aureus*. J Bacteriol 183:1113-23.
163. Yun, H. S., Y. Kim, S. Oh, W. M. Jeon, J. F. Frank, and S. H. Kim. 2012. Susceptibility of *Listeria monocytogenes* biofilms and planktonic cultures to hydrogen peroxide in food processing environments. Biosci Biotechnol Biochem 76:2008-13.
164. Zafar, U., L. B. Johnson, M. Hanna, K. Riederer, M. Sharma, M. G. Fakih, M. C. Thirumoorthi, R. Farjo, and R. Khatib. 2007. Prevalence of nasal colonization among patients with community-associated methicillin-resistant *Staphylococcus aureus* infection and their household contacts. Infection Control and Hospital Epidemiology 28:966-969.
165. Zhang, Q., Q. Chang, R. A. Cox, X. Gong, and L. J. Gould. 2008. Hyperbaric oxygen attenuates apoptosis and decreases inflammation in an ischemic wound model. J Invest Dermatol 128:2102-12.
166. Zhu, Y., E. C. Weiss, M. Otto, P. D. Fey, M. S. Smeltzer, and G. A. Somerville. 2007. *Staphylococcus aureus* biofilm metabolism and the influence of arginine on polysaccharide intercellular adhesin synthesis, biofilm formation, and pathogenesis. Infect Immun 75:4219-26.